ROLE OF HYPOTHALAMIC *SIM1* IN HYPERPHAGIC OBESITY

APPROVED BY SUPERVISORY COMMITTEE

Andrew R. Zinn, M.D., Ph.D.

Joel K. Elmquist, D.V.M., Ph.D.

Jay Horton, M.D.

Amelia J. Eisch, Ph.D.

To my dear husband Joel, my family and God.
Without your support this would not have been possible.

ACKNOWLEDGEMENTS

There are so many people who have mentored me and assisted me in reaching this point, and I owe you all a debt of gratitude.

First of all, I would like to thank the past and present members of my lab who have been intimately involved in my research and the process of graduate school: Andrew Zinn, Bassil Kublaoui, Purita Ramos, Terry Gemelli, Lane Jaeckle Santos and Elizabeth Bhoj. Thank you Andrew and Bassil for mentoring, guiding and supporting me. Thanks Purita and Terry for all of your help in the lab and teaching me research techniques. Thanks Elizabeth and Lane for being my sistes-in-arms in the process of graduate school and your helpful insights into my work. Thank you especially Lane for being such a good friend and having the patience to be a constant sounding board and supporter. Thank you also Miguel for letting me borrow your wife so often and for being there for me yourself.

I also thank my committee members, Joel Elmquist, Jay Horton, Keith Parker and Amelia Eisch for their guidance during my training. Keith's sense of humor and astute questions will be missed. I especially thank Amelia and Joel for their help with techniques that were new to me and our lab.

I am also thankful to all of our collaborators and colleagues, who are too numerous to list here. The Integrative Biology program provided a wonderful learning experience, made possible largely through the coordination of Priyarama Sen. A number of other graduate students were particularly influential during my studies: Anne Marie

Corgan, Yuri Kim, Liliana Carbajal-Hernandez, Jessica Ables, Bret Evers, James Deng, Elhadji Dioum, and Andrew Bitmansour are a few.

Thank you Stuart Ravnik for not only recruiting the girl with the blue hair, but also for sticking with me for the last 5 years and helping with teaching opportunities.

I would not have made it to graduate school without the support and mentoring of numerous teachers and professors in high school and undergraduate, particularly David Marcey, Andrea Huvard and Barbara Collins.

In addition, I would like to thank my friends from undergraduate, home, and church who have supported me through this process, especially Cora and Nate Silva, Steve Carriere, Lindsay Severs, Jon Gonzales, Burke Wallace, Sarah Polster, Kristin Fricke and the whole Johnson family. An enormous thanks goes to Sarah Wright, the only non-scientist besides Joel brave enough to read and edit my dissertation. Thanks to both the FOPC and UPUMC church families, who provided support and prayers.

I am immensely thankful for the many members of my family, who have helped me to become who I am and supported me both financially and emotionally – my parents Jan Petersen-Smith and Dave Smith, my brother Brian Smith, my Grandma Earlene and Dave, Leslie, Sara and Jennifer Petersen. The new members of my family – especially Tod and Helene Tolson – have been so supportive and encouraging as well. And there is no way I would have made it this far without the help of my amazing husband Joel. Thank you for everything and for helping me to make a home with all of our fuzzy little children.

ROLE OF HYPOTHALAMIC *SIM1* IN HYPERPHAGIC OBESITY

by

KRISTEN PETERSEN TOLSON

DISSERTATION

Presented to the Faculty of the Graduate School of Biomedical Sciences

The University of Texas Southwestern Medical Center at Dallas

In Partial Fulfillment of the Requirements

For the Degree of

DOCTOR OF PHILOSOPHY

The University of Texas Southwestern Medical Center at Dallas

Dallas, Texas

October, 2009

ROLE OF HYPOTHALAMIC *SIM1* IN HYPERPHAGIC OBESITY

Kristen Petersen Tolson, Ph.D.

The University of Texas Southwestern Medical Center at Dallas, 2009

Andrew Robert Zinn, M.D., Ph.D.

Single-minded 1 (*SIM1)* mutations are one of the few known causes of monogenic obesity in both humans and mice. *Sim1* encodes a transcription factor essential for formation of the hypothalamic paraventricular nucleus (PVN), and haploinsufficiency of mouse *Sim1* causes hyperphagic obesity with increased linear growth and enhanced sensitivity to a high-fat diet. While the role for *Sim1* in the formation of the hypothalamus has been described, its post-developmental, physiologic functions have not been well established. Here I present my work in elucidating the role of hypothalamic *Sim1* in hyperphagic obesity.

First, I show that overexpression of *SIM1* in transgenic mice causes no obvious phenotype on a low-fat chow diet but confers resistance to diet-induced obesity on a high fat diet. I show this change to be due to reduced food intake with no change in energy expenditure. Additionally, the *SIM1* transgene completely rescues the hyperphagia and partially rescues the obesity of agouti yellow mice, in which melanocortin signaling is

abrogated. Next, I investigate the hypothesis that altered PVN neuropeptide expression mediates the hyperphagia of *Sim1*$^{+/-}$ mice. I show oxytocin (Oxt) mRNA and peptide are markedly decreased in *Sim1*$^{+/-}$ mice, and that *Sim1*$^{+/-}$ mice are hypersensitive to an Oxt receptor antagonist, while repeated Oxt injections decrease the food intake and weight gain of *Sim1*$^{+/-}$ mice. Finally, I demonstrate that postnatal CNS deficiency of *Sim1* causes hyperphagic obesity by conditionally deleting *Sim1* after birth. I also generate viable conditional *Sim1* homozygotes, demonstrating that adult *Sim1* expression is not essential for neuronal survival. Furthermore, I show that the phenotype of both conventional heterozygotes and conditional *Sim1* homozygotes was not attributable to hypocellularity of the PVN or changes in projections to the hindbrain.

My work indicates that *Sim1* controls food intake but not energy expenditure, supports the importance of Oxt neurons in feeding regulation, suggests that reduced Oxt neuropeptide is one mechanism mediating the hyperphagic obesity of *Sim1*$^{+/-}$ mice, and demonstrates that *Sim1*'s role in feeding regulation is not limited to formation of the PVN. Collectively, these studies support a physiological role for *Sim1* in hyperphagic obesity after the development of the PVN.

TABLE OF CONTENTS

PRIOR PUBLICATIONS

Tolson KP, Gemelli T, Gautron L, Elmquist JK, Zinn AR, Kublaoui BM. Postnatal *Sim1* deficiency causes hyperphagic obesity and reduced *Mc4r* and *Oxytocin* expression. *Manuscript in submission*.

Kublaoui BM, Gemelli T, **Tolson KP**, Wang Y, Zinn AR. (2008). Oxytocin deficiency mediates hyperphagic obesity of *Sim1* haploinsufficient mice. Mol Endocrinol. 22(7):1723-34.

Kublaoui BM, Holder JL Jr, **Tolson KP**, Gemelli T, Zinn AR. (2006). *SIM1* overexpression partially rescues agouti yellow and diet-induced obesity by normalizing food intake. Endocrinology. 147(10):4542-9.

LIST OF FIGURES

LIST OF ABBREVIATIONS

3V – third ventricle

aCSF – artificial cerebrospinal fluid

ad libitum – free-feeding

α-MSH – alpha melanocyte-stimulating hormone

Agrp – agouti related peptide

ANOVA – analysis of variance

ARC – arcuate nucleus

Arnt2 – aryl hydrocarbon receptor nuclear translocator 2

Avp – arginine vasopressin

A^y – Agouti yellow

BAC – bacterial artificial chromosome

bHLH – basic helix loop helix

BMI – body mass index

CaMKII – calcium/calmodulin-dependent protein kinase II

CCK – cholecystokinin

c-Fos – FBJ murine osteosarcoma viral oncogene homolog

cHet – conditional *Sim1* heterozygote (Cre^+, $Sim1^{+/fl}$)

cKO – conditional *Sim1* homozygote (Cre^+, $Sim1^{fl/fl}$)

CLAMS – Comprehensive Lab Animal Monitoring System

CNS – central nervous system

CRH – corticotropin-releasing hormone

Cre – Cre recombinase

Cre159 – CaMKII-Cre 159 mouse line

Cre93 – CaMKII-Cre 93 mouse line

DAPI – 4',6-diamidino-2-phenylindole

DIO – diet-induced obesity

DNA – deoxyribonucleic acid

DMV – dorsal motor nucleus of the vagus

DVC – dorsal vagal complex

FI – food intake

GABA – γ-Aminobutyric acid

GFP – green fluorescent protein

HF – high fat

HSTG18 – high copy number *SIM1* transgene mouse line

HSTG26 – low copy number *SIM1* transgene mouse line

ICV – intracerebroventricular

IP – intraperitoneal

LF – low fat

LH – lateral hypothalamus

MC4R – melanocortin 4 receptor

mRNA – messenger RNA

MTII – melanotan II

n – number of subjects in the study

NMR – nuclear magnetic resonance

Npy – neuropeptide Y

NTS – nucleus of the solitary tract

OVT – $d(CH_2)_5$, $Tyr(Me)^2$,Orn^8-Oxytocin

Oxt – oxytocin

P – postnatal day

PAS – Per Arnt Sim

PBS – phosphate buffered saline

PCR – polymerase chain reaction

POMC – pro-opiomelanocortin

PVN – paraventricular nucleus

qPCR – quantitative real time PCR

RNA – ribonucleic acid

RT – reverse transcriptase

SEM – standard error of the mean

SIM1 – single-minded 1 (capital denotes human gene, first letter only capital denotes mouse gene, non-italicized denotes protein)

SON – supraoptic nucleus

SST – somatostatin

TRH – thyrotropin-releasing hormone

WT – wild type

Chapter I

Introduction

Obesity

While changes in the environment over the last few decades have resulted in the current epidemic of obesity (Figure I.1), much of the variance in individual response to this environment is genetically determined (Maes et al., 1997; Farooqi and O'Rahilly, 2005; Keith et al., 2006; Wardle et al., 2008). Adult and childhood obesity are rapidly increasing in prevalence, with around 66.3% of U.S. adults overweight, 32.2% obese, and nearly 5% extremely obese (Ogden et al., 2006). The same study reported that childhood obesity has a prevalence of 17.1% among 2-19 year olds in the United States, with an additional 16.5% of children overweight (Ogden et al., 2006). Obesity is also no longer an affliction solely of Western society; it has increased worldwide by >75% since 1980 (Flegal et al., 1998) and there are now over 1 billion people who are overweight or obese (Froguel and Boutin, 2001).

Obesity predisposes to many health problems including type 2 diabetes mellitus, hypertension, dyslipidemia, liver disease, early coronary and carotid artery pathology, orthopedic problems, obstructive sleep apnea, psychosocial problems and more (Kortelainen, 1997; Barlow and Dietz, 1998). These medical issues both are costly and debilitating. Therefore, there is an urgent need for more research into the biology of feeding, energy homeostasis, and obesity. However, existing nonsurgical treatment options for obesity are surprisingly limited and ineffective (Bray and Tartaglia, 2000) – for most people, no more than a 5%–10% loss of body weight can be maintained through diet, exercise, and use of the few available anti-obesity medications (Yanovski and Yanovski, 2002). Additionally, many of these therapeutics have undesirable and sometimes dangerous side effects, as they affect more than one physiological pathway.

Therefore, there is an urgent need for more research into the biology of feeding, energy homeostasis, and obesity.

While obesity has been and often still is perceived as a problem with sloth, gluttony and poor will power, incontrovertible evidence now shows that genetic factors play a dominant role in determining body weight within a given environment (Barsh et al., 2000). Obesity clusters within families (Allison et al., 1996), and twin studies have shown that the concordance of body mass index (BMI) is much higher between monozygotic than dizygotic twins (74% versus 32%, respectively), despite sharing the same environments (Stunkard et al., 1990; Barsh et al., 2000). Moreover, the BMI of adopted children is linearly related to that of both of their biological parents and is unrelated to that of either adoptive parent, even when there is no direct contact with the biological parents and the adoptive parents provide the daily menu (Stunkard et al., 1986). Taken together with other data, the studies suggest an estimated heritability for obesity of 50% to 90% (Barsh et al., 2000). While common obesity is polygenic, rare single gene mutations that cause obesity in animal models or in humans have delineated central nervous system pathways critical for energy homeostasis, and the molecules encoded by these genes are promising pharmacologic targets.

Central nervous system control of energy balance

The leptin-melanocortin pathway

Neuroanatomic, pharmacologic, and genetic studies (reviewed in (Cone, 2005; Morton et al., 2006)) have led to the current models of central nervous system regulation of energy homeostasis. A prominent model and area of study involves leptin, a

circulating hormone secreted by adipocytes in proportion to body fat stores, which acts as an adiposity signal. This model is especially interesting as all of the currently known causes of monogenic obesity in humans occur in this pathway (Figure I.2), and multiple mouse models of obesity have been generated with mutations in this pathway (Cummings and Schwartz, 2003; Farooqi and O'Rahilly, 2005). The results of leptin replacement therapy with people with congenital leptin deficiency are both dramatic and exciting (Figure I.3) but have not been replicated in common obesity, likely because of leptin resistance (Schwartz et al., 2000; Farooqi and O'Rahilly, 2005).

Leptin binds to receptors in multiple areas of the brain (Balthasar, 2006), particularly the arcuate nucleus (ARC), which lies near the third ventricle (3V) and the median eminence (ME). The ME is effectively outside of the blood brain barrier, allowing circulating leptin to access the ARC. The ARC contains two populations of neurons that appear to act in opposition to one another: the orexigenic Neuropeptide y/Agouti related peptide (*Npy/Agrp*) neurons and the anorexigenic Pro-opiomelanocortin/Cocaine and amphetamine related transcripts (*Pomc*) neurons (Schwartz et al., 2000; Cone, 2005). Leptin receptor activation stimulates *Pomc* neurons which release α-MSH (alpha melanocyte stimulating hormone), and inhibits *Npy/Agrp* neurons from releasing Npy and Agrp (Schwartz et al., 2000; Cone, 2005). In the ARC, 30% of *Pomc* neurons have the signaling-competent long form of the leptin receptor (Cheung et al., 1997). Intraperitoneal leptin injection increases hypothalamic *Pomc* mRNA (Schwartz et al., 1997), while fasting induces a low leptin state and decreases it. *Pomc* mRNA is also depressed in mice and rats that lack a functioning leptin receptor (Mizuno et al., 1998).

These ARC neurons project to other central nervous system (CNS) sites, including the paraventricular nucleus (PVN) (Schwartz et al., 1997), which is the area of focus of this work (Figure I.4) and will be discussed in more detail below. α-MSH is the principal endogenous ligand of both the CNS melanocortin 3 and 4 receptors (Mc3r and Mc4r). Intracerebroventricular (ICV) administration of α-MSH markedly reduces food intake in rodents. The effect of α-MSH on feeding is principally mediated through the Mc4r (Huszar et al., 1997; Schioth et al., 1999), while Mc3r is involved in energy partitioning (Abbott et al., 2000; Butler et al., 2000; Chen et al., 2000). α-MSH binds to the Mc4r on neurons within and/or innervating the PVN, where it acts to inhibit feeding. Blockade of the Mc4r impairs leptin's ability to reduce food intake and body weight (Satoh et al., 1998). Agrp is a competitive inhibitor of α-MSH at the Mc4r, and its release potently stimulates feeding. Npy binds to Npy receptors that also stimulate feeding, and *Npy/Agrp* neurons also release inhibitory γ-Aminobutyric acid (GABA) onto *Pomc* neurons (Cowley et al., 2001). *Agrp* mRNA expression is increased by fasting or by mutations in leptin or the leptin receptor. Unsurprisingly, overexpression of Agrp leads to obesity and central injection of Agrp stimulates food intake and reverses leptin-induced feeding inhibition (Schwartz et al., 2000; Cone, 2005).

Integration of adiposity and satiety signals by second order pathways

Altered feeding in most mouse models of obesity affects termination of feeding (meal size). Npy-induced hyperphagia arises from consumption of larger meals at a similar frequency (Leibowitz and Alexander, 1991), and leptin mediates hypophagia by reducing meal size (Flynn et al., 1998). A major determinant of meal size is the onset of

satiety, a neuroendocrine response involving the gastrointestinal (GI) tract and the brainstem in a reflex arc. Satiety signals differ from adiposity signals as they respond to the immediate state of food intake rather than the long term state of body fuel stores. Signals from the GI tract, mainly the stomach and duodenum, are transmitted via the vagus nerve to the nucleus of the tractus solitarius (NTS) (Travers et al., 1987), leading to inhibition of further food intake by a reflex arc (Figure I.5). Studies in the decerebrate rat suggest that a connection between the cerebrum and hindbrain is necessary for proper regulation of feeding (Grill and Kaplan, 2002). Neuroanatomical studies demonstrate ample connections between hypothalamic nuclei, such as the PVN, and the NTS. Negative feedback signals transmitted from the GI tract to the NTS are mediated by gastric stretch receptors and cholecystokinin (CCK) receptors on vagal nerve afferent termini. CCK is released from the mucosal cells of the duodenum in response to the presence in the gut lumen of fatty acids and certain amino acids (Moran and Schwartz, 1994). It binds to nearby CCK-A receptors on vagal nerve endings, which transmit a negative feeding signal to the NTS. CCK's satiety action is neuroendocrine rather than endocrine, as both vagotomy and selective afferent vagotomy abolish the effect (Moran, 2000).

Several studies point to an interaction between the adiposity signal in the PVN and the satiety signal in the NTS. Infusion of a gastric load prior to initiation of feeding in rats leads to a slight decrease in subsequent food intake (Emond et al., 2001). By itself ICV injection of leptin causes no acute change in food intake, but greatly diminishes food intake after a gastric load. In the same study, both an intragastric load and leptin administration led to similar activation of PVN neurons, and their combined effect was

synergistic. By itself leptin had no effect on NTS neuronal activation, but it caused a synergistic response when given with a gastric load. A similar interaction has been demonstrated between leptin and CCK (Moran, 2000). In this study, ICV administration of leptin by itself did not reduce food intake, but it augmented the reduction of feeding due to intraperitoneal (IP) administration of CCK. Again, PVN and medial NTS neurons were synergistically activated by leptin and CCK, as reflected by c-Fos immunoreactivity.

The PVN in the anterior hypothalamus acts as an integration site for many pathways involved in energy homeostasis, and anatomic PVN lesions result in hyperphagic obesity (Leibowitz et al., 1981). The PVN is also one of the main sites of single-minded 1 (*Sim1*) expression. In addition to inputs from ARC neurons containing Npy/Agrp and Pomc/Cart (Elmquist et al., 1999), the PVN has receptors for other orexigenic and anorexigenic neurotransmitters including serotonin, galanin, norepinephrine, and opioids. The balance between these orexigenic and anorexigenic signals to the PVN determines food intake, with leptin acting on both sets of pathways to reduce feeding. The PVN has five major neuronal subtypes, distinguished on the basis of the neuropeptide they produce: oxytocin (Oxt), vasopressin (Avp), thyrotropin releasing hormone (Trh), corticotropin releasing hormone (Crh), and somatostatin (Sst). Three of these neuropeptides, Oxt, Trh, and Crh, have been shown to inhibit feeding when injected centrally (discussed in further detail below). There is also Mc4r immunoreactivity in the PVN, but the precise location of Mc4 receptors that signal to PVN neurons is unclear. Cowley et al. (Cowley et al., 1999) presented electrophysiologic and immunolocalization data showing relevant Mc4r receptors on presynaptic GABAergic interneurons within the

PVN. Balthasar et al. (Balthasar et al., 2005) showed genetic evidence that Mc4r in *Sim1*-expressing neurons in the PVN or possibly amygdala regulates food intake but not energy expenditure. It is not known whether the interneurons studied by Cowley et al. (Cowley et al., 1999) express *Sim1*. Neither study excluded the possibility that Mc4r also acts presynaptically elsewhere in the brain on neurons that project to the PVN (Balthasar et al., 2005).

SIM1 and hyperphagic obesity

Now recognized as one of the six known genes involved in monogenic obesity (Cummings and Schwartz, 2003), *Sim1* is a mouse homolog of Drosophila Single-minded which encodes a basic helix loop helix-Per Arnt Sim (bHLH-PAS) transcription factor (Ema et al., 1996; Fan et al., 1996). The PAS domain is found in many plant, animal, and prokaryotic proteins that sense environmental or developmental signals such as redox potential, xenobiotics, and cellular oxygen (Gu et al., 2000). A subfamily of PAS proteins also contain a basic helix loop helix (bHLH) domain; these bHLH-PAS proteins heterodimerize with other bHLH-PAS proteins to regulate nuclear transcription of target genes. One of the best studied bHLH-PAS proteins, the aryl hydrocarbon (dioxin) receptor (AHR), heterodimerizes with its partner ARNT and translocates to the nucleus in a ligand-dependent fashion (Hankinson, 1995). By contrast, no ligand has been identified for SIM1, which is thought to constitutively heterodimerize with its partner ARNT2 and activate or repress nuclear target genes, based on subcellular localization studies of *Drosophila* SIM during development (Ward et al., 1998) and studies of epitope-tagged mouse SIM1 or eGFP-SIM1 fusion proteins in transfected cells (Woods and Whitelaw,

2002; Yamaki et al., 2004). Multiple bHLH-PAS family members have been shown to undergo regulated translocation to the nucleus (Hankinson, 1995; Kallio et al., 1998; Ward et al., 1998; Dekanty et al., 2005; Kwon et al., 2006; Teh et al., 2006) and the natural localization of Sim1 has remained enigmatic, largely due to the lack of a specific antibody. Sim1 has an atypical nuclear localization signal that is potentially a substrate for phosphorylation (Yamaki et al., 2004). The potential phosphorylation of Sim1, particularly as a mechanism by which signal transduction and transcriptional regulation is controlled, has not been studied. Protein phosphorylation of transcription factors can modulate nuclear translocation, DNA binding activity, protein stability, and protein-protein interactions including interactions with transcriptional co-activators. A number of bHLH-PAS proteins – including CLOCK, hPER2, BMAL, ARNT and HIF2-α – are known to undergo serine/threonine phosphorylation, which has been shown to modulate their activity and in some cases their nuclear localization (Conrad et al., 1999; Long et al., 1999; Lee et al., 2001; Toh et al., 2001; Kondratov et al., 2003; Kewley and Whitelaw, 2005; To et al., 2006).

Mouse *Sim1* is required for terminal migration and differentiation of the neurons of the PVN, as well as supraoptic (SON) and anterior periventricular (aPV) nuclei of the hypothalamus (Michaud et al., 1998), which produce the neuropeptides Avp, Oxt, Crh, Trh, and Sst. *Sim1* is prominently expressed in PVN neuronal progenitor cells where it heterodimerizes with its partner Arnt2 (Michaud et al., 2000). The direct transcriptional targets of Sim1/Arnt2 are not known, although several plexin genes that guide neuronal migration are directly or indirectly regulated by *Sim1* (Xu and Fan, 2007). Based on overlapping phenotypes and epistasis relationships of knockout mice, *Sim1* is thought to

act in parallel with the transcription factor Otp to maintain expression of another transcription factor, Pou3f2 (Brn2), which then controls the differentiation of Oxt, Avp, and Crh neurons in the PVN (Michaud et al., 1998; Acampora et al., 1999; Michaud et al., 2000; Wang and Lufkin, 2000; Hosoya et al., 2001). *Sim1* is part of an evolutionarily conserved developmental pathway: zebrafish *Sim1* is required for development of neurons that produce isotocin, the fish homolog of Oxt (Eaton and Glasgow, 2006). Recent data have shown that *Sim1* is not required for survival of PVN progenitor neurons as previously thought, at least up until birth, but is essential for proper migration (Xu and Fan, 2007). *Sim1* expression is detectable in the developing mouse hypothalamus as early as embryonic day e10.5 (Fan et al., 1996). Expression of *Sim1* precedes and is required for expression of the previously mentioned PVN neuropeptides (Michaud et al., 1998). It is not known if *Sim1* is also required for postnatal development of PVN neuronal projections. In adults, *Sim1* is expressed in the PVN and SON as well as in the basomedial amygdala (Holder et al., 2004), where it may regulate gene expression. Precedent for dual action of developmental transcription factors comes from POU domain proteins involved in the formation of anterior pituitary cells and subsequent production of growth hormone, prolactin, and thyroid stimulating hormone (Holder et al., 2000; Burbach, 2002).

We described a girl with severe early onset hyperphagic obesity (Figure I.6), accelerated linear growth, and a balanced chromosome translocation (Figure I.7) that disrupted one allele of *SIM1* (Holder et al., 2000). We hypothesized that half-normal dosage, or haploinsufficiency, of *SIM1* was responsible for her obesity phenotype, which closely resembles that of patients with *MC4R* mutations (Farooqi et al., 2003). Consistent

with this hypothesis, a number of patients have been reported with Prader-Willi-like phenotypes and visible chromosome deletions encompassing *SIM1* (Villa et al., 1995; Gilhuis et al., 2000; Faivre et al., 2002; Varela et al., 2006). No clear-cut *SIM1* loss of function point mutations have been identified in any severely obese human (Hung et al., 2007). However, in a recent candidate obesity gene study, nonsynonymous *SIM1* sequence variants were seen in 6/379 obese adults vs. 0/378 lean controls (Ahituv et al., 2007), similar to the frequencies of nonsynonymous *MC4R* mutations (8 in obese group vs. 2 in lean group), mutations of which are the most common monogenic cause of early onset morbid obesity (Farooqi et al., 2003). It was also recently reported that Pima Indians have a common variation in *SIM1* that is associated with a higher BMI (Traurig et al., 2009).

Prior to these studies and lacking any clear-cut human loss of function *SIM1* point mutations, confirmation of the gene's role in obesity came from mouse models. *Sim1* heterozygous knockout ($Sim1^{+/-}$) mice show hyperphagic obesity and increased linear growth (Michaud et al., 2001; Holder et al., 2004). Both the girl with the (heterozygous) translocation and $Sim1^{+/-}$ mice showed normal energy expenditure (Holder et al., 2000; Michaud et al., 2001; Kublaoui et al., 2006a). Furthermore, $Sim1^{+/-}$ mice have increased susceptibility to high fat (HF) diet-induced obesity (DIO) due to exacerbation of their hyperphagia (Holder et al., 2004). Based on the similar human and mouse phenotypes associated with loss of function mutations of *SIM1* or *MC4R* and expression of both genes in the PVN, we hypothesized that normal *Sim1* dosage is required for proper hypothalamic Mc4r signaling (Holder et al., 2000; Holder et al., 2004). We subsequently confirmed that *Sim1* haploinsufficiency impairs melanocortin

agonist-induced activation of PVN neurons in the *Sim1*$^{+/-}$ mouse model (Kublaoui et al., 2006a). Hypothalamic *Mc4r* RNA level was not different in *Sim1*$^{+/-}$ vs. *Sim1*$^{+/+}$ mice (Holder et al., 2004), but expression specifically in the PVN was not measured and correct interpretation of the results may be confounded by the fact that *Mc4r* is expressed in multiple areas in the hypothalamus. The best evidence that *Mc4r* acts directly in *Sim1* neurons comes from the previously mentioned studies by Brad Lowell, Joel Elmquist, and colleagues (Balthasar et al., 2005). They developed mice with an inactivated *Mc4r* allele that can be conditionally reactivated by Cre recombinase, as well as BAC transgenic mice expressing Cre recombinase under the control of *Sim1* regulatory sequences. Using these mice, they showed that selective expression of *Mc4r* in *Sim1* neurons in the PVN and amygdala rescued the hyperphagia but not the reduced energy expenditure phenotype of *Mc4r*$^{-/-}$ mice. This result was surprising and unexpected, as neuroanatomic studies suggested that PVN neurons, which send direct projections to sympathetic preganglionic neurons in the spinal cord (Saper et al., 1976; Swanson and Kuypers, 1980), would regulate energy expenditure. However, their finding was consistent with the normal energy expenditure of *Sim1*$^{+/-}$ mice (Michaud et al., 2001; Kublaoui et al., 2006a), as well as our finding that *SIM1* transgenic overexpression reduced food intake but did not change energy expenditure in DIO and *A*^{y} mouse models (Kublaoui et al., 2006b). Recently, we showed that hypothalamic expression of *Oxt* is severely reduced and expression of other PVN neuropeptides (*Crh, Trh, Avp, Sst*) moderately reduced in *Sim1*$^{+/-}$ mice (Kublaoui et al., 2008). These mice are hypersensitive to the orexigenic effect of an Oxt receptor antagonist administered centrally. In addition, central administration of Oxt partially rescued the hyperphagia and

reduced the weight gain of *Sim1*$^{+/-}$ mice at a dose that did not affect wild-type mice. These data suggest that reduced Oxt neuropeptide is one mechanism mediating the hyperphagic obesity of *Sim1*$^{+/-}$ mice.

A key question is whether the mechanism of hyperphagic obesity in *Sim1*$^{+/-}$ mice involves either a fixed developmental defect or a post-developmental, physiologic role of *Sim1* in feeding regulation, possibly through regulation of *Mc4r* expression, or a combination of the two. *Sim1* homozygous knockout (*Sim1*$^{-/-}$) mice lack the PVN entirely (Michaud et al., 1998). Since anatomic PVN lesions result in hyperphagic obesity (Leibowitz et al., 1981), a simple hypothesis to explain the phenotype of *Sim1*$^{+/-}$ mice is that they have a reduced number of PVN neurons compared to *Sim1*$^{+/+}$ (wild type) mice. Michaud et al. (Michaud et al., 2001) reported that *Sim1*$^{+/-}$ mice have a 24% mean reduction in the number of PVN neurons compared to controls, with no specific subtype affected. They concluded that the defect was developmental and that *Sim1*$^{+/-}$ mice have a "congenital PVN lesion". However, this conclusion is not consistent with a previous study showing that bilateral PVN lesions in weanling rats (as opposed to adults) did not cause hyperphagic obesity (Bernardis, 1984), suggesting that developmental plasticity can compensate for even severe PVN lesions early in life. We re-examined the PVN cell number of *Sim1*$^{+/-}$ mice using a *Sim1*-GFP BAC transgene to mark *Sim1* neurons and found no difference in relative GFP-positive PVN cell counts in *Sim1*$^{+/-}$ versus *Sim1*$^{+/+}$ mice (Kublaoui et al., 2006a). However, the studies of Michaud et al. (Michaud et al., 2001) and Kublaoui et al. (Kublaoui et al., 2006a) were not done using unbiased stereologic cell counting and therefore neither may be regarded as conclusive. To further test whether *Sim1* functions physiologically as well as developmentally, we generated

BAC transgenic mice overexpressing human *SIM1* (Kublaoui et al., 2006b). The PVN of these transgenic mice was histologically normal. The mice grew normally on a chow diet, ruling out a nonspecific growth-stunting effect, but were resistant to high fat diet-induced hyperphagia and obesity compared to nontransgenic littermates. Furthermore, the transgene partially suppressed the hyperphagia and obesity of Agouti yellow (A^y) mice, a model in which hypothalamic melanocortin signaling is abrogated by ectopic expression of Agouti, an extra-hypothalamic analogue of Agrp. These results supported a physiologic role for *Sim1* in feeding regulation and suggest that *Sim1* acts downstream of Mc4r signaling. Yang et al. (Yang et al., 2006) reported further evidence that hypothalamic *Sim1* physiologically regulates feeding in adult mice. They acutely modulated *Sim1* expression in the PVN of adult mice by stereotaxic injection of adenoviral constructs expressing either a *Sim1* cDNA or a *Sim1* siRNA. Overexpression of *Sim1* in the PVN reduced food intake by a peak of 20% seven days after injection, whereas siRNA inhibition of *Sim1* PVN expression increased food intake by a peak of 22% six days after injection.

Oxytocin and feeding

There are conflicting data regarding the role of Oxt in satiety. Neuroanatomic and pharmacologic studies have characterized a subset of parvocellular PVN Oxt neurons that respond to leptin and project to the NTS (Kirchgessner et al., 1988; Blevins et al., 2004). Oxt has been shown to modulate feeding behavior in rats (Arletti et al., 1989; Olson et al., 1991b), and third ventricular injection of an Oxt antagonist in mice attenuated the effect of leptin on food intake (Blevins et al., 2004). However, wild-type

and *Oxt*$^{-/-}$ mice ingest similar amounts of standard chow under ad libitum baseline conditions, after overnight food deprivation when drinking water is available, and after systemic administration of either CCK or D-fenfluramine (Mantella et al., 2003; Rinaman et al., 2005). On the other hand, *Oxt*$^{-/-}$ mice display an increased intake of both sweet and non-sweet carbohydrate solutions (Sclafani et al., 2007). Oxt receptor deficient mice have been generated but no characterization of their food intake or body weight has been published (Takayanagi et al., 2005). These data could suggest that Oxt marks the identity of neurons projecting from the PVN to the NTS but is not itself critical for their action in meal termination, which could be mediated by classical neurotransmitters such as GABA or glutamate. Alternatively, Oxt may be an important physiologic regulator of feeding in normal mice, but there could be developmental mechanisms that compensate for its absence in *Oxt*$^{-/-}$ mice. Functional and developmental compensation by hypothalamic neurons has been demonstrated, most notably in *Npy/Agrp* neurons. Despite compelling pharmacological evidence for a prominent role for these two peptides in energy homeostasis, mice deficient in *Npy*, *Agrp*, or both have no demonstrable feeding phenotype (Qian et al., 2002). Conversely, partial ablation of *Npy/Agrp* neurons postnatally leads to the expected lean phenotype, and complete ablation in adulthood leads to starvation (Qian et al., 2002; Beuckmann et al., 2004; Bewick et al., 2005; Gropp et al., 2005; Luquet et al., 2005). Developmental compensation by these neurons appears to take place postnatally because neonatal ablation had minimal effects on body weight or feeding regulation (Luquet et al., 2005). Another possible explanation may be species differences in Oxt action between mice as rats. Taken together, available data suggest the following pathway involved in the regulation of feeding: the adiposity signal (leptin) is

sensed in the ARC, transmitted to the PVN and LHA by the melanocortin system (Pomc/α-MSH/Mc4r), and relayed by parvocellular *Oxt* neurons (although perhaps not via Oxt itself) to the NTS to modulate satiety. Certainly this is an oversimplification and other CNS pathways are involved; for instance, there is considerable evidence that leptin acts via distributed pathways throughout the CNS to regulate feeding (Balthasar, 2006; Dhillon et al., 2006; Farooqi et al., 2007). However, the data suggest that this pathway could be a key pathway controlling food intake. Interestingly, postmortem brains of patients with Prader-Willi syndrome, a well known human genetic disorder characterized by severe hyperphagia, show reduced numbers of PVN parvocellular Oxt neurons, consistent with a role for these neurons in human satiety (Swaab et al., 1995).

Significance

Sim1 encodes a hypothalamic transcription factor that has been shown to be involved in both human and mouse obesity. Previous work has implicated defective hypothalamic melanocortin and oxytocinergic signaling in the pathophysiology of hyperphagic obesity in *Sim1* mutant mice. There is a compelling need for selective and efficient treatments for the obesity epidemic: possible targets of these therapeutics are the second order neurons and the networks that specifically affect food intake and energy expenditure. If a physiologic function of *Sim1* is confirmed, then *Sim1* and its transcriptional targets become candidates for novel pharmacologic approaches to modulate food intake and treat obesity and identifying the transcriptional targets of Sim1 and defining the molecular link between *Sim1* dosage, Mc4r signaling, and PVN neuropeptide expression would be extremely significant.

In this dissertation, I will describe our studies using mouse model systems to investigate and understand the role of hypothalamic *Sim1* in regulating food intake. These experiments test the hypothesis that *Sim1* acts physiologically to regulate food intake, and help elucidate its function in hypothalamic development and hyperphagic obesity.

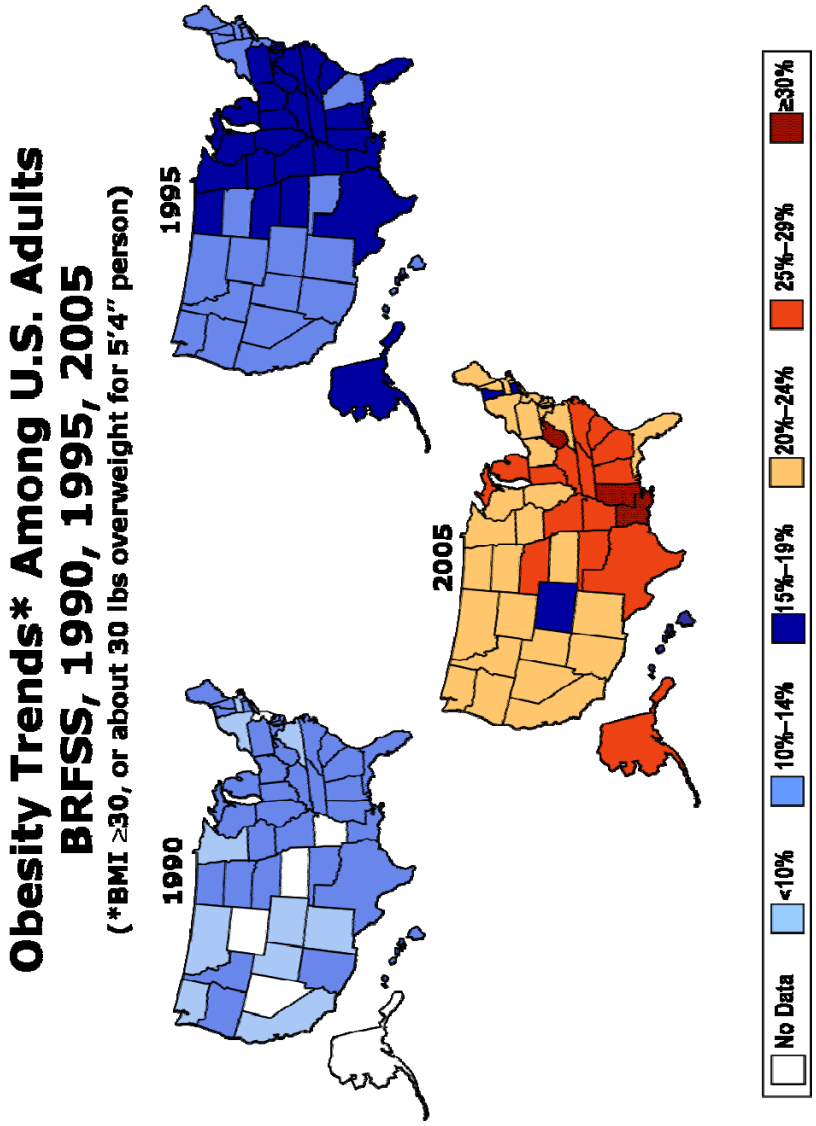

Figure I.1 Obesity trends in the U.S. as reported by the CDC. Obesity in adults in the U.S. in 1990, 1995 and 2005, reported as percentages per state. From the CDC's Behavioral Risk Factor Surveillance System (BRFSS).

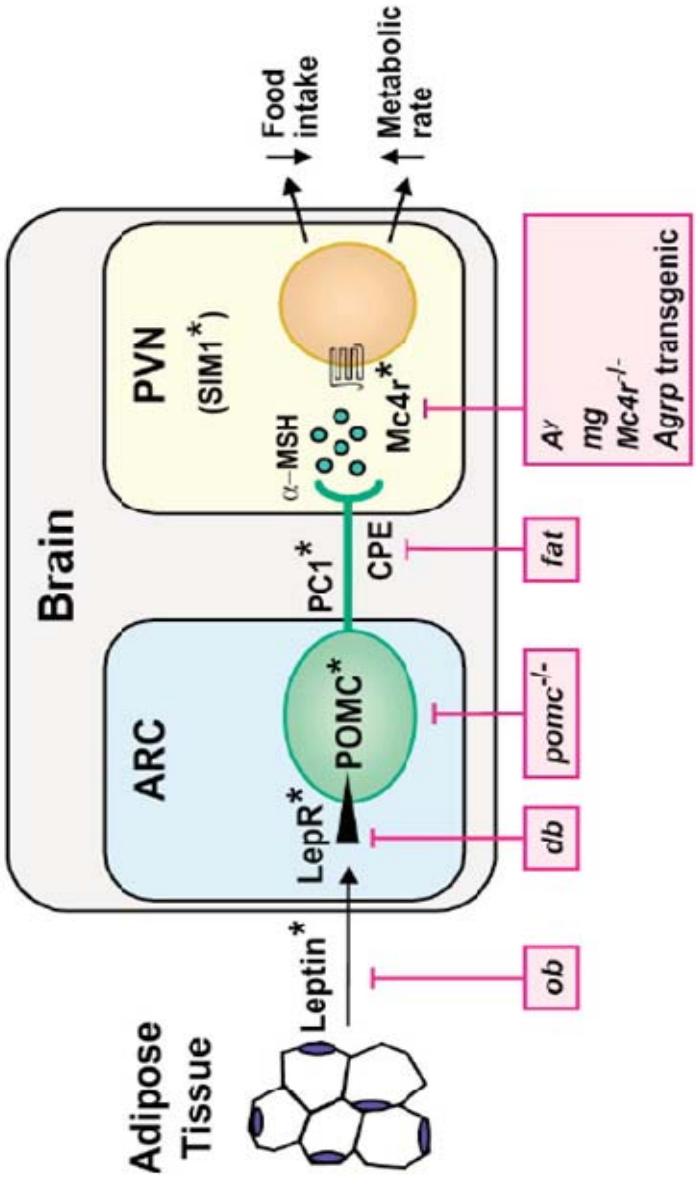

Figure I.2 Known causes of monogenic obesity. Genes which, when mutated, cause severe early onset obesity. Mutations in humans indicated by asterisks, mutants in mice shown in pink. ARC, hypothalamic arcuate nucleus; POMC, proopiomelanocortin; PC1, prohormone convertase 1; CPE, carboxypeptidase E; PVN, paraventricular nucleus; Mc4r, melanocortin-4 receptors. From (Cummings and Schwartz, 2003).

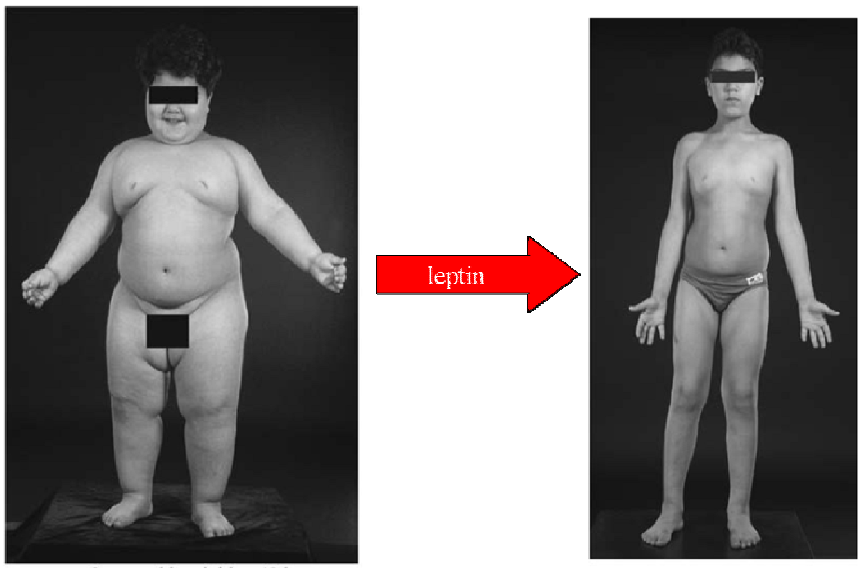

Figure I.3 Effects of leptin therapy in leptin deficiency. Clinical response in a 3-year-old boy with congenital leptin deficiency. Modified from (Farooqi and O'Rahilly, 2005).

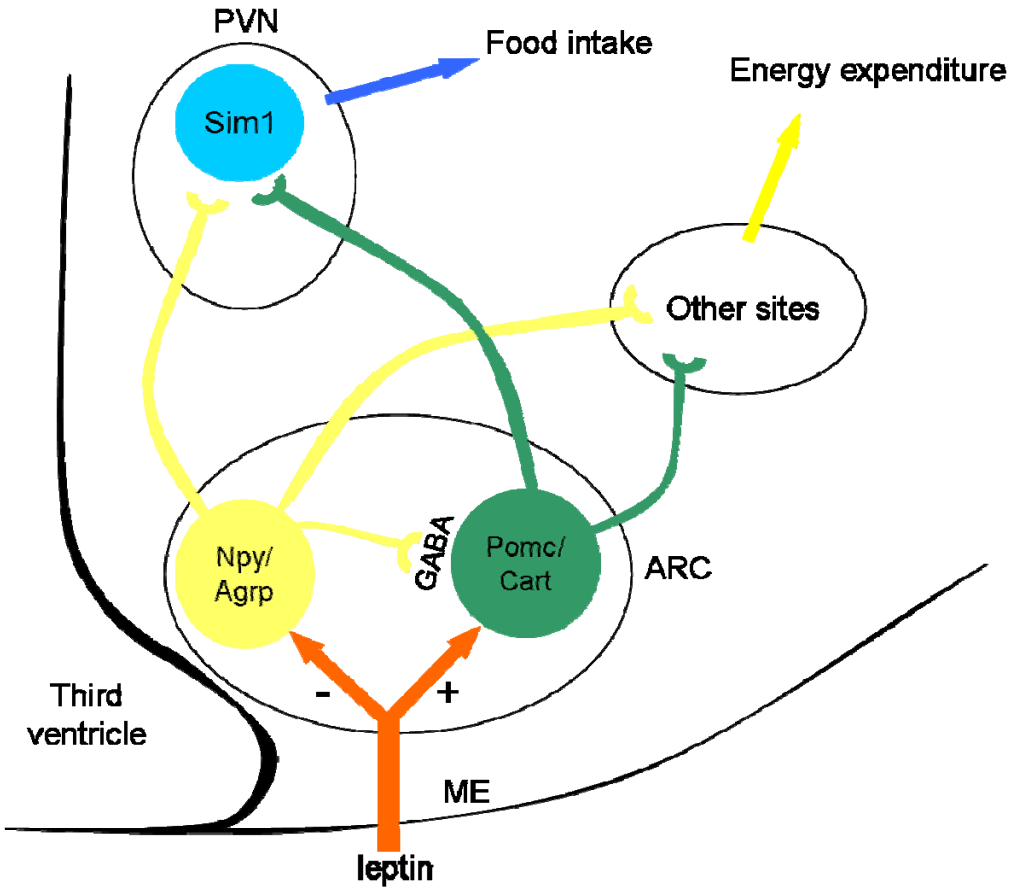

Figure I.4 Simplified schematic of hypothalamic pathways regulating food intake. Leptin enters the arcuate nucleus (ARC) via the median eminence (ME), where it inhibits *Npy/Agrp* neurons and stimulates *Pomc* neurons. *Npy/Agrp* neurons directly and indirectly inhibit *Pomc* neurons, through GABA release on *Pomc* neurons and Agrp antagonizing the Mc4r. These neurons project to multiple sites to regulate food intake and energy expenditure.

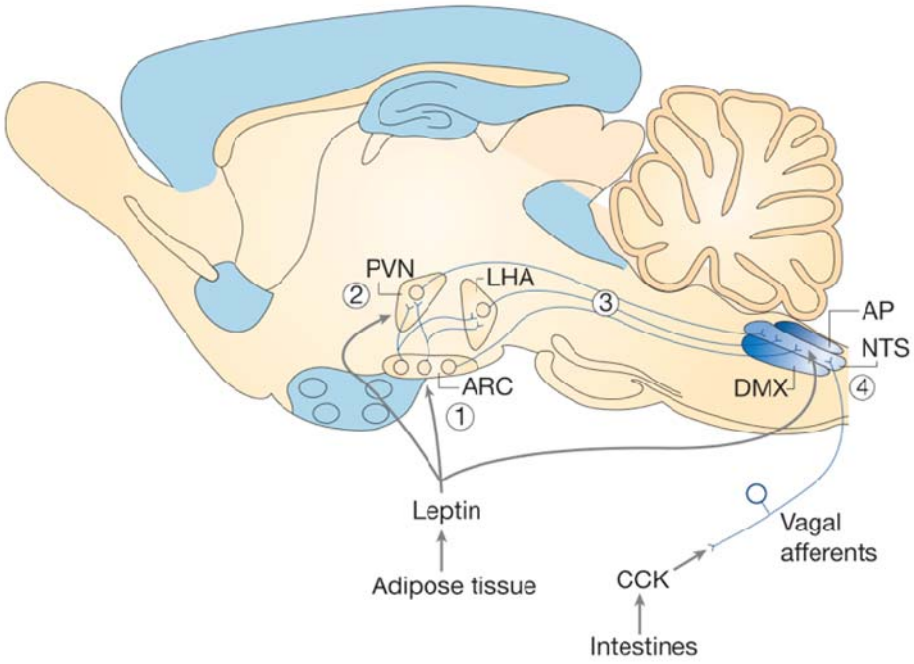

Figure I.5 Pathways from hypothalamus to hindbrain integrating adiposity (leptin) and satiety (CCK) signals. The hypothalamus is a key target for leptin action, whereas the satiety effect of CCK involves activation of vagal afferent fibers that terminate in the NTS. Integration of these inputs can involve the actions of leptin in the ARC (1) or other hypothalamic areas (2) involving neurons that project to the NTS (3) and influence the response to CCK (4). In addition, leptin can act directly in the NTS. AP, area postrema; DMX, dorsal motor nucleus of the vagus nerve; LHA, lateral hypothalamic area; NTS, nucleus of the solitary tract; PVN, paraventricular nucleus. From (Morton et al., 2006).

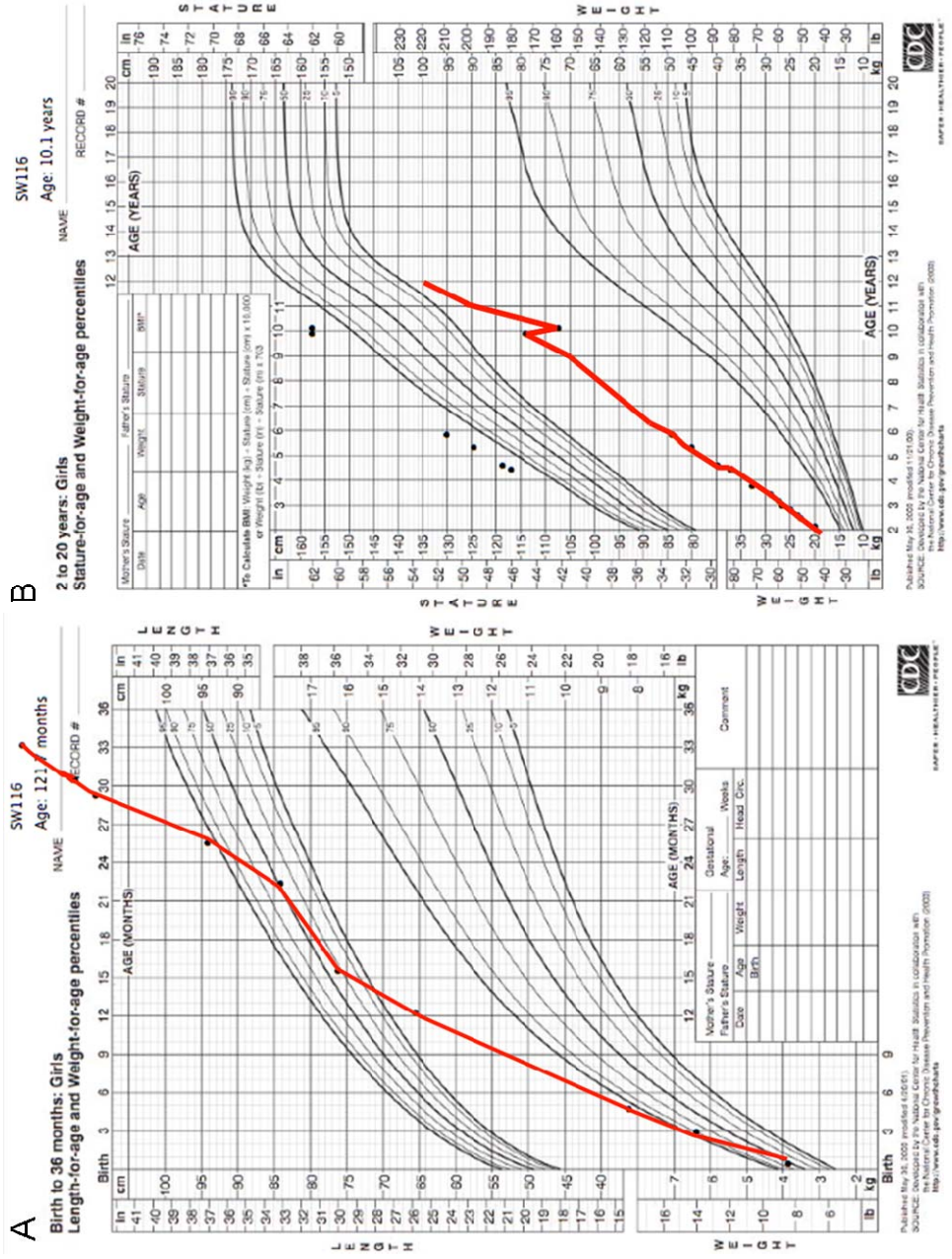

Figure I.6 Growth curves of SW116. ***A***, Weight from birth to 36 months. ***B***, Weight from 2 to 12 years.

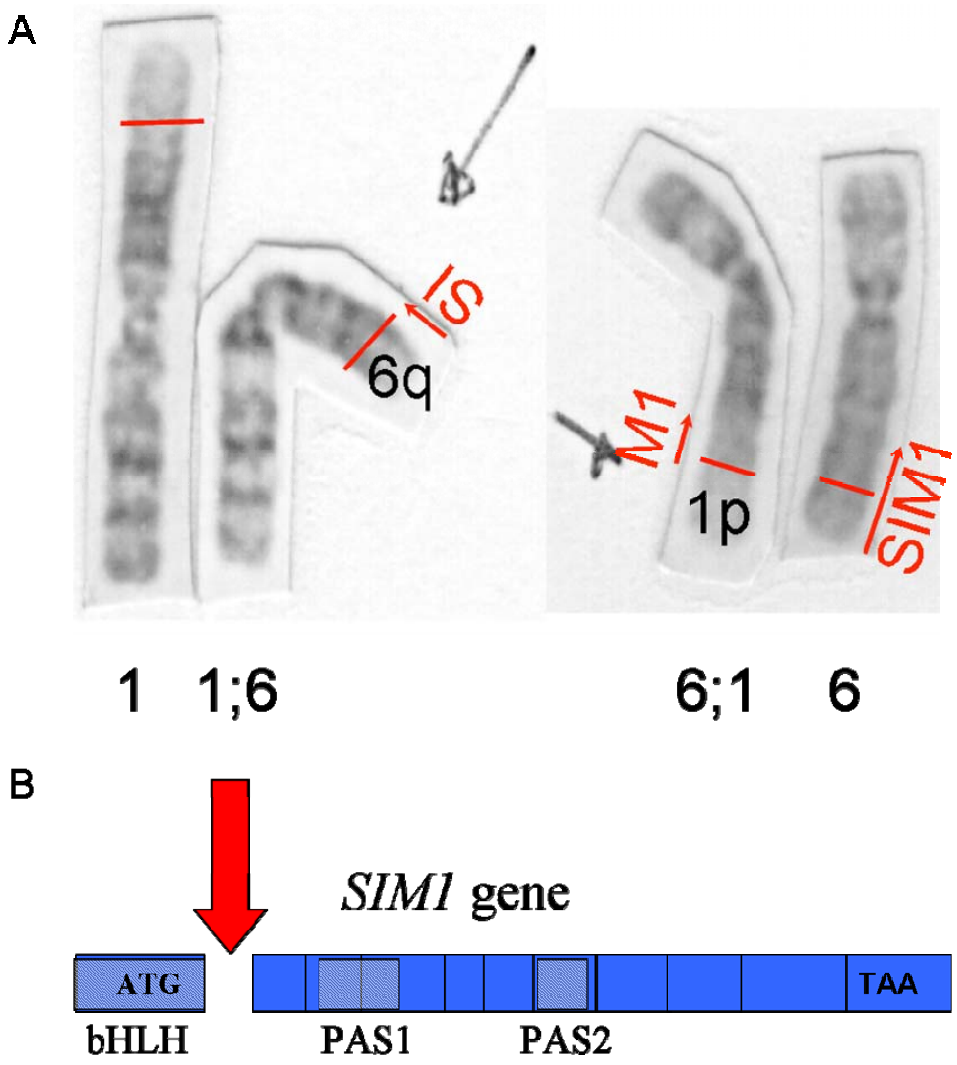

Figure I.7 The balanced translocation in proband SW116. A, partial karyotype of SW116 showing balanced translocation. B, Schematic showing that the breakpoint interrupted *SIM1* and separated the start codon and bHLH domain from the rest of the gene. Modified from (Holder et al., 2000).

Chapter II

Overexpression of *SIM1* in mice

INTRODUCTION

Single-minded 1 (*SIM1*), which encodes a member of the bHLH-PAS (basic helix-loop-helix Per Arnt Sim) family of nuclear transcription factors (Emmons et al., 1999), is one of six genes associated with human monogenic obesity (Farooqi and O'Rahilly, 2005). *SIM1* was first implicated in body weight regulation by a balanced translocation that disrupted the gene in a girl with early-onset obesity, hyperphagia, and accelerated linear growth (Holder et al., 2000). Visible deletions of the region of chromosome 6 containing *SIM1* have also been associated with early-onset obesity in boys and girls (Turleau et al., 1988; Villa et al., 1995; Gilhuis et al., 2000; Faivre et al., 2002). Heterozygous disruption of the murine *Sim1* gene leads to an analogous phenotype of hyperphagic obesity, increased linear growth, and enhanced sensitivity to diet-induced obesity (DIO) (Michaud et al., 2001; Holder et al., 2004). Homozygous mutant mice die shortly after birth and exhibit failure of terminal differentiation of the neurons of the paraventricular (PVN) and supraoptic nuclei of the hypothalamus (Michaud et al., 1998). In adult mice the *Sim1* gene is expressed in the PVN and supraoptic nuclei as well as the basomedial amygdala and a subset of lateral hypothalamic neurons (Holder et al., 2004).

The phenotype of *Sim1* heterozygous mice is similar to that of melanocortin 4 receptor (*Mc4r*) knockout mice (Huszar et al., 1997), and the girl with heterozygous *SIM1* disruption (Holder et al., 2000) clinically resembles children with heterozygous *MC4R* mutations (Vaisse et al., 1998; Yeo et al., 1998). The triad of hyperphagic obesity, increased linear growth, and enhanced DIO sensitivity is also seen in other mouse mutations, including Agouti yellow (A^{y}) (Miller et al., 1993; Lu et al., 1994), brain-derived neurotrophic factor (*Bdnf*) conditional knockout (Rios et al., 2001), and

hypomorphic alleles of *TrkB*, the Bdnf receptor (Xu et al., 2003). Impaired hypothalamic melanocortin signaling is proposed to underlie this phenotype in all of these models (Wisse and Schwartz, 2003), leading us to hypothesize a similar signaling defect in humans or mice with *Sim1* haploinsufficiency (Holder et al., 2000; Holder et al., 2004). Although coexpression of *Mc4r* and *Sim1* within hypothalamic neurons has not been directly demonstrated, expression of *Mc4r* specifically in *Sim1* neurons of the PVN and amygdala completely rescued the hyperphagia of *Mc4r* null mice (Balthasar et al., 2005), further supporting a cellular interaction between *Sim1* and *Mc4r* in appetite regulation.

Two mechanisms have been proposed for this interaction. *Sim1* heterozygotes may have a developmental defect leading to reduced numbers of PVN neurons, including Mc4r neurons (Michaud et al., 2001). Alternatively, adult *Sim1* heterozygotes may have abnormal transcriptional regulation of target genes impinging on the Mc4r signaling pathway (Holder et al., 2004). The *in vivo* transcriptional targets of Sim1 are not known, but *Mc4r* does not appear to be directly regulated by Sim1 because hypothalamic *Mc4r* expression was not reduced in *Sim1* heterozygotes (Holder et al., 2004). Experiments testing proposed mechanisms of interaction between Sim1 and Mc4r using *Sim1* loss-of-function mutations are confounded by the absence of mature PVN neurons in *Sim1* homozygous knockout mice. As an alternative means to test whether Sim1 modulates Mc4r signaling in adult mice, we overexpressed *Sim1* via BAC transgenesis. We show that the transgene conferred resistance to DIO and also rescued the hyperphagia of A^y mice, in which melanocortin signaling is abrogated. Our findings support a postdevelopmental, physiologic role for *Sim1* in feeding regulation.

RESULTS

Generation of SIM1 transgenic mice

A human *SIM1* BAC transgene was used to distinguish its expression from that of the endogenous mouse *Sim1* gene. The amino acid sequences of human *SIM1* and mouse *Sim1* proteins are 96% identical (Chrast et al., 1997). The BAC clone contains the *SIM1* transcription unit and 65 kb of 5'- and 58 kb of 3'- flanking sequences (Figure II.1A). The 5' end of the insert contains part of an RNA helicase gene whose pattern of expression is different from *SIM1*, suggesting that all *SIM1* 5' regulatory sequences are present within the BAC. Two transgenic lines were obtained, a high copy number line (HSTG18) and a low copy number line (HSTG26) (Figure II.1, B and C). Human *SIM1* mRNA was quantitated in the hypothalamus by real-time PCR using primers with identical binding sites in human *SIM1* and mouse *Sim1* transcripts (Figure II.1D). The HSTG18 line displayed approximately 35-fold expression and the HSTG26 line displayed 2.5-fold expression of the human *SIM1* mRNA relative to the mouse *Sim1* mRNA. These measurements were corroborated by direct sequencing of RT-PCR products (data not shown). Despite abundant hypothalamic *SIM1* expression, HSTG18 mice had no visible phenotype (Figure II.1E) and normal PVN histology (Figure II.1, F and G).

Growth and feeding behavior of SIM1 transgenic mice

Three-week-old mice were weaned onto chow containing 4% [low fat (LF)] or 35% [high fat (HF)] dietary fat, allowed to feed *ad libitum*, and weighed weekly (Figure II.2, A–D). Growth of transgenic and wild-type mice on the LF diet was indistinguishable. By

contrast, transgenic mice gained considerably less weight on the HF diet than their wild-type littermates. The high-expressing HSTG18 mice (Figure II.2, A and B) were more resistant to DIO than the low-expressing HSTG26 mice (Figure II.2, C and D). The transgenes had similar effects on males and females.

Subsequent studies used the high-expressing HSTG18 line. We measured weekly food intake of male HSTG18 mice and wild-type littermates on LF and HF diets (Figure II.3, A–D). On LF, weekly food intake differed significantly between transgenic and wild-type mice at only five time points, and cumulative food intake did not differ significantly at any time point, although there was a trend toward decreased food intake in the transgenic mice. On HF, *SIM1* transgenic mice ate significantly less than their wild-type littermates at almost every time point after 5–6 weeks of age, reflected by both weekly and cumulative food intake measures.

Energy expenditure, activity, and body composition of SIM1 transgenic mice

To determine whether resistance to DIO in *SIM1* transgenic mice was due solely to decreased food intake, we measured energy expenditure, locomotor activity, and feeding efficiency in transgenic mice and wild-type littermates on LF and HF diets (Figure II.4, A–F). Regardless of diet, *SIM1* transgenic mice exhibited normal energy expenditure and locomotor activity in both the light and dark cycles. *SIM1* transgenic mice also exhibited normal feeding efficiency. Regardless of diet, the oxygen consumption rate, carbon dioxide production rate, and respiratory quotients of transgenic mice were the same as wild-type littermates (data not shown). In both wild-type and transgenic mice, the respiratory quotient was appropriately lower in mice fed a HF diet (data not shown).

Body composition of *SIM1* transgenic mice on LF was no different from that of wild-type littermates (data not shown). On HF, *SIM1* transgenic mice had significantly less fat mass than wild-type littermates (15.3 vs. 18.9%, $P < 0.01$).

Pomc regulation by HF in SIM1 transgenic mice

Pomc expression in the hypothalamus is induced after switching mice from a LF to a HF diet and has been proposed to be part of the physiologic hypophagic response (Ziotopoulou et al., 2000). Because reduced *Sim1* dosage impairs this response (Holder et al., 2004), we asked whether overexpression of *SIM1* affects hypothalamic *Pomc* induction by HF. Figure II.5A shows that in contrast to wild-type mice, *Pomc* was not induced by HF in *SIM1* transgenic mice. *Npy* and *Agrp* mRNA levels did not show any significant changes in response to the HF diet and did not differ significantly between wild-type and transgenic mice (Figure II.5, B and C).

Effect of SIM1 transgene on A^y obesity

Given that *Sim1* is expressed in Mc4r PVN neurons (Balthasar et al., 2005) and *Sim1* heterozygous mice are resistant to the anorectic effects of hypothalamic melanocortin signaling (Kublaoui et al., 2006a), we asked whether overexpression of *SIM1* would rescue the phenotype of A^y mice. Figure II.6 shows that the *SIM1* transgene partially rescued A^y obesity. The effect was more prominent in females than males. To investigate the mechanism of the partial rescue of A^y obesity by the *SIM1* transgene, food intake and feeding efficiency were measured in A^y mice and littermates that carry the *SIM1* transgene (Figure II.6, E–H). The transgene completely normalized food intake of A^y

mice but had no effect on feeding efficiency. Body composition analysis revealed that A^y/*SIM1* transgenic mice had reduced fat mass, compared with A^y mice. Fat mass was reduced by 17% in females and 19% in males. Lean mass was also slightly reduced in females (4%) but not males (Figure II.7).

DISCUSSION

The phenotype of *Sim1* haploinsufficiency is strikingly similar to that of *Mc4r* knockout mice, and both genes are expressed within the PVN, lateral hypothalamus, and amygdala. *Sim1* is necessary during fetal development for normal terminal differentiation of PVN neurons but continues to be expressed in the PVN, amygdala, and lateral hypothalamus in adult mice, suggesting that it may also function physiologically in energy homeostasis. To test this hypothesis, we generated *SIM1* BAC transgenic mice and asked whether overexpression of *SIM1* leads to either a lean phenotype or resistance to DIO, opposite to the phenotype of reduced *Sim1* expression. We used a human *SIM1* BAC clone to differentiate it from the mouse gene. Human and mouse Sim1 proteins are 96% identical in amino acid sequence. The BAC we chose includes extensive 5'- and 3'-flanking sequences and showed a copy number-dependent hypothalamic expression level, suggesting that it contains all the necessary regulatory elements to drive appropriate *SIM1* expression. Furthermore, the BAC insert spans a genomic region similar to that of a mouse BAC that drives enhanced green fluorescent protein expression (Gong et al., 2003) with the same pattern as the endogenous *Sim1* gene (Fan et al., 1996; Ziotopoulou et al., 2000). Two transgenic lines were generated, a high expresser and a low expresser. Neither line had a weight phenotype on a LF chow diet. Whereas it might seem surprising

for overexpression of a developmental transcription factor to have only subtle phenotypic effects, SIM1 acts as a heterodimer, and its dimerization partner, ARNT2 (aryl hydrocarbon receptor nuclear translocator-2) in the hypothalamus (Michaud et al., 2000), may be limiting in the transgenic mice. Alternatively, there could be translational regulation of the *SIM1* transcript. No suitable SIM1 antibody is presently available to test this possibility.

Although neither transgenic line showed any body weight phenotype on a chow diet, we previously showed that *Sim1* heterozygous mice have enhanced susceptibility to DIO (Holder et al., 2004). Consequently we examined the effect of the transgene on weight gain of animals fed a HF diet. The high-expressing line of mice was resistant to DIO, whereas the low-expressing line showed a similar trend that did not reach statistical significance, probably due to inter-animal variability. These data suggest a dose-dependent action of *SIM1* on feeding behavior. We examined the mechanism of DIO resistance in the high-expressing line. These mice ate significantly less of the HF diet than their wild-type littermates but showed no difference in basal metabolic rate or total energy expenditure. Additionally, *Sim1* heterozygous mice are hyperphagic but have normal energy expenditure (Michaud et al., 2001; Kublaoui et al., 2006a). Our results are consistent with the findings of Balthasar *et al.* (Balthasar et al., 2005), who showed that *Mc4r*- and *Sim1*-expressing neurons in the PVN or amygdala function solely in the control of food intake, with energy expenditure being regulated by Mc4r neurons elsewhere in the brain. The fact that *SIM1*-overexpressing mice on a LF diet are not lean may be due to redundant mechanisms that defend normal body weight.

Overexpression of *SIM1* partially rescued the obesity of the A^y mouse, suggesting that Sim1 acts downstream of Mc4r. There is also direct evidence from the *Sim1* heterozygous mouse that Sim1 functions downstream of the MC4R (Kublaoui et al., 2006a). The fact that the transgene completely rescued the hyperphagia of A^y mice but had no effect on their feeding efficiency and only partially rescued their body weight suggests that it has little or no effect on their energy expenditure, which is known to be reduced (Yen et al., 1983; Yen et al., 1984; Yen et al., 1994). This inference is also consistent with the model that Mc4r PVN neurons act specifically in feeding regulation (Balthasar et al., 2005; Kublaoui et al., 2006a) and with the findings of normal energy expenditure in both *Sim1* heterozygous mice (Michaud et al., 2001; Kublaoui et al., 2006a) and *SIM1* transgenic mice.

Short-term exposure to the HF diet induced hypothalamic *Pomc* expression in wild-type but not *SIM1* transgenic mice. The mechanism of this induction is not clear, but it may be part of the physiologic response to dietary fat (Ziotopoulou et al., 2000), whereby the increased caloric density of the HF diet leads to increased *Pomc* expression causing a compensatory reduction in food intake. The lack of *Pomc* induction by the HF diet in the transgenic mice may reflect an already maximal activation of Mc4r signaling and negative feedback on *Pomc* expression. The mechanism of feedback is unclear but could involve projections from the PVN to the arcuate nucleus (Cummings and Schwartz, 2003). The lack of change in *Npy* or *Agrp* expression argues against a leptin-mediated effect.

The increased weight of *Sim1* heterozygotes is due mostly to increased fat mass (Holder et al., 2004). However, they also exhibit increased lean mass and increased

length. The *SIM1* transgenic mice on HF had decreased fat as well as lean mass, compared with wild-type littermates. A^y and $Mc4r^{-/-}$ mice are also longer than littermates (Wolff, 1963; Huszar et al., 1997; Martin et al., 2006). The mechanism of the changes in lean mass in any of these models is unknown.

Sim1 has been implicated in the regulation of food intake in the homeostatic response to dietary fat (Holder et al., 2004). Reduction and increase in *Sim1* dosage have opposite effects on body weight regulation. Reduced gene dosage leads to increased sensitivity to DIO, and increased gene dosage leads to resistance, with higher *SIM1* expression correlated with greater resistance. The molecular mechanisms underlying this *Sim1* dosage effect are unclear. The most parsimonious explanation for the phenotype of *SIM1* overexpression is that in addition to its developmental role, *Sim1* has a physiologic function in energy homeostasis. Taken together with our previous work and the work of Balthasar *et al.* (Balthasar et al., 2005), we propose that Sim1 acts downstream of Mc4r within PVN neurons to regulate food intake. Identification of relevant Sim1 transcriptional targets in hypothalamic melanocortin neurons is needed to elucidate the molecular mechanism of its effect on feeding regulation.

METHODS

Animals

Unless otherwise stated, C57BL/6 mice from the National Cancer Institute, aged 6–9 weeks, were used. A^y mice were purchased from Jackson Laboratories (Bar Harbor, ME). Mice were fed *ad libitum* and kept on a 12-h light,12-h dark cycle (0700–1900 h light). All experimental protocols were approved by the University of Texas Southwestern

Institutional Animal Care and Use Committee and are in accord with accepted standards of humane animal care.

Generation of SIM1 transgenic mice

CsCl-purified supercoiled DNA from BAC clone RP11–621C20 was microinjected into C57BL/6 fertilized pronuclei. Three founders showed germline transmission of the transgene, and transgenic lines were established and maintained by backcrossing to C57BL/6 mice. *Sim1* transgenic mice were genotyped using PCR primers specific for the human *SIM1* gene, 5'-CAA TTG AGA CCT TAA GGG TGC T-3' and 5'-CTC ACA TCG GCC TCC TTC ACA-3'. All experiments used mice from N10 or later generations. RT-PCR with human-specific primers confirmed that the transgene was expressed in kidney and brain, like endogenous mouse *Sim1*. Two lines showed relatively low expression; one of these was not studied further.

Transgene copy number determination

*Bam*HI-digested mouse liver DNAs were hybridized with a 1:1 mixture of ^{32}P-radiolabeled human *SIM1* and mouse *Sim1* genomic fragments that detected bands of approximately 5 kb (mouse *Sim1*) and approximately 10 kb (human *SIM1*). Hybridization intensities were quantitated using a STORM phosphor imager (Amersham, Piscataway, NJ).

Real-time PCR

Real-time PCR was performed as previously described (Holder et al., 2004). Briefly, hypothalami from fresh brains were dissected with a block (David Kopf Instruments,

Tujunga, CA), using the following landmarks: posteriorly, posterior aspect of median eminence; anteriorly, 5 mm anterior to the median eminence; dorsally, the thalamus; laterally, medial to the dentate gyrus. Total RNA was extracted using Tripure reagent (Roche Applied Science, Indianapolis, IN). Quantitative real-time PCR was performed using an MJ Research Opticon instrument (Bio-Rad, Hercules, CA) and the QuantiTect HotStart SYBR green qPCR kit (QIAGEN, Valencia, CA). Measurements were normalized to *β-actin* mRNA levels. Primers sequences were 5'-GCC CTC CTG CTT CAG ACC TC-3' and 5'-CGT TGC CAG GAA ACA CGG-3' (*Pomc*), 5'-CAG CAG AGG ACA TGG CCA GAT ACT AC-3' and 5'-GGG CGT TTT CTG TGC TTT CCT TCA TT-3' (*Npy*), 5'-TCC CAG AGT TCC CAG GTC TAA GTC-3' and 5'-GCG GTT CTG TGG ATC TAG CAC CTC-3' (*Agrp*), 5'-GAC GAT GCT CCC CGG GCT GTA TTC-3' and 5'-TCT CTT GCT CTG GGC CTC GTC ACC-3' (*β-actin*), 5'-GAG GCA GGC AGG TAC TT-3' and 5'-CTG ACC ACA CTA TCT TCA T-3' (human *SIM1* and mouse *Sim1*). All reactions were subjected to 40 cycles of amplification (denaturation at 94 C for 15 sec, annealing at 53 C for 30 sec, and extension at 72 C for 30 sec). Standard curves were generated using reference cDNA prepared from normal mouse hypothalamus and used to normalize measurements from experiment to experiment. All measurements were made in the exponential phase of the real-time PCR, as described by the manufacturer (Bio-Rad). Reactions were performed in triplicate and the results averaged. The coefficient of variation was less than 15% for each set of measurements.

Nissl staining

Mice were deeply anesthetized with pentobarbital (7.5mg per 0.15 ml, ip) and transcardially perfused with 10 ml heparinized saline (10 U/ml, 2 ml/min) followed by 10 ml phosphate-buffered 4% paraformaldehyde (2 ml/min). Brains were removed, postfixed for 24 h in 4% paraformaldehyde, and then equilibrated in 30% sucrose in PBS for 72 h. Brains were coronally sectioned (8 μm) on a cryostat. Sections containing the PVN were from bregma -0.58 to -1.22 mm according to *The Mouse Brain in Stereotaxic Coordinates* (Paxinos and Franklin, 2001). Sections were delipidated in 1:1 alcohol/chloroform overnight and then rehydrated through 100 and 95% alcohol to distilled water. Sections were stained in 0.1% cresyl violet solution for 3–5 min and rinsed in distilled water. They were then dehydrated through 95 and 100% ethanol for 3 minutes each and cleared with xylene for 3 minutes.

Growth and feeding studies

Mice were genotyped and weaned onto their respective diets at 3 weeks of age and fed *ad libitum* with either a low-fat diet (Teklad, Madison, WI; 2.94 kcal/g, with 46.8% available carbohydrate, 4.0% available fat, and 24.0% available protein) or a high-fat diet (Research Diets, New Brunswick, NJ; 5.24 kcal/g, with 26.3% available carbohydrate, 34.9% available fat, and 26.2% available protein). Cohorts used to measure food intake were individually housed. Otherwise mice were group housed. Food consumption and body weight were measured weekly, and data were analyzed and plotted as mean ± SE. Feeding efficiency was calculated by dividing the change in body mass (milligrams) by the food intake (kilocalories) over a 2-week period.

Metabolic and body composition studies

Indirect calorimetry was performed using a 12-cage equal flow CLAMS calorimeter (Columbus Instruments, Columbus, OH). Mice were habituated to the metabolic cages for 2 d prior to beginning data acquisition. Nuclear magnetic resonance analysis of body composition was performed using a Bruker minispec mq10 nuclear magnetic resonance analyzer. Live mice were individually analyzed by the machine, and then the collected data were further analyzed and plotted as mean ± SE.

Data analysis

Data were analyzed using Microsoft Excel (Redmond, WA) and plotted using Prism software (GraphPad Software, San Diego, CA). Unless otherwise noted, means were compared using unpaired, two-tailed *t* tests, with Welch's correction if *F* test indicated unequal sample variances. Multiple comparisons were performed using one-way ANOVA with Newman-Keuls multiple comparison *post hoc* test. Differences were considered statistically significant if $P < 0.05$.

ACKNOWLEDGEMENTS

This research was conducted in collaboration with Bassil Kublaoui, J. Lloyd Holder Jr., Terry Gemelli, and Andrew R. Zinn and is Copyright 2006, The Endocrine Society. This work was supported by grants from the American Heart Association, the American Diabetes Association, the Texas Higher Education Coordinating Board, and National Institutes of Health Grant P20 RR020691.

We thank Ward Wakeland and Fanglin Wei for assistance generating transgenic mice, Ed Esplin for initially characterizing transgene expression, Yuhe Zhao for genotyping and growth studies, and John Shelton and James Richardson for help with brain sections. We thank Michael Brown for reviewing the manuscript.

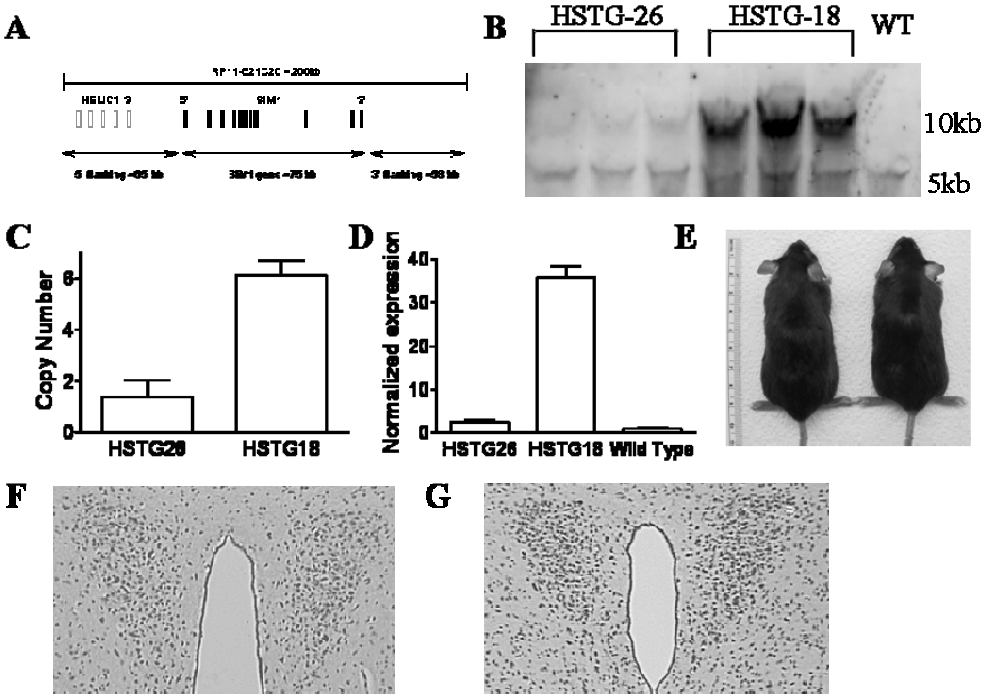

Figure II.1 Generation of *SIM1* transgenic mice. ***A***, Map of human *SIM1* BAC clone. ***B***, Southern blot showing human *SIM1* transgene (10 kb band) in transgenic mice and mouse *Sim1* gene (5 kb band) in transgenic and wild-type mice. ***C***, Quantitation of Southern blot showing approximate copy number of human *SIM1* transgene in both lines. ***D***, Quantitation of total human *SIM1* plus mouse *Sim1* transcripts in transgenic versus wild-type mouse hypothalamus by real-time PCR. ***E***, Gross appearance of 20 week old male wild-type (left) and transgenic (right) mice on a LF diet. ***F***, Nissl stain of coronal section of adult brain through the PVN in female wild-type and ***G***, transgenic HSTG18 mice.

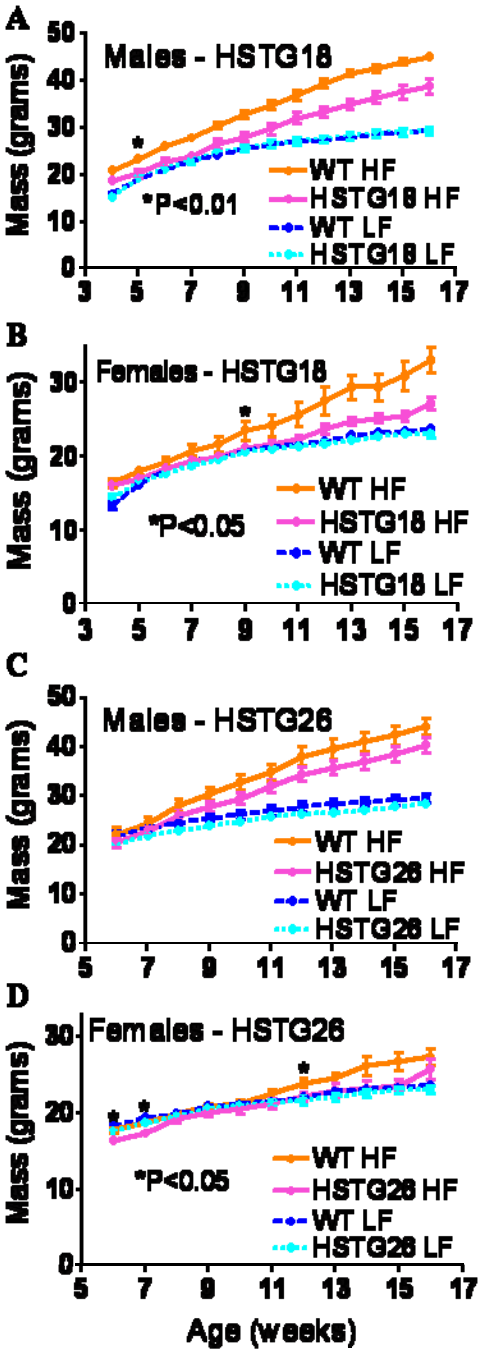
A
Males - HSTG18
Mass (grams)
*P<0.01
WT HF
HSTG18 HF
WT LF
HSTG18 LF
B
Females - HSTG18
Mass (grams)
*P<0.05
WT HF
HSTG18 HF
WT LF
HSTG18 LF
C
Males - HSTG26
Mass (grams)
WT HF
HSTG26 HF
WT LF
HSTG26 LF
D
Females - HSTG26
Mass (grams)
*P<0.05
WT HF
HSTG26 HF
WT LF
HSTG26 LF
Age (weeks)

Figure II.2 Growth curves of transgenic lines on HF and LF diet. ***A***, Males, HSTG18 vs. wild-type littermates. Curves on LF are superimposed. LF: transgenic n=8, wild-type n=12. HF: transgenic n=5, wild-type n=10. *P<0.01 from 5 weeks onward on HF. ***B***, Females, HSTG18 vs. wild-type littermates. LF: transgenic n=5, wild-type n= 8. HF: transgenic n=15, wild-type n=7. *P<0.05 from 9 weeks onward on HF. ***C***, Males, HSTG26 vs. wild-type littermates. LF: transgenic n=9, wild-type n=9. HF: transgenic n=11, wild-type n=7. Weights were not significantly different on either diet. ***D***, Females, HSTG26 vs. wild-type littermates. LF: transgenic n=9, wild-type n=9. Weights were not significantly different on a low fat diet. HF: transgenic n=9, wild-type n=9. *P<0.05 at weeks 6, 7 and 12. Mice were group housed with the same sex and weighed weekly.

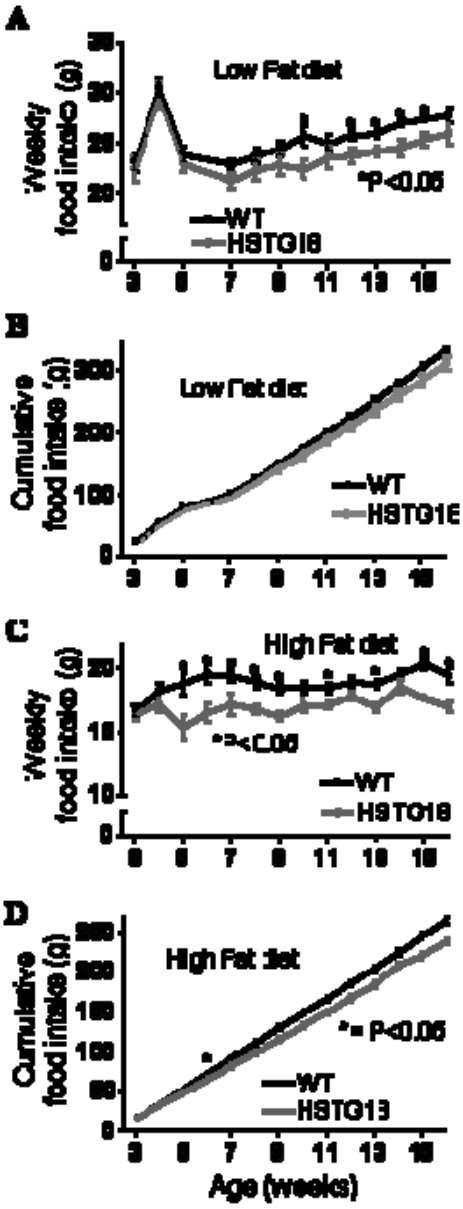

Figure II.3 Feeding studies of male HSTG18 transgenic mice vs. wild-type littermates. ***A***, Weekly and ***B***, cumulative food intake on LF diet. *P<0.05. ***C***, Weekly and ***D***, cumulative food intake on HF diet. *P<0.05 from 6 weeks onward. Mice were weaned onto their respective diets at 3 weeks of age and individually housed. Food intake was determined weekly.

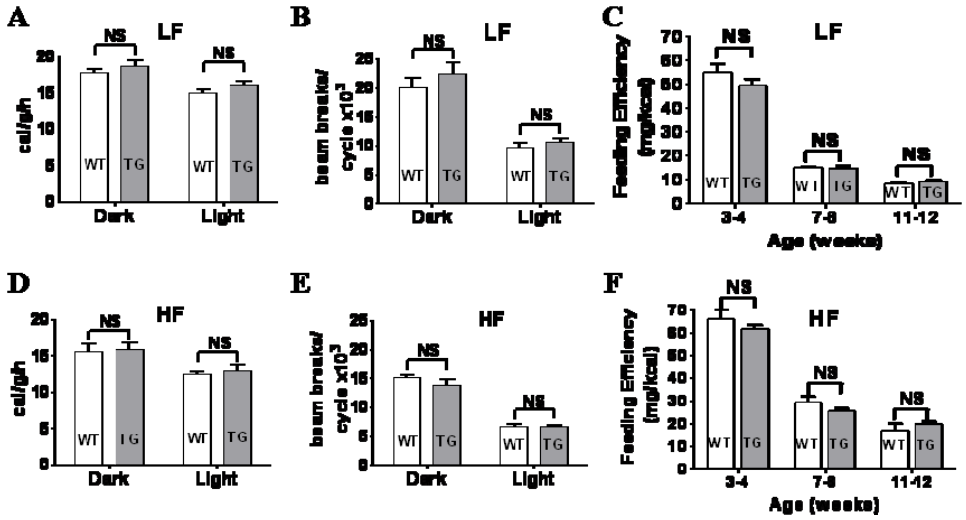

Figure II.4 Energy expenditure, activity, and feeding efficiency in HSTG18 transgenic vs. wild-type mice. ***A***, ***D***, Energy expenditure of males during light and dark cycles. ***B***, ***E***, Total activity of males during light and dark cycles. C, F, Feeding efficiency of males at various ages. ***A***, ***B***, ***C***, LF diet. ***D***, ***E***, ***F***, HF diet. Mice were habituated to the CLAMS metabolic cages for two days before the data were collected over the following three days. For ***A-F***, transgenic n=6, wild-type n=6.

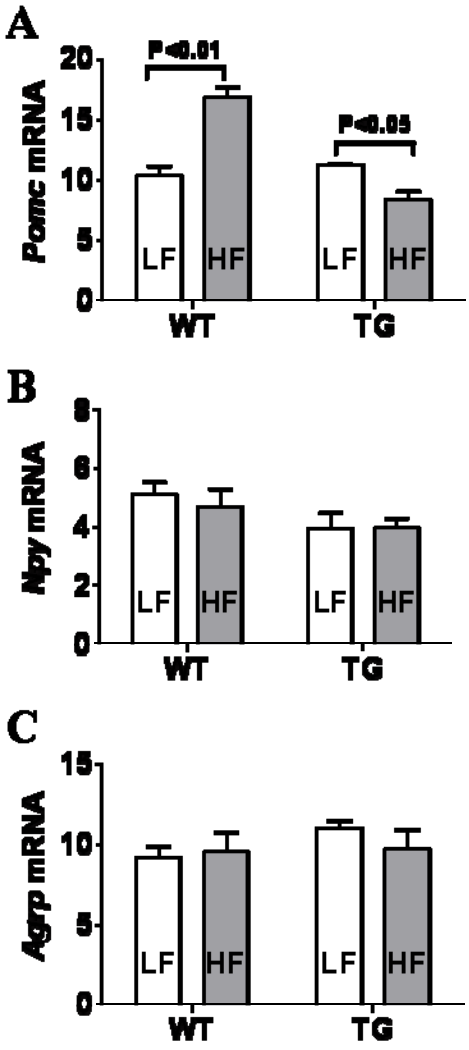

Figure II.5 *Pomc, Npy,* and *Agrp* expression in HSTG18 transgenic *vs.* wild-type mice. ***A***, Wild-type mice but not *SIM1* transgenic mice induce hypothalamic *Pomc* when fed a HF diet. ***B***, ***C***, *Npy* and *Agrp* expression is not affected by diet or genotype (n = 4 for each condition).

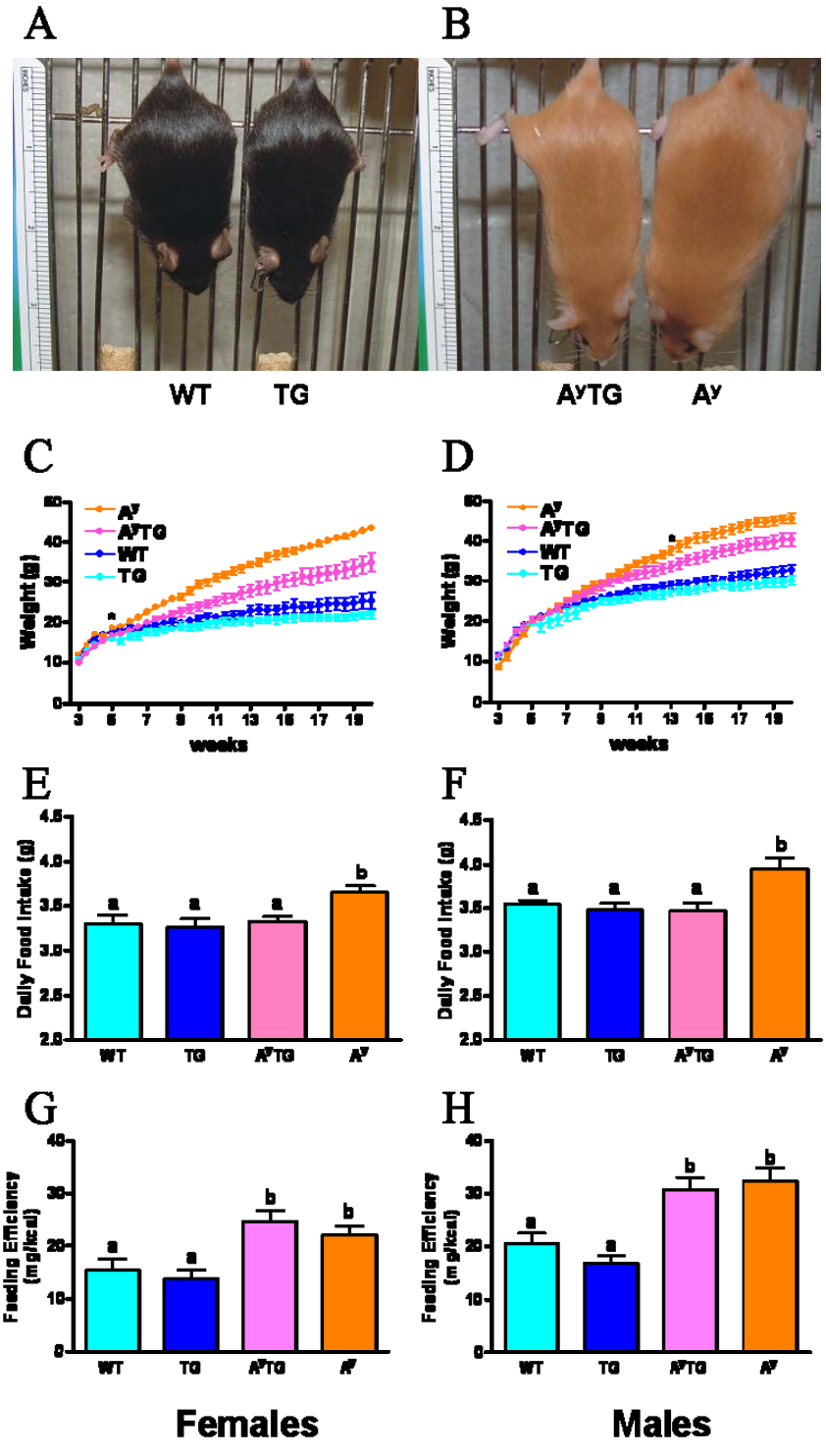
A
B
WT
TG
AyTG
Ay
C
D
Weight (g)
weeks
Ay
AyTG
WT
TG
E
F
Daily Food Intake (g)
G
H
Feeding Efficiency (mg/kcal)
Females
Males

Figure II.6 Partial rescue of obesity and normalization of food intake of A^y mice by *SIM1* transgene. ***A***, Gross appearance of wild-type and HSTG18 transgenic mice. ***B*** Gross appearance of A^y and A^y/HSTG18 transgenic mice. ***C***, Mean weight of females on LF diet. Wild-type n=5, HSTG18 n=4, A^y n=7, A^y/HSTG18 n=5. *P<0.05 from week 5 onward for A^y/HSTG18 vs. A^y. ***D***, Mean weight of males on LF diet. Wild-type n=12, HSTG18 n=7, A^y n=6, A^y/HSTG18 n=10. *P<0.05 from week 13 onward for A^y/HSTG18 vs. A^y. ***E***, Average daily food intake in females age 5-7 weeks. ***F***, Average daily food intake in males age 5-7 weeks. ***G***, Average feeding efficiency in females age 6-7 weeks. ***H***, Average feeding efficiency in males age 6-7 weeks. Multiple groups were compared using one-way ANOVA with Newman-Keuls Multiple Comparison post hoc test. Groups with different letters are significantly different P<0.01. Groups with the same letter are not significantly different.

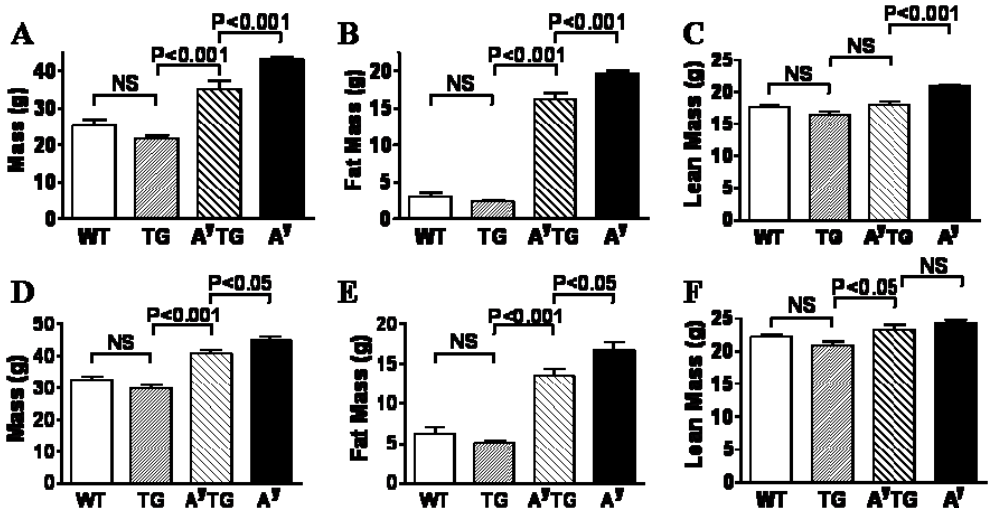

Figure II.7 Body composition of wild-type, HSTG18 transgenic, A^y, and A^y/HSTG18 transgenic mice. ***A,D*** Total body mass. ***B,E*** Fat mass. ***C,F*** Lean mass. ***A-C***, females: wild-type n=5, HSTG18 n=4, A^y n=7, A^y/HSTG18 n=5. ***D-F***, males: wild-type n=12, HSTG18 n=7, A^y n=6, A^y/HSTG18 n=10.

Chapter III

Aberrant neuropeptide expression in *Sim1* deficient mice

INTRODUCTION

Single-minded 1 (*SIM1*) encodes a member of the basic helix-loop-helix Per Arnt Sim family of nuclear transcription factors (Ward et al., 1998) and is one of six genes implicated in human monogenic obesity (Hung et al., 2007). A balanced chromosomal translocation that disrupts one allele of *SIM1* was identified in a girl with severe early-onset obesity, hyperphagia, and accelerated linear growth (Holder et al., 2000). Recently, nonsynonymous *SIM1* sequence variants were found in 6 of 379 obese adults *vs.* 0/378 lean controls (Ahituv et al., 2007), similar to the frequencies of nonsynonymous *MC4R* mutations (eight in obese group *vs.* two in lean group in the same study), the most common monogenic cause of early-onset morbid obesity and also associated with tall stature (Farooqi et al., 2003).

Heterozygous inactivation of the murine *Sim1* gene (*Sim1*$^{-/-}$) leads to an analogous phenotype of hyperphagic obesity and increased linear growth, with enhanced sensitivity to diet-induced obesity (Michaud et al., 2001; Holder et al., 2004). Homozygous S*im1* knockout mice die shortly after birth and exhibit failure of terminal migration and differentiation of the neurons of the paraventricular (PVN), supraoptic (SON), and anterior periventricular nuclei of the hypothalamus (Michaud et al., 1998; Xu and Fan, 2007), which produce the neuropeptides arginine vasopressin (Avp), oxytocin (Oxt), CRH, TRH, and somatostatin (Sst). Michaud *et al.* (Michaud et al., 2001) reported that *Sim1*$^{+/-}$ mice have a 24% reduction in PVN cellularity measured by Nissl staining, with no specific neuropeptide subtype affected, leading them to propose that the phenotype of hyperphagic obesity is due to a hypothalamic developmental defect. By contrast, we found no difference in the number of PVN *Sim1* neurons in *Sim1*$^{+/-}$ *vs.*

Sim1$^{+/+}$ mice, using a *Sim1*-enhanced green fluorescent protein (GFP) transgenic reporter to mark these neurons (Kublaoui et al., 2006a). In the absence of a gross neuroanatomic defect in *Sim1*$^{+/-}$ mice, it is unclear which PVN neurons are important for the regulation of feeding behavior by *Sim1*. Of the neuropeptides produced in the PVN, Oxt (Arletti et al., 1989, 1990; Olson et al., 1991b; Olson et al., 1991a), TRH (Choi et al., 2002; Steward et al., 2003), and CRH (Krahn et al., 1986; Krahn et al., 1990; Vettor et al., 2002; Valassi et al., 2008) have consistently been shown to have an anorectic effect when given centrally to rodents.

Sim1 is expressed postdevelopmentally in the PVN and supraoptic nucleus (SON) as well as the basomedial amygdala and a subset of lateral hypothalamic neurons (Holder et al., 2004). The *Sim1*$^{+/-}$ phenotype is suggestive of defective hypothalamic melanocortin signaling (Wisse and Schwartz, 2003), and we hypothesized that *Sim1* physiologically regulates body weight by modulating PVN Mc4r signaling (Holder et al., 2004). Consistent with this hypothesis, PVN neurons of *Sim1*$^{+/-}$ mice showed impaired activation in response to peripheral injection of melanotan II, a melanocortin receptor agonist (Kublaoui et al., 2006a). Furthermore, transgenic overexpression of human *SIM1* partially suppressed both diet-induced and Agouti yellow (A^y) obesity by reducing feeding (Kublaoui et al., 2006b). Moreover, viral-mediated overexpression of *Sim1* in the PVN of adult mice reduced food intake, whereas small interfering RNA-mediated inhibition of *Sim1* expression increased food consumption (Yang et al., 2006). These findings suggest that *Sim1* acts postdevelopmentally to regulate feeding.

Leptin secreted by adipocytes activates receptors in the arcuate nucleus (ARC), increasing proopiomelanocortin expression and stimulating release of α-MSH by ARC

neurons that project to the PVN and LH (Schwartz et al., 1997). This hypothalamic adiposity signal is integrated with hindbrain satiety signals such as cholecystokinin (CCK), mediated by vagal afferents (Matson et al., 1997; Matson and Ritter, 1999; Matson et al., 2000; Matson et al., 2002; Morton et al., 2005). Neuroanatomic evidence suggests that the PVN is central to this interaction (Schwartz et al., 2000; Baskin et al., 2001). In rats, the neurons responsible for this interaction may be parvocellular oxytocinergic neurons in the posterior PVN projecting to the hindbrain and spinal cord (Kirchgessner et al., 1988; Rinaman, 1998; Blevins et al., 2003; Liu et al., 2003b). Fourth ventricular injection of an Oxt receptor antagonist attenuated the effect of leptin on food intake, suggesting that Oxt itself is an important signal in addition to classical neurotransmitters (Blevins et al., 2004). Interestingly, patients with Prader-Willi syndrome, a human genetic disorder characterized by severe obesity, have a 42% reduction of parvocellular PVN Oxt neurons (Swaab et al., 1995). Additionally, the levels of circulating Oxt in these patients are abnormally low for their degree of obesity (Hoybye, 2004). The gene regulatory network that controls Oxt cell development is conserved in vertebrate species as diverse as zebrafish, chicks, and mice (Caqueret et al., 2005; Eaton and Glasgow, 2006). Zebrafish *Sim1* is required for the development of neurons that produce isotocin, the fish homolog of Oxt (Eaton and Glasgow, 2006). It is not known whether the *Oxt* gene is also a transcriptional target of *Sim1*.

To further examine the effect of *Sim1* haploinsufficiency on PVN neuronal function, we evaluated expression of PVN neuropeptides in *Sim1*$^{+/-}$ mice. We also compared the regulation of Oxt and CRH in these mice in response to fasting and refeeding. We further investigated the effect of an oxytocin receptor antagonist, OVT

($d(CH_2)_5$, $Tyr(Me)^2$,Orn^8-Oxytocin) on food intake in *Sim1*$^{+/-}$ *vs.* wild-type mice and tested whether PVN Oxt neurons in wild-type mice are activated by an Mc4r-selective agonist. Finally, we measured the effect of chronic intracerebroventricular (ICV) Oxt injections on food intake and body weight of *Sim1*$^{+/-}$ and wild-type mice. Our findings support the role of PVN Oxt neurons and Oxt itself in the regulation of feeding and suggest a neuroendocrine mechanism for the hyperphagia of *Sim1*$^{+/-}$ mice.

RESULTS

Sim1$^{+/-}$ *Mice Exhibit Reduced Expression of PVN Oxt*

To determine which PVN neurons are sensitive to reduced *Sim1* dosage, we compared the hypothalamic mRNA levels of the neuropeptides CRH, TRH, Oxt, Sst, and Avp in *Sim1*$^{+/-}$ and wild-type mice. All mRNAs were decreased in *Sim1*$^{+/-}$ mice, with the greatest reduction (-80%) in *Oxt* (Figure III.1). We next performed immunostaining for Oxt and CRH, for which suitable antibodies were available, to determine whether the reductions in hypothalamic mRNAs resulted in reduced PVN neuropeptide levels. Oxt but not CRH immunoreactivity was demonstrably reduced (Figure III.2). Although difficult to determine in the absence of another marker of Oxt neurons, the marked reduction in Oxt immunoreactivity may reflect a decreased number of Oxt neurons rather than reduced staining within existing neurons (Figure III.2). The reduction in Oxt immunoreactivity was evident throughout the PVN. There was a similar reduction in Oxt peptide expression in the SON (data not shown).

Sim1$^{+/-}$ Mice Fail to Regulate Hypothalamic Oxt in Response to Feeding State

Wild-type mice showed reduced *Oxt* mRNA levels in the hypothalamus with fasting that were restored with refeeding, whereas *CRH* mRNA displayed the opposite pattern (Figure III.3). This was consistent with previous studies (Verbalis et al., 1986; Jang and Romsos, 1998). By contrast, *Oxt* mRNA in *Sim1$^{+/-}$* mice was not changed by fasting or refeeding, although these mice showed normal regulation of *CRH* expression in response to feeding state (Figure III.3).

Oxt Is Colocalized in a Subset of Sim1 Neurons in the PVN

To determine whether PVN *Sim1* neurons coexpress Oxt, we used a *Sim1*-GFP transgenic mouse line as reported previously (Kublaoui et al., 2006a). Figure III.4A shows two color immunofluorescent detection of Oxt (*red*) and GFP (*green*) in PVN sections harvested from a wild-type mouse not pretreated with colchicine. The result shows that Oxt is colocalized with GFP in a subset of *Sim1* neurons in the PVN.

PVN Oxt Neurons Are Activated by Central Injection of an Mc4r-Selective Agonist

To determine whether PVN Oxt neurons might be germane to the defective melanocortin response of *Sim1$^{+/-}$* mice, we treated wild-type mice ICV with the Mc4r agonist cyclo(*β*-Ala-His-D-Phe-Arg-Trp-Glu)- NH_2 and tested the response of Oxt neurons using induction of c-Fos immunoreactivity as a marker of neuronal activation. This agonist is highly selective for the Mc4r (>90-fold selectivity over Mc3r and >3400- fold selectivity over Mc5r) (Bednarek et al., 2001). In mice it acts centrally to reduce 2 hour food intake by 50% at a dose of 1 μg (Navarro et al., 2005). Figure III.4B shows two color

immunofluorescent detection of c-Fos (*red*) and Oxt (*green*) in hypothalamic sections harvested 6 h after ICV injection of the Mc4r agonist or artificial cerebrospinal fluid (aCSF) from a wild-type mouse pretreated with colchicine. The result shows that c-Fos was robustly induced in many PVN Oxt neurons at this time point. A control colchicine-pretreated animal that received aCSF vehicle showed negligible c-Fos immunoreactivity. PVN Oxt immunoreactivity decreased after Mc4r agonist treatment in both wild-type and *Sim1*$^{+/-}$ mice (data not shown). This decrease, coupled with the already low level of Oxt immunoreactivity in *Sim1*$^{+/-}$ mice, precluded simultaneous detection or quantitation of c-Fos- and Oxt-positive neurons in these animals.

Central Oxt Receptor Antagonist Administration Exacerbates Hyperphagia of Sim1$^{+/-}$ *Mice*

We hypothesized that reduced Oxt neuropeptide levels in *Sim1*$^{+/-}$ mice might render these mice hypersensitive to further inhibition of Oxt signaling. To test this hypothesis, we treated *Sim1*$^{+/-}$ mice and wildtype littermates ICV with the Oxt receptor antagonist OVT (d(CH_2)$_5$, Tyr(Me)^2,Orn^8-Oxytocin). An OVT dose of 0.5 μg did not affect feeding of wild-type mice but increased the food intake of the already hyperphagic *Sim1*$^{+/-}$ mice by approximately 50% (Figure III.5).

Central Oxt Injection Rescues Hyperphagic Obesity of Sim1$^{+/-}$ *Mice*

To further substantiate the role of Oxt deficiency in the phenotype of *Sim1*$^{+/-}$ mice, we tested whether Oxt replacement could rescue their hyperphagia and obesity. *Sim1*$^{+/-}$ mice and wild-type littermates were injected twice daily ICV with either 10 ng of Oxt or

vehicle (aCSF). Daily food intake and body weight were measured over 12 days. Oxt normalized food intake of *Sim1*$^{+/-}$ mice but had no effect on food intake of wild-type mice (Figure III.6A), arguing against a nonspecific anorectic effect such as nausea. Repeated Oxt injections also led to decreased weight gain compared with vehicle treatment in *Sim1*$^{+/-}$ mice but not their wild-type littermates (Figure III.6B). Mice were weighed again after a 12 day washout period after completion of ICV injections. *Sim1*$^{+/-}$ mice that had previously received Oxt or aCSF gained a similar amount of weight (Figure III.6C).

Wild-Type Mice Are Insensitive to High Doses of ICV Oxt but Respond to the Oxt Receptor Antagonist OVT

Having shown that food intake of *Sim1*$^{+/-}$ mice was sensitive to both OVT and Oxt at doses that did not change food intake of wild-type mice, we sought to investigate the dose-response of wild-type mice to both agents. ICV Oxt has been consistently shown to reduce food intake of rats at doses of 1–4 nmol (~1–4 μg) (Arletti et al., 1989, 1990; Olson et al., 1991b) but not mice (Gimpl and Fahrenholz, 2001). ICV OVT blocks anorexia in rats at doses of 9 nmol (~9 μg). Doses of Oxt as high as 1 μg failed to inhibit food intake in wild-type mice (Figure III.7A). On the other hand, OVT was capable of increasing food intake in wild-type mice at a dose of 1.5 μg (Figure III.7B).

DISCUSSION

We previously showed that *Sim1*$^{+/-}$ mice have normal hypothalamic *Mc4r* mRNA levels but blunted anorexia and activation of PVN neurons in response to the Mc3r/Mc4r agonist melanotan II (Kublaoui et al., 2006a). The total number of PVN neurons was

unchanged in *Sim1*$^{+/-}$ mice, and these neurons appeared to induce c-Fos normally in response to another stimulus, hypertonic saline. We also showed that overexpression of *SIM1* rescued hyperphagia of *A*^{y} mice, with no effect on energy expenditure (Kublaoui et al., 2006b). These findings led us to propose that *Sim1* functions downstream of Mc4r in the PVN.

Sim1 is necessary for the development of all PVN neurons. Given that mouse *Sim1* is required for the development of neurons of the PVN, SON, and anterior periventricular nucleus expressing AVP, Oxt, CRH, TRH, and Sst, we hypothesized that one or more of these neuronal populations may be affected by *Sim1* haploinsufficiency and that this may mediate the hyperphagic obesity of *Sim1*$^{+/-}$ mice. Microarray expression profiling revealed that Oxt mRNA was reduced in the hypothalamus of *Sim1*$^{+/-}$ mice compared with controls (data not shown). These results were confirmed in the present study using quantitative RT-PCR, revealing a marked (~80%) reduction in *Oxt* expression in *Sim1*$^{+/-}$ mice, with a similar decrease in Oxt peptide as measured by immunohistochemistry. The reduction in Oxt peptide in the PVN appeared to be global and likely affected both magnocellular and parvocellular neurons, although these populations cannot be distinguished morphologically or anatomically in mice ((Castel and Morris, 1988) and J. Elmquist, personal communication). Other PVN neuropeptide mRNAs were reduced in *Sim1*$^{+/-}$ mice, but to a much lesser degree than Oxt.

It is unclear whether reduced Oxt expression in *Sim1*$^{+/-}$ mice was due to a decreased number of Oxt neurons or to decreased Oxt expression in most of these neurons below the threshold for immunodetection. Presently we have no way other than Oxt expression to mark these neurons. By contrast, CRH neurons did not show

measurable reduction in either number or peptide expression, suggesting that *Sim1* haploinsufficiency preferentially affects Oxt neurons. These findings are consistent with a conserved role for *Sim1* in development of Oxt (or isotocin in zebrafish) neuronal lineages (Eaton and Glasgow, 2006).

The Oxt promoter has not been well characterized, even in the well-known context of regulation by estrogen (Ivell and Walther, 1999; Koohi et al., 2005). Inspection of the upstream or downstream 5 kb of genomic sequence with Regulatory VISTA (rVISTA) (Loots et al., 2002) and the UCSC Genome Browser (Kent et al., 2002) did not reveal any conserved binding sites for Sim1 or its heterodimer partner Arnt2, suggesting that if Sim1 physiologically regulates Oxt expression, the mechanism is indirect.

There is a large body of literature supporting the role of Oxt and Oxt neurons in regulation of feeding in both humans and rodents. Patients with Prader-Willi syndrome have a 42% reduction of parvocellular PVN Oxt neurons (Swaab et al., 1995). Plasma Oxt levels are elevated in subjects with common obesity and decrease after gastric banding (Stock et al., 1989), suggesting that there may be Oxt resistance analogous to leptin resistance. Centrally administered Oxt has been shown to reduce food intake in rats, and this effect is blocked by Oxt receptor antagonists (Arletti et al., 1989, 1990; Olson et al., 1991b). Oxt is secreted into the bloodstream by magnocellular neurons in response to exogenous CCK, and serum Oxt levels are directly proportional to the degree of inhibition of food intake by this treatment (Verbalis et al., 1993). Despite these observations, peripheral administration of Oxt at physiological levels does not modulate food intake in rats, suggesting that peripheral release takes place in parallel with central

effects on feeding. Peripheral administration of Oxt in rats at high doses has been shown to reduce food intake by some investigators (Arletti et al., 1989, 1990) but not others (Verbalis et al., 1993).

Neuroanatomic and pharmacological studies in rats point to parvocellular PVN Oxt neurons that project monosynaptically to the hindbrain as being important in satiety. Oxt receptor expression in the mouse hindbrain is greatest in the nucleus of the solitary tract (NTS). A known satiety center (Gould and Zingg, 2003), and there is evidence that Oxt preferentially regulates food intake in the hindbrain (Blevins et al., 2004). Furthermore, oxytocinergic projections to the nucleus of the solitary tract in newborn rats come solely from the PVN (Rinaman, 1998). Disruption of PVN oxytocinergic fibers projecting to the hindbrain leads to hyperphagic obesity (Kirchgessner et al., 1988). Furthermore, PVN Oxt neuron axonal projections interact with NTS neurons that are activated by CCK (Blevins et al., 2003). Finally, Baskin and colleagues (Blevins et al., 2003; Blevins et al., 2004) characterized a subset of parvocellular PVN Oxt neurons that both respond to leptin and project to the NTS and showed that injection of OVT into the fourth ventricle attenuated the effect of leptin on food intake. These results support the notion that PVN parvocellular Oxt neurons transmit hypothalamic adiposity signals to the NTS, where they are integrated with gut satiety signals. Furthermore, there is evidence that the parvocellular PVN itself also integrates adiposity signals such as leptin with satiety signals from the NTS. This integration is then followed by modulation of NTS neurons that reduce meal size. This evidence comes from the work of Moran and colleagues (Emond et al., 1999), who showed that leptin modulates CCK induced c-Fos in both the PVN and NTS, as well as the work of Verbalis and colleagues (Olson et al.,

1992), who showed that CCK activates oxytocinergic parvocellular PVN neurons that then project to the dorsal vagal complex (dorsal motor nucleus of the vagus and NTS).

Further evidence for the role of PVN Oxt neurons in feeding regulation comes from a report showing an effect of ghrelin on these neurons (Olszewski et al., 2007). In this study, Levine and colleagues showed that the Oxt receptor antagonist OVT exacerbated ghrelin-induced hyperphagia. Others have shown that parvocellular and magnocellular PVN Oxt neurons are activated by insulin (Griffond et al., 1994). Hypothalamic Oxt has also been implicated in the regulation of food intake during pregnancy (Douglas et al., 2007).

Studies of a *Sim1*-GFP transgenic mouse showed that essentially all cells in the PVN expressing NeuN, a marker of neurons but not glial cells, were also GFP positive (our unpublished results). Based on these and other data (Balthasar et al., 2005), we proposed that all adult mouse PVN neurons express *Sim1* (Kublaoui et al., 2006a). Here we showed that Oxt colocalized in a subset of Sim1 neurons (Figure III.4A). Colocalization of Oxt and Mc4r has been previously demonstrated in mouse PVN neurons (Liu et al., 2003). It is also clear from the work of Balthasar *et al.* (Balthasar et al., 2005) that *Mc4r* is expressed in PVN Sim1 neurons. Together, the data indicate that a subset of PVN neurons coexpress *Sim1*, *Mc4r*, and *Oxt*. Our previous results suggest that Sim1 functions downstream of Mc4r (Kublaoui et al., 2006a), and we show here that proper *Oxt* expression is dependent upon Sim1. Thus, there may exist a molecular pathway from Mc4r to Sim1 to Oxt within PVN neurons, although the notion of a linear relationship is likely an oversimplification of the relevant circuits.

Our results further bolster the relevance of PVN Oxt neurons in the melanocortin feeding circuitry by showing that these neurons are activated by a centrally administered Mc4r-selective agonist (Figure III.4B). Regulation of Oxt neurons by melanocortin agonists is not limited to the PVN but has also been shown in the SON, where α-MSH induces the release of Oxt from the dendrites of magnocellular neurons while inhibiting its secretion from nerve terminals in the posterior pituitary (Sabatier et al., 2003; Sabatier, 2006).

A key question is whether reduced expression of Oxt is causally related to the hyperphagia of *Sim1*$^{+/-}$ mice. To answer this question, we examined the effect of both an Oxt receptor antagonist and Oxt on food intake in *Sim1*$^{+/-}$ *vs.* wild-type. We reasoned that if Oxt simply marks absent or defective PVN neurons in *Sim1*$^{+/-}$ mice but is not itself involved in feeding regulation, then treatment with Oxt or an Oxt receptor antagonist should not differentially affect food intake of *Sim1*$^{+/-}$ *vs.* wild-type mice. On the other hand, if Oxt deficiency is mechanistically related to the hyperphagia of *Sim1*$^{+/-}$ mice, then administration of an Oxt receptor antagonist might exacerbate and administration of Oxt might ameliorate their hyperphagia.

The results of our pharmacological experiments clearly support the conclusion that Oxt neuropeptide deficiency *per se* contributes to the hyperphagic obesity in *Sim1*$^{+/-}$ mice. Further experiments are required to address the neuronal mechanism of Oxt action. For instance, Oxt may act as a neuromodulator of synaptic signaling by classical neurotransmitters released in the NTS by parvocellular PVN neuronal projections.

Despite the large body of evidence implicating Oxt in food intake regulation, wild-type and *Oxt*$^{-/-}$ mice ingest similar amounts of standard chow *ad libitum*, after

overnight food deprivation when drinking water is available, and after systemic administration of either CCK or D-fenfluramine (Mantella et al., 2003; Rinaman et al., 2005). On the other hand, *Oxt*$^{-/-}$ mice display an increased intake of both sweet and non-sweet carbohydrate solutions (Sclafani et al., 2007). Oxt receptor-deficient mice have been generated, but no characterization of their food intake or body weight has been published (Takayanagi et al., 2005). There are several possible explanations for the apparent discrepancy between genetic models and anatomic and pharmacological data. Oxt may mark the identity of neurons projecting from the PVN to the NTS but not be critical for their action in meal termination, which could be mediated by classical neurotransmitters such as GABA or glutamate. Our results argue against this possibility. Alternatively, Oxt may be an important physiological regulator of feeding in normal mice, but there could be developmental mechanisms that compensate for its absence in *Oxt*$^{-/-}$ mice. Functional and developmental compensation by hypothalamic neurons has been demonstrated, most notably in Npy/Agrp neurons. Despite compelling pharmacological evidence for a prominent role for these two peptides in energy homeostasis, mice deficient in Npy, Agrp, or both have no demonstrable feeding phenotype (Qian et al., 2002). On the other hand, partial ablation of Npy/Agrp neurons postnatally leads to the expected lean phenotype, and complete ablation in adulthood leads to starvation (Qian et al., 2002; Beuckmann et al., 2004; Bewick et al., 2005; Gropp et al., 2005; Luquet et al., 2005). Developmental compensation by these neurons appears to take place postnatally, because neonatal ablation had minimal effects on body weight or feeding regulation (Luquet et al., 2005). We hypothesize that similar developmental compensation explains the absence of a feeding phenotype in *Oxt*$^{-/-}$ mice. These

compensatory mechanisms may involve compensation by other PVN neuropeptides implicated in feeding regulation, *i.e*. CRH or TRH. These compensatory mechanisms may be intact in *Oxt*$^{-/-}$ mice and impaired in *Sim1*$^{+/-}$ mice, which show moderately decreased mRNA levels of CRH and TRH.

Another explanation for the lack of a feeding phenotype in *Oxt*$^{-/-}$ mice may be species differences. Our results do not support this possibility. Whereas ICV Oxt consistently reduces food intake of rats (Arletti et al., 1989, 1990; Olson et al., 1991b), no such hypophagic effect has been demonstrated in mice (Gimpl and Fahrenholz, 2001). We too could not find such an effect of ICV Oxt on wild-type mice. On the other hand, we were able to demonstrate that OVT increased food intake in wild-type mice. These results in wild-type mice, coupled with our results in *Sim1*$^{+/-}$ mice, support the hypothesis that Oxt exerts a tonic inhibition of feeding in mice. This is consistent with the work of Blevins *et al.* (Blevins et al., 2003) in rats, who also concluded that Oxt exerts a tonic stimulatory effect on NTS neurons that reduce meal size by showing that fourth ventricular administration of OVT blunted CCK-induced satiety.

Further experiments are needed to determine the site of action of Oxt in rescuing the hyperphagia of *Sim1*$^{+/-}$ mice and whether *Sim1* haploinsufficiency leads to a developmental reduction in Oxt neurons or a postdevelopmental reduction of *Oxt* expression. Any reduction in the number of PVN neurons must be subtype specific. Because there is no difference in the total PVN *Sim1* neuron count of *Sim1*$^{+/-}$ mice *vs.* wild-type mice (Kublaoui et al., 2006a), a reduction in the number of Oxt neurons may be due to fate switching. Additional experimental approaches, such as conditional postnatal *Sim1* inactivation, are needed to determine whether the decrease in Oxt expression in

Sim1$^{+/-}$ mice is developmental or regulatory. Regardless, our results support the importance of the oxytocinergic pathway from the PVN to the NTS in feeding regulation and suggest that reduced *Oxt* expression is responsible for much of the hyperphagia of *Sim1*$^{+/-}$ mice (Figure III.8). Further study of the PVN to NTS oxytocinergic pathway may be relevant to our understanding of other genetic causes of human obesity such as Prader-Willi syndrome or *MC4R* mutations.

METHODS

Animal Care

C57BL6 mice (6–8 wk of age) from the National Cancer Institute were used unless otherwise stated. Mice were kept on a 12 hour light, 12 hour dark cycle and fed a low-fat chow diet (Global diet 2016; Teklad, Madison, WI) *ad libitum*. Generation, breeding, and genotyping of *Sim1*$^{+/-}$ mice were previously described (Holder et al., 2004). All experimental protocols were approved by the University of Texas Southwestern Institutional Animal Care and Use Committee.

Real-Time PCR

Hypothalami from fresh brains were dissected with a block (David Kopf Instruments, Tujunga, CA) as described (Shinyama et al., 2003), using the following landmarks: posteriorly, posterior aspect of median eminence; anteriorly, 5 mm anterior to the median eminence; dorsally, the thalamus; laterally, medial to the dentate gyrus. Total RNA was extracted using Tripure reagent (Roche Applied Science, Indianapolis, IN). Quantitative

real time PCR was performed using an ABI 3700 instrument (Applied Biosystems, Foster City, CA) and the QuantiTect HotStart SYBR green qPCR kit (QIAGEN, Valencia, CA). Neuropeptide measurements were normalized to *β-actin* or *GAPDH* mRNA levels. Primers sequences were 5'-GAG GAC CTG CGA CTA GAC TGA C-3' and 5'-CAG CAG CTC TGC CAA GAA GTA-3' (Sst); 5'-GTT GAG AGA CTG AAG AGA AAG G-3' and 5'-GGA CGA CAG AGC CAC CAG-3' (CRH); 5'-CTT TGA TCT TCG TGC TAA CTG GT- 3' and 5'-CTT CAA CGT CTT CCT CCT TCT C-3' (mTRH); 5'-CTC TGA CAT GGA GCT GAG ACA G-3' and 5'-AGG GCA GGT AGT TCT CCT CCT-3' (AVP); 5'-TGGCTTACTGGCTCTGACCT-3' and 5'-AGG CAG GTA GTT CTC CTC CTG- 3' (Oxt). Taqman primers were used for determining Oxt and CRH mRNA levels for feeding state experiments (4331182 and 4351372; Applied Biosystems, Foster City, CA). 5'-GAC GAT GCT CCC CGG GCT GTA TTC-3' and 5'-TCT CTT GCT CTG GGC CTC GTC ACC-3' (*β-actin*) and GAPDH (4352339E, Applied Biosystems) were used for normalization. All reactions were performed at 53ºC annealing temperature.

Cannulation (ICV)

Mice were anesthetized with ketamine (117 mg/kg) and xylazine (7.92 mg/kg). After shaving the head and applying a microbicide, each animal was placed in a stereotaxic chamber (Stoelting, Wood Dale, IL). A sagittal section was cut and the skin was clipped back. Bregma coordinates were visually determined, and the location of the lateral ventricle was calculated (0.2 mm posterior; 1.0 mm lateral; 2.1 mm deep to skull surface). The site of cannulation on the skull surface was marked. The skull was punctured using an engraving Dremel bit. The guide cannula (C315GS-4/spc; Plastics

One, Roanoke, VA) was inserted and glued to the skull surface with dual cure paste (031458550; Den-mat, Santa Maria, CA). A dummy cannula (or dust cap) was placed inside the guide cannula (C315DCS-4/spc; Plastics One). The scalp was closed with dissolvable sutures. Upon waking, the animal was injected ip with 0.1 mg/kg of Buprenex (buprenorphine hydrochloride) for analgesia. Mice were then allowed to recover for 1 week. Cannula placement was tested by examining the effect of 0.2 μg of angiotensin II on drinking behavior as described elsewhere (Johnson and Epstein, 1975).

Injections (ICV)

Individually housed mice were habituated to handling and injections with aCSF for at least 1 week before experimentation. Single injections were made manually using an internal cannula (C315IS-4/spc; Plastics One) connected to PE-50 tubing and a Hamilton syringe. Drug or vehicle (2 μl) was injected over a 30-sec period.

OXT Wild-Type *vs.* *Sim1*$^{+/-}$. Female mice (6–12 weeks of age) were equally divided into the following groups matched for age and weight (wild-type aCSF, n = 7; wild-type Oxt, n = 7; *Sim1*$^{+/-}$ aCSF, n = 5; and *Sim1*$^{+/-}$ Oxt, n = 8). After 1 week of habituation to twice daily ICV injection, mice were injected with 10 ng of Oxt (H2510; Bachem Bioscience, Inc., King of Prussia, PA) or vehicle, twice a day for 12 days (at the onset of the dark cycle and 6 hours later). Food intake and body weight were recorded daily. Food intake was analyzed by two-way ANOVA (group *vs.* time) and body weight change was analyzed with one-way ANOVA (group). Both analyses were done with a Bonferroni posttest to determine intergroup significance. On day 24, 12 days after the last injection, body weight was measured again and compared with body weight on day 12.

Posttreatment body weight change for the groups was compared using one-way ANOVA with a Bonferroni posttest.

Wild-Type OVT *vs.* *Sim1*$^{+/-}$. Mice were ICV injected at the onset of the dark cycle with 2 µl aCSF to determine baseline food intake. Mice were injected 24 h later with 0.5 µg OVT (d(CH_2)$_5$, Tyr(Me)^2,Orn^8-Oxytocin; H4928, Bachem). Food intake was measured at 1 hour intervals for 6 hours. The experiment was repeated the following week. Food intake from the two aCSF measurement days was averaged for each mouse, and food intake from the two OVT measurement days was averaged for each mouse. OVT food intake was normalized to aCSF food intake for each mouse. Means were calculated for each treatment and compared using a paired *t* test.

Wild-Type Oxt. After 1 week of habituation to daily ICV injection, 6- to 10-week-old female wild-type mice were injected at the onset of the dark cycle with aCSF, 50 ng, 250 ng or 1µg of OXT. Food intake was normalized to aCSF food intake. Means were calculated for each treatment, and the groups at each time point were compared using one-way ANOVA.

Wild-Type OVT. After 1 week of habituation to daily ICV injection, 6- to 10-week-old female wild-type mice were injected at the onset of the dark cycle with aCSF on day 1 and 1.5 µg OVT on day 2. Food intake was normalized to aCSF food intake for each mouse. Means were calculated for each treatment, and the groups at each time point were compared using a paired *t* test.

Immunohistochemistry

For colocalization of c-Fos and Oxt, 8-week-old female C57BL/6 mice received 1 μg colchicine ICV 24 hours before subsequent experimental procedures. For c-Fos experiments, mice were ICV injected with 3 μg of the Mc4r-selective agonist or vehicle (aCSF) 4 hours before intracardiac perfusion. The Mc4r selective agonist cyclo(*β*-Ala-His-D-Phe-Arg-Trp-Glu)-NH_2 was purchased from Phoenix Pharmaceuticals (Burlingame, CA). *Sim1*-GFP transgenic mice were not colchicine treated, and immunohistochemistry was performed as described previously (Kublaoui et al., 2006a). Mice were deeply anesthetized with pentobarbital (7.5 mg /0.15 ml, ip) and transcardially perfused with 10 ml of heparinized saline (10 U/ml, 2 ml/min) followed by 10 ml of phosphate-buffered 4% paraformaldehyde (2 ml/min). Brains were removed, postfixed for 24 hours in 4% paraformaldehyde, and then equilibrated in 30% sucrose in PBS for 72 hours. Immunohistochemistry was performed as described elsewhere (Beuckmann et al., 2004; Kublaoui et al., 2006a). Briefly, brains were coronally sectioned (35 μm) on a freezing microtome (Leica SM 2000R; Wetzlar, Germany) and stored in PBS at 4 C. Sections were incubated for 16 hours in mouse anti-Oxt antiserum (MAB5296, 1:5000, Millipore Corp., Billerica, MA) or rabbit anti-CRH antiserum (AB-02, 1:800; Advanced Targeting Systems, San Diego, CA) and then incubated with either Cy-3 affiniPure goat antimouse IgG secondary antiserum or Cy-3 affiniPure goat antirabbit IgG secondary antiserum (115–165-166, 111–165-003, 1:400; Jackson ImmunoResearch Laboratories, Inc., West Grove, PA) for 2 hours at room temperature. Sections were placed in 4’,6-diamidino-2-phenylindole (DAPI) (0.2 μg /ml, 236276; Roche, Indianapolis, IN) and then mounted and coverslipped using Vectashield (H-1000; Vector Laboratories,

Burlingame, CA). Images of sections containing PVN were captured on an Olympus BX61 microscope using Cytovision software (Applied Imaging Corp., San Jose, CA). For fluorescent c-Fos and Oxt double labeling, sections were incubated for 16 hours in rabbit anti-Fos antiserum (Ab-5; 1:3000 dilution; Calbiochem, La Jolla, CA) and mouse anti-Oxt antiserum. Sections were then incubated with Cy-3 goat antirabbit IgG secondary antiserum and Cy-2 affiniPure goat antimouse IgG secondary antiserum (115–225-166, 1:400; Jackson ImmunoResearch) for 2 hours at room temperature. Sections were treated with DAPI and mounted as described above. For fluorescent GFP and Oxt double labeling, sections were incubated for 48 hours in rabbit anti-GFP antiserum (A6455, 1:5000; Molecular Probes, Eugene, OR) and mouse anti-Oxt antiserum. Sections were then incubated with fluorescein isothiocyanate goat antirabbit IgG secondary antiserum and Cy-2 affiniPure goat antimouse IgG secondary antiserum (115-225-166, 1:400; Jackson ImmunoResearch) for 2 hours at room temperature. Sections were treated with DAPI and mounted as described above. Cell counts and densitometry were determined using ImageJ software (National Institutes of Health, Bethesda, MD). Each side of a section was counted separately, and counts from six sides were averaged for each animal. Densitometry was performed on images that were captured with identical settings using the Integrated Density function after background subtraction.

Data Analysis

Data were analyzed using Microsoft Excel and plotted using Prism software (GraphPad Software, San Diego, CA). Values are means ± SEM. Unless otherwise noted, means were compared using two-tailed *t* tests, with Welch's correction if *F* test indicated

unequal sample variances. Differences were considered statistically significant if $P < 0.05$.

ACKNOWLEDGEMENTS

This research was conducted in collaboration with Bassil Kublaoui, Terry Gemelli, Yu Wang and Andrew R. Zinn and is Copyright 2008, The Endocrine Society. This work was supported by grants from the American Diabetes Association (1-05-RA-154) and National Institutes of Health (5K08DK073228 and 1RL1DK081185).

We thank Lane Jaeckle Santos, Elizabeth Keohane Bhoj, Clay Williams, John Shelton, James Richardson, Laurent Gautron, Toshiro Kishi, and Joel Elmquist for their assistance and Michael Schwartz for helpful discussions.

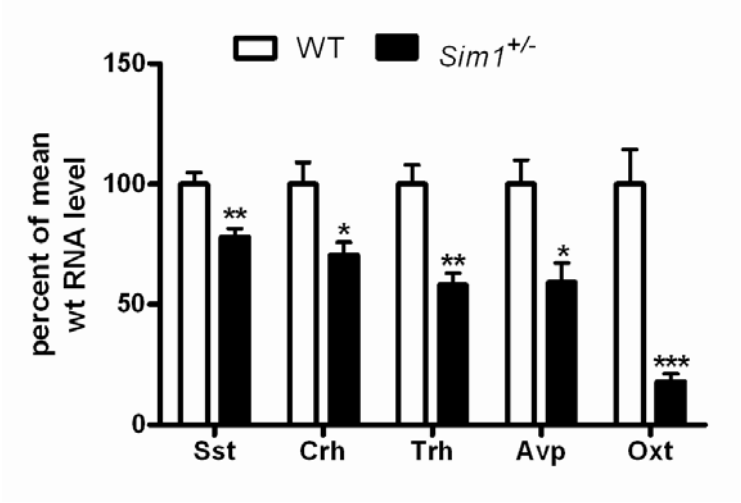

Figure III.1 *Sim1*$^{+/-}$ mice exhibit reduced mRNA expression of PVN neuropeptides. Real-time PCR showing hypothalamic expression of *Sst*, *Crh*, *Trh*, *Avp* and *Oxt* mRNA in *Sim1*$^{+/-}$ mice compared to wild-type mice (n=5 for each group). Groups were compared using a two-tailed unpaired t-test (*p<0.05; **p<0.01; ***p<0.001). Error bars indicate SEM.

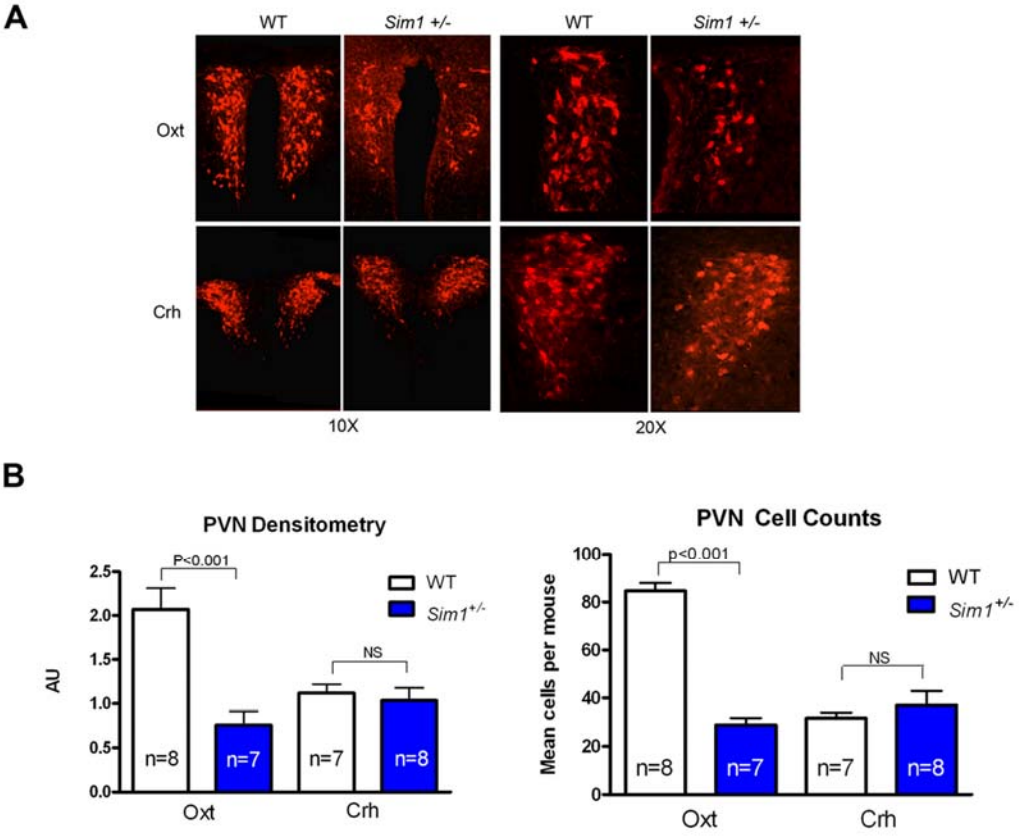

Figure III.2 *Sim1*$^{+/-}$ mice exhibit reduced expression of PVN Oxt but not Crh peptide. ***A***, Representative images of immunohistochemical analysis of Oxt and Crh peptides in PVN of *Sim1*$^{+/-}$ mice compared to wild-type mice (captured with 10X and 20X objectives). ***B***, Cell counts and densitometry measurements of Oxt and Crh immunohistochemistry. For ***B***, groups were compared using a two-tailed unpaired t-test (*p<0.05; **p<0.01; ***p<0.001). Error bars indicate SEM. Numbers of animals are shown in the figure.

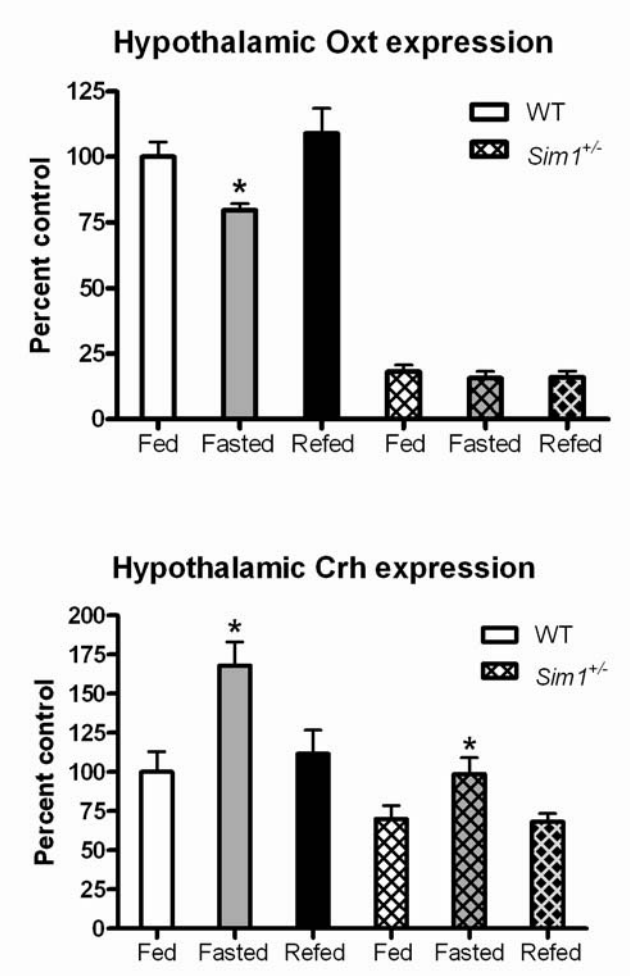

Figure III.3 *Sim1*$^{+/-}$ mice fail to regulate *Oxt* mRNA expression in response to feeding state. Real-time PCR showing hypothalamic expression of *Crh* and *Oxt* mRNAs in fed, fasted and refed *Sim1*$^{+/-}$ mice vs. wild-type mice (n=5 for all groups except wt fasted and *Sim1*$^{+/-}$ refed, where n=4). Each sub-group (e.g. wt Oxt) was analyzed using one-way ANOVA with Newman Keuls multiple comparison post-test. (*$p<0.05$ indicates that the fasted group is significantly different from the fed or refed groups).

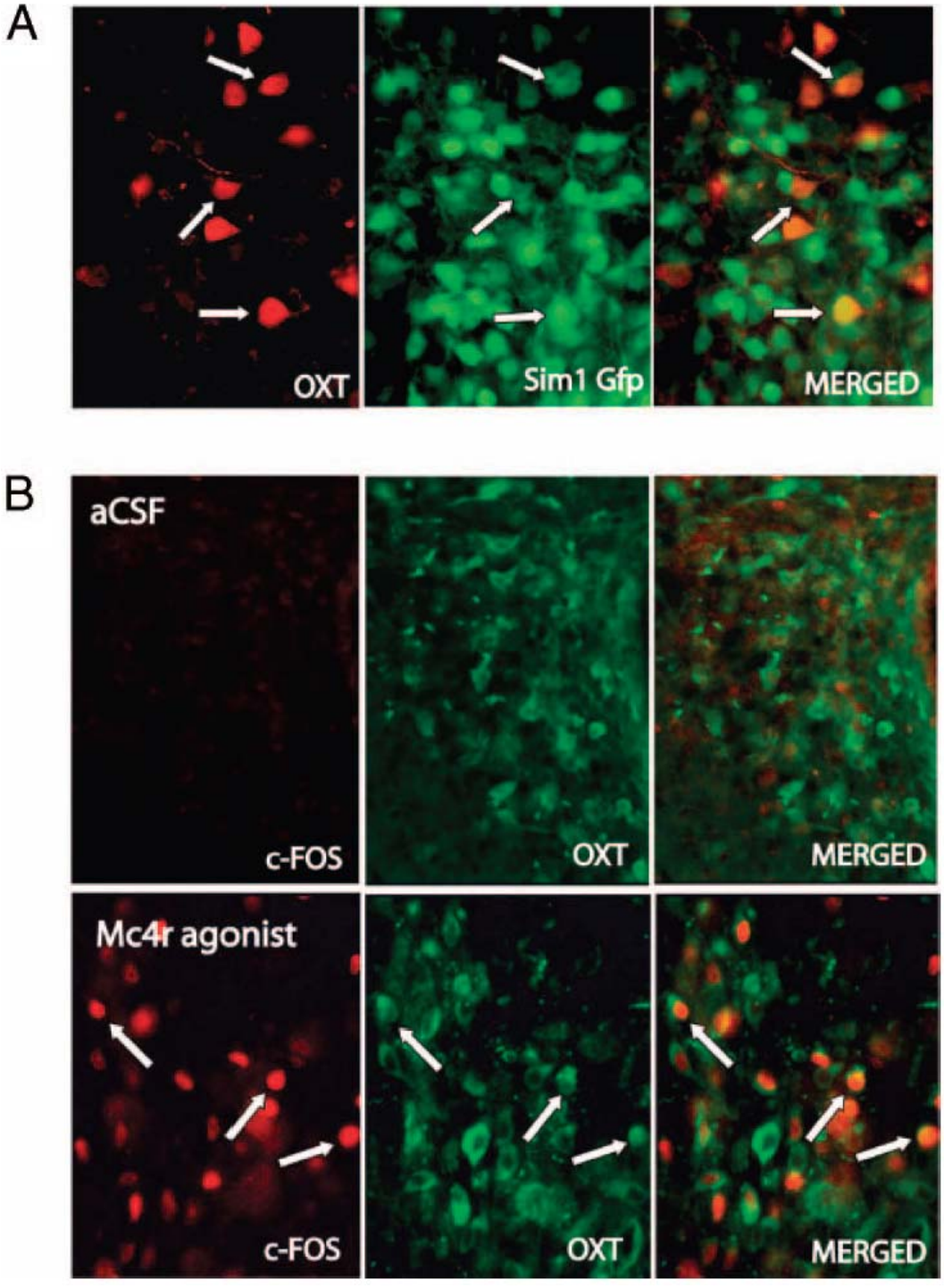
A
OXT
Sim1 Gfp
MERGED
B
aCSF
c-FOS
OXT
MERGED
Mc4r agonist
c-FOS
OXT
MERGED

Figure III.4 Oxt is colocalized with *Sim1* in PVN neurons and PVN Oxt neurons are activated by central Mc4r selective agonist injection. ***A***, Representative image showing colocalization of Oxt is in CY3 (red) and *Sim1*-GFP is in FITC (green), captured at 20X. Mice were not pretreated with colchicine. ***B***, Colocalization of Oxt and c-Fos after aCSF or Mc4r selective agonist (3µg) ICV. After Mc4r selective agonist treatment, most c-Fos^{+} neurons in the region shown are Oxt^{+} and many Oxt^{+} neurons are c-Fos^{+} (arrows). c-Fos is in CY3 (red) and Oxt is in CY2 (green), captured at 20X. Mice were pretreated with colchicine.

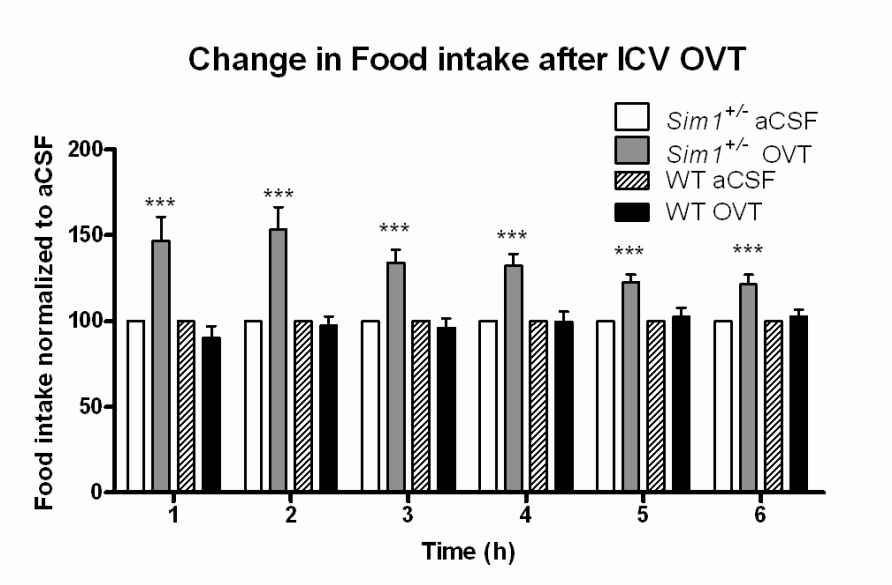

Figure III.5 Central administration of Oxt antagonist OVT exacerbates hyperphagia of *Sim1*$^{+/-}$ mice at a dose that does not affect food intake of wild-type mice. After one week of habituation to daily ICV injection, mice were injected at the onset of the dark cycle with aCSF on day 1 and 0.5µg OVT on day 2. OVT food intake was normalized to aCSF food intake for each mouse. Means were calculated for each treatment and compared using a paired t-test (n=14 for wt group, n=11 for *Sim1*$^{+/}$ group,***p<0.001.)

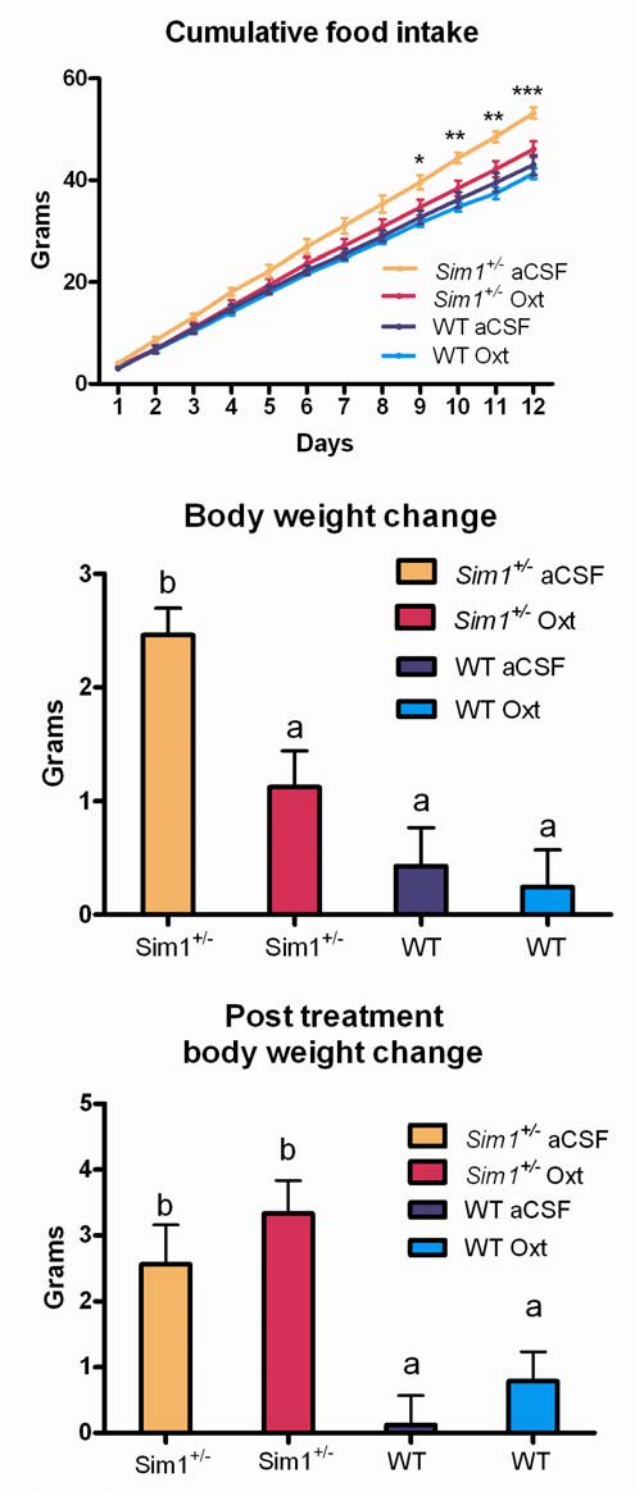
Cumulative food intake
Grams
Days
Sim1+/- aCSF
Sim1+/- Oxt
WT aCSF
WT Oxt
*
**
**
***
Body weight change
Grams
Sim1+/- aCSF
Sim1+/- Oxt
WT aCSF
WT Oxt
b
a
a
a
Sim1+/-
Sim1+/-
WT
WT
Post treatment
body weight change
Grams
Sim1+/- aCSF
Sim1+/- Oxt
WT aCSF
WT Oxt
b
b
a
a
Sim1+/-
Sim1+/-
WT
WT

Figure III.6 Central Oxt injection rescues hyperphagia and reduces weight gain of *Sim1*$^{+/-}$ mice but does not affect food intake or weight gain of wild-type mice.
A, B, After one week of habituation to twice daily ICV injection, mice were injected twice daily with either aCSF or 10ng Oxt. Food intake and body weight were measured daily for 12 days. Food intake was analyzed by two-way ANOVA (group vs. time) and body weight change with one-way ANOVA (group). Both analyses were done with a Bonferroni post-test to determine intergroup significance. ***C***, 12 days after the last injection (day 24) body weight was measured again and compared to body weight on day 12. Groups were compared using one-way ANOVA with a Bonferroni post-test. For A, *$p<0.05$; **$p<0.01$; ***$p<0.001$. For ***B*** and ***C***, groups with different letters are statistically different ($p<0.05$). n=7 for WT aCSF, n=5 for *Sim1*$^{+/-}$ aCSF, n=7 for WT Oxt, n=8 for Het Oxt.

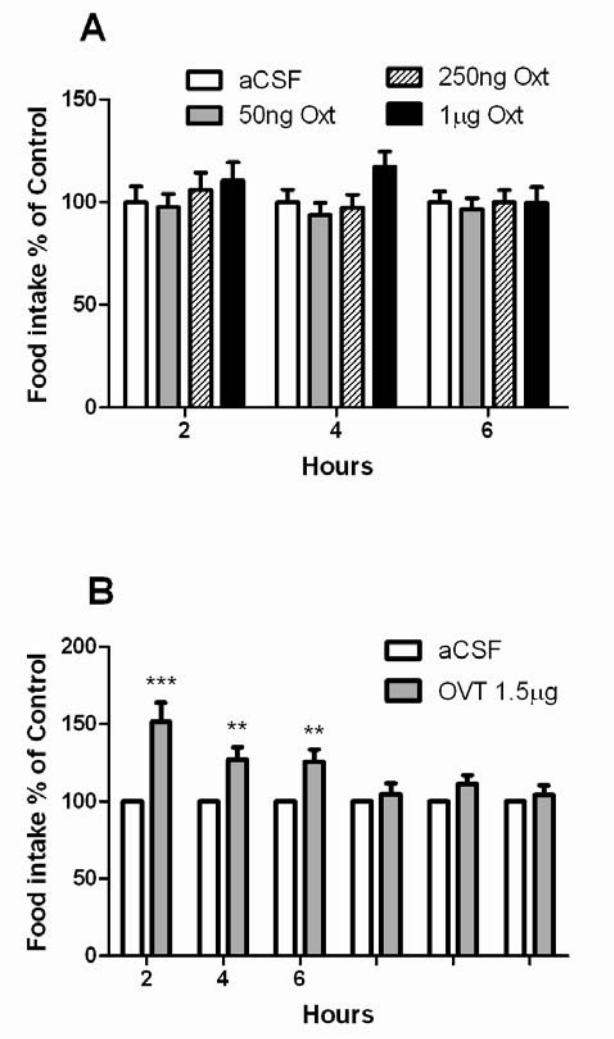

Figure III.7 Wild-type mice are insensitive to high doses of ICV Oxt but are sensitive to the Oxt antagonist OVT. ***A***, After one week of habituation to daily ICV injection, mice were injected at the onset of the dark cycle with either aCSF or 50ng, 250ng or 1μg of Oxt. Food intake was normalized to aCSF food intake for each mouse. Means were calculated for each treatment, and the groups at each time point were compared using one-way ANOVA (n=9, p=NS). ***B***, After one week of habituation to daily ICV injection, mice were injected at the onset of the dark cycle with aCSF on day 1 and 1.5μg OVT on day 2. Food intake was normalized to aCSF food intake for each mouse. Means were calculated for each treatment and the groups at each time point were compared using a paired t-test. (n=11, *p<0.05; **p<0.01; ***p<0.001).

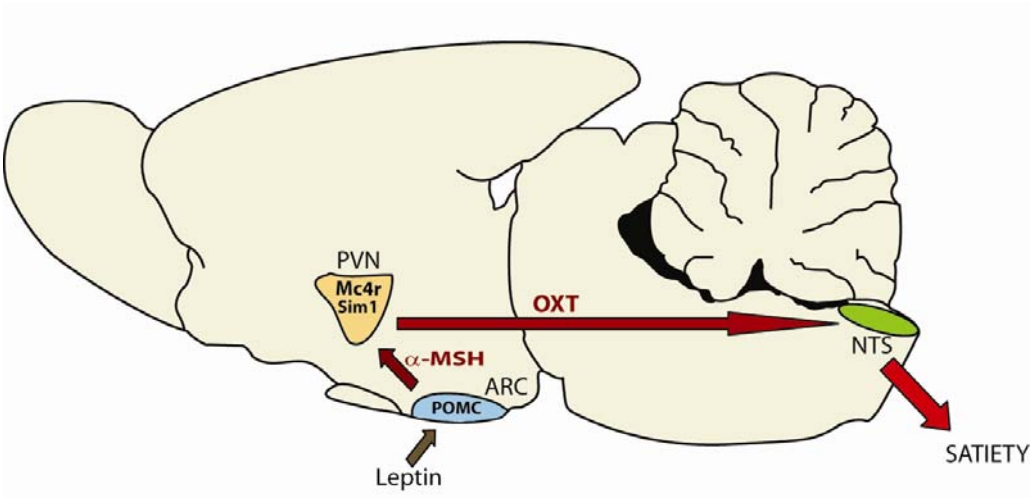

Figure III.8 Model showing ARC adiposity signals, e.g., leptin relayed via α-MSH to PVN parvocellular Oxt/Sim1 neurons projecting to the hindbrain, where they are integrated with satiety signals. PVN *Sim1* neurons may also integrate satiety signals from reciprocal projections from the NTS (not shown) with adiposity signals from the ARC and elsewhere in the brain.

Chapter IV

Conditional knockout of *Sim1*

INTRODUCTION

Single-minded 1 (*SIM1*) encodes a hypothalamic transcription factor in the bHLH-PAS (basic helix loop helix-Per Arnt Sim) family (Ward et al., 1998) and is one of only a handful of genes associated with human monogenic obesity (Holder et al., 2000; Farooqi and O'Rahilly, 2005). *Sim1* homozygous mice (*Sim1*$^{-/-}$) die perinatally and lack the anterior periventricular, paraventricular (PVN), and supraoptic (SON) hypothalamic nuclei (Michaud et al., 1998) due to failure of terminal migration and differentiation of the *Sim1* neurons (Xu and Fan, 2007). These nuclei, responsible for the production of multiple neuropeptides including oxytocin (Oxt), vasopressin, corticotropin-releasing hormone, thyrotropin-releasing hormone, and somatostatin, has long been implicated in energy balance from studies in multiple animal models (Heinbecker et al., 1944; Leibowitz et al., 1981). *Sim1* heterozygotes (*Sim1*$^{+/-}$) show hyperphagic obesity, increased linear growth and enhanced susceptibility to diet-induced obesity (Holder et al., 2004), associated with defective melanocortin 4 receptor (Mc4r) signaling (Kublaoui et al., 2006a) and reduced hypothalamic *Oxt* expression (Kublaoui et al., 2008); the phenotype is partially rescued by intracerebroventricular (ICV) Oxt administration (Kublaoui et al., 2008).

Whether the obesity phenotype of *Sim1*$^{+/-}$ mice is the result of a developmental or post-developmental hypothalamic defect is uncertain. Michaud et al. reported a mean reduction of 24% in the PVN cellularity of *Sim1*$^{+/-}$ mice and attributed their hyperphagic obesity to this congenital lesion of the hypothalamus (Michaud et al., 2001). Using a *Sim1*-GFP reporter transgene, we found no difference in the number of *Sim1*-expressing cells in *Sim1*$^{+/+}$ vs. *Sim1*$^{+/-}$ mice (Kublaoui et al., 2006a). Furthermore, we showed that

Sim1 transgenic overexpression did not affect hypothalamic morphology but partially rescued C57/Bl6 diet-induced obesity as well as hyperphagia and obesity of Agouti yellow mice, which have defective Mc4r signaling (Kublaoui et al., 2006b). Subsequently, Yang et al. (2006) reported that viral-mediated changes in *Sim1* hypothalamic expression in adult mice were inversely correlated with food intake, also supporting a physiologic role for *Sim1* in regulating food intake.

In order to dissociate the neuroanatomic and physiologic functions of *Sim1* in feeding regulation, we used two CamKII-Cre lines, Cre93 and Cre159, to conditionally delete *Sim1* in the postnatal brain (Minichiello et al., 1999; Rios et al., 2001). We bred viable conditional postnatal CNS homozygous *Sim1* knockout mice and measured their growth and feeding behavior. We examined the cellularity of germline *Sim1* heterozygotes and conditional postnatal *Sim1* homozygotes using unbiased stereology, as well as PVN projections to the hindbrain and median eminence in germline *Sim1* heterozygotes using retrograde tract tracing. We also assessed the expression of *Sim1*, *Oxt* and *Mc4r* mRNAs in the hypothalamus of mice with conditional postnatal *Sim1* deletion.

Another significant question is which neuronal subtype in the PVN is responsible for the hyperphagic obesity of $Sim1^{+/-}$ mice. The PVN has five major neuronal subtypes, distinguished on the basis of the neuropeptide they produce: oxytocin (Oxt), vasopressin (Avp), thyrotropin releasing hormone (Trh), corticotropin releasing hormone (Crh), and somatostatin (Sst). Oxt, Trh, and Crh have all been shown to have anorectic effects when injected into the hypothalamus, and all three neuropeptide mRNAs are reduced in *Sim1* heterozygotes, especially *Oxt*. Previous studies by others have implicated *Oxt* neurons in

feeding behavior (Arletti et al., 1989; Olson et al., 1991b; Blevins et al., 2003), and *Oxt* neurons projecting from the PVN to the NTS are thought to form part of the link between adiposity and satiety signals (Kirchgessner et al., 1988; Blevins et al., 2003). Also of note, *Sim1* is part of a conserved genetic pathway for *Oxt* neuron development (Eaton and Glasgow, 2006). Although *Oxt* neurons are present in *Sim1*$^{+/-}$ mice, *Oxt* mRNA and peptide levels are dramatically reduced and central injections of Oxt rescue their hyperphagia (Kublaoui et al., 2008).

To test whether conditional *Sim1* deficiency in *Oxt* neurons is sufficient to cause hyperphagic obesity, we used an Oxt-Cre transgene to conditionally delete *Sim1* specifically in *Oxt* neurons. Oxt-Cre transgenic mice were generated by Dr. David Olson in the laboratory of Dr. Bradford Lowell at Beth Israel Deaconess Medical Center, Boston, MA. We created *Oxt*-neuron specific *Sim1* heterozygotes and homozygotes and measured their growth and feeding behavior. We also assessed the expression of *Sim1*, and *Oxt* mRNAs in the hypothalamus of these mice.

RESULTS

Validation of Cre-loxP Sim1 inactivation

Previously, germline *Sim1* heterozygous mice were generated using a floxed *Sim1* allele that contained 3 loxP sites and a *pGK-Neo* cassette crossed with an EIIa-Cre transgene (Holder et al., 2004). From the same floxed *Sim1* line, a 2 loxP allele was created by excising the *pGK-Neo* cassette. These two loxP sites flank the first exon of *Sim1*, which contains the start codon and the first 17 amino acids of *Sim1*.

To confirm that recombination of this floxed *Sim1* allele would recapitulate a *Sim1* null allele, we used a ubiquitously expressed EIIa-Cre to achieve germline deletion and studied the progeny. Three week old mice were weaned onto a high fat diet containing about 35% dietary fat (HF), allowed to feed *ad libitum*, and weighed weekly (Figure IV.1, A–B). After one week on the HF diet, both male and female *Sim1* heterozygotes weighed significantly more than their controls. At 8 weeks of age, *Sim1* heterozygous males weighed 44% more (Figure IV.1 A) and *Sim1* heterozygous females weighed 73% more (Figure IV.1 B) than control littermates on the HF diet. Similar sex differences have been observed previously (Holder et al., 2004). Heterozygotes of either gender continued to gain weight until the experiment was terminated at 12 weeks of age. PCR showed that the recombined floxed *Sim1* allele was the expected size (Figure IV.1 C); the 371bp band shows the wild type allele and the 160bp band shows the recombined allele. These results recapitulated the previously reported phenotype of *Sim1* heterozygotes (Holder et al., 2004), confirming the utility of the floxed *Sim1* allele.

Expression of CamKII-Cre in the PVN and SON

To conditionally delete *Sim1* postnatally, we obtained two CamKII-Cre lines that have been previously described, CamKII-Cre93 and CamKII-Cre159, hereafter referred to as Cre93 and Cre159 (Minichiello et al., 1999; Rios et al., 2001). In both of these lines, the Cre transgene expression is driven by the α-calcium/calmodulin-dependent protein kinase II (CamKII) promoter, which is expressed in postmitotic neurons (Minichiello et al., 1999). Cre93 was reported to begin expression shortly after birth with wide activation at P21 (Rios et al., 2001), and Cre159 expression was not reported until after P15, with full

recombination occurring around P28 (Minichiello et al., 1999; Rios et al., 2001). Both lines showed transgene expression in the hypothalamus, but the PVN and SON were not specifically examined at the time.

To confirm expression of the Cre transgene in these hypothalamic nuclei, both lines were crossed to a Rosa26-eYFP line, which contains a STOP cassette flanked by loxP sites inserted between the Rosa26 promoter and eYFP and expresses eYFP only in cells producing Cre recombinase (Srinivas et al., 2001). We then performed immunohistochemistry on adult progeny to detect eYFP in the PVN and SON. Cre93, Rosa26-eYFP double transgenic mice exhibited strong staining in the PVN as well as the SON in both males and females (Figure IV.2, A-D). Cre159, Rosa26-eYFP double transgenic mice also showed staining in the PVN (Figure IV.3, A-B) in both sexes, although it was not as strong as the Cre93 staining, and staining in the SON was negligible (data not shown). Some eYPF expression at P10 was also noted (data not shown), which is earlier than the previously reported start of expression at P15 (Minichiello et al., 1999; Rios et al., 2001), but still well after the formation of the PVN and SON.

Growth and feeding behavior of conditional postnatal Sim1 heterozygous mice

Some Cre transgenes cause weight phenotypes themselves (Schmidt-Supprian and Rajewsky, 2007). To control for possible effects of the Cre93 and 159 transgenes on weight, three week old transgenic mice were weaned onto a low fat diet (LF). Cre93 mice and wild type littermates were weighed weekly from age 9-18 weeks (Figure IV.4, A-B), with no observable difference in weight. Cre159 mice and wild type littermates were

weighed every three weeks from age 9-18 weeks (Figure IV.4, C-D), also with no observable difference in weight.

To achieve conditional postnatal *Sim1* heterozygous deletion, we first crossed the floxed *Sim1* mice ($Sim1^{fl/fl}$) to the Cre93 line. Genotyping of tail and liver biopsies of progeny (not shown) confirmed the absence of germline recombination due to aberrant transgene expression ("delta effect"). Three week old progeny were weaned onto a HF diet and weighed weekly (Figure IV.5, A–B). After two weeks on the HF diet, both male and female heterozygotes (cHet93: Cre93, $Sim1^{+/fl}$) weighed significantly more than their littermate controls. At 8 weeks of age, heterozygous males weighed 23% more (Figure IV.5 A) and heterozygous females weighed 36% more (Figure IV.5 B) than control littermates on the HF diet. Heterozygotes of either gender continued to gain weight until the experiment was terminated at 12 weeks of age. To determine if the obesity of the cHet93 mice was due to hyperphagia, male cHet93 mice and littermate controls were weaned at 3 weeks on a LF diet, individually housed, and their body weights and food intakes measured weekly. cHet93 mice also became significantly obese on a LF diet after 5 weeks of age (Figure IV.6 A), preceded by significant hyperphagia at 4 weeks of age (Figure IV.6 B). The cumulative excess food intake by cHet93 mice was an average of 80 grams per mouse over the 9 week period they were monitored. Additionally, measurements of the $Cre93^{+}$ and $Sim1^{+/fl}$ littermates confirmed that in the absence of *Sim1* recombination the Cre transgene or the floxed *Sim1* allele alone did not cause weight or feeding differences

Effects of conditional postnatal homozygous deletion of Sim1 on body weight, length, food intake, and gross appearance

Conventional homozygous inactivation of *Sim1* results in death shortly after birth (Michaud et al., 2001; Holder et al., 2004). To determine if conditional postnatal homozygous *Sim1* inactivation also results in lethality, we generated cKO mice (Cre, $Sim1^{fl/fl}$) by crossing cHet mice with $Sim1^{fl/fl}$ mice. Male cHet mice caused aberrant germline recombination in their progeny, so only the progeny of female cHet mice were used. Genotyping of tail biopsies or postmortem livers (data not shown) confirmed the absence of germline recombination in these progeny.

Conditional postnatal *Sim1* homozygotes created with the Cre93 transgene (cKO93: Cre93, $Sim1^{fl/fl}$) were viable and showed no visible signs of illness. *Sim1* has been suggested to act in a dose-dependent manner (Kublaoui et al., 2006b), so we weaned cKO93, cHet93 mice and littermate controls at 3 weeks of age onto a LF diet measured their and body weights weekly. cKO93 mice developed even more severe obesity than cHet93 mice (Figure IV.7 A) and exhibited increased length (Figure IV.7 B). A similar, but less dramatic weight phenotype was observed in cKO159 (cKO159: Cre159, $Sim1^{fl/fl}$) and cHet159 (cHet159: Cre93, $Sim1^{+/fl}$) mice on a LF diet (Figure IV.8, A-B).

To determine if the obesity of cKO93 mice was due to hyperphagia, mice were weaned at onto a LF diet, housed individually, and their food intake and body weights measured weekly. The mice exhibited hyperphagia before becoming grossly obese (Figure IV.9 A), with male cKO93 mice consuming about 25% more calories per week and female cKO93 mice consuming about 40% more calories per week than littermate

controls (Figure IV.9 B). The obesity phenotype was clearly observable at age 12 weeks on the LF diet (Figure IV.9 C).

Stereologic analysis of the number of cells in the PVN of germline Sim1 heterozygotes and conditional postnatal Sim1 homozygotes

We used unbiased stereologic analyses to determine whether a reduction in cellularity of the PVN accounts for the hyperphagic obesity of $Sim1^{+/-}$ or cKO93 mice, . There was no statistically significant difference in the number of Nissl-stained cells in the PVN of wild-type vs. germline *Sim1* heterozygotes ($p = 0.2433$) (Figure IV.10), in agreement with our previous results using nonstereologic methods (Kublaoui et al., 2006a). Additionally, there was no statistically significant difference in the number of PVN cells or between controls vs. cKO93 ($p = 0.0952$) (Figure IV.10). Thus loss of PVN neurons did not explain the hyperphagic obesity observed in these mice.

Retrograde tract tracing in germline Sim1 heterozygotes

Another possible cause of the hyperphagic obesity of $Sim1^{+/-}$ mice is faulty development of projections of PVN *Sim1* neurons to the hindbrain or the median eminence (ME). To test this possibility, we used retrograde tract tracing to examine these projections in adult mice. Projections to the ME were traced using Fluoro-Gold (FG) (Figure IV.11, A-D), and retrograde tract tracing from the dorsal vagal complex (DVC) was accomplished by using the cholera toxin b subunit (CTb) (Figure IV.11, E-H). The results clearly demonstrated the presence of intact projections from the PVN to the DVC and ME that

were qualitatively indistinguishable from those seen in wild-type controls. We did not attempt to quantitate projections due to injection site variability.

Expression of Sim1, Oxt and Mc4r mRNAs in conditional postnatal Sim1 inactivation

As no suitable antibodies are available for Sim1 immunohistochemistry, we assessed the efficiency of *Sim1* recombination in the conditional postnatal *Sim1* heterozygotes and homozygotes by measuring hypothalamic *Sim1* mRNA levels. We found *Sim1* to be reduced by around 60% in cHet93 and over 90% in cKO93 (Figure IV.12 A) compared to control littermates. The Cre159 transgene showed a more moderate reduction of *Sim1* mRNA of about 30% in the cHet159 and about 40% in the cKO159 (Figure IV.13 A) compared to controls, probably accounting for the less severe weight phenotypes observed in these mice.

As oxytocin has been implicated in the hyperphagic obesity of $Sim1^{+/-}$ (Kublaoui et al., 2008), we also used qPCR to measure *Oxt* levels. The amount of *Oxt* reduction correlated well with *Sim1* reduction: *Oxt* expression was reduced in the cHet93 by around 50% and the cKO93 by around 90% (Figure IV.12 B), and in the cHet159 by around 30% and the cKO159 by around 40% (Figure IV.13 B), all compared to their respective control littermates.

We previously reported that *Mc4r* expression in the whole hypothalamus was not decreased in *Sim1* heterozygotes (Holder et al., 2004). However, we observed a trend toward decreased *Mc4r* expression in the whole hypothalamus of the cKO93 compared to controls that was not statistically significant (data not shown). Using laser capture

microdissection to isolate the PVN, we saw a significant decrease in *Mc4r* expression in both germline *Sim1* heterozygotes (30%) as well as cKO93 (70%) (Figure IV.12 C).

Expression of Oxt-Cre in the PVN and SON

We obtained Oxt-Cre transgenic mice from Dr. David Olson in the laboratory of Dr. Bradford Lowell. Their initial data generated from crossing these Oxt-Cre mice to Rosa26-eYFP reporter mice showed, at maximum, recombination in 35% of Oxt neurons of the PVN and SON (Figure IV.14 A). In our hands, we saw a greater amount of recombination in the PVN and SON (Figure IV.14 C-D). To confirm that this recombination was in oxytocin neurons, we then performed a double immunohistochemistry for Oxt and eYFP (Figure IV.15 A-D), with Oxt represented by red and eYFP represented by green. The yellow coloring indicating colocalization of eYFP and Oxt was extensive, suggesting that recombination was occurring largely in oxytocin neurons. Mice were not pretreated with colchicine, so the extent of oxytocin expression may be greater than we observed.

Growth of mice with oxytocin neuron conditional Sim1 deletion

To test whether conditional *Sim1* deficiency in Oxt neurons is sufficient to cause hyperphagic obesity, we crossed Oxt-Cre mice with *Sim1* floxed mice. Three week old mice were weaned onto a HF diet and weighed weekly (Figure IV.16 A–B). The $OxtCre^{+}$ and $Sim1^{+/fl}$ littermates confirm that the Cre transgene and floxed allele do not cause significant weight differences on their own. No significant differences were seen between cHet-Oxt (OxtCre, $Sim1^{+/fl}$) and the littermate controls even at 20 weeks of age, although

the male data (Figure IV.16 A) suggested a possible trend towards obesity. We then used cHet-Oxt mice to breed cKO-Oxt (OxtCre, $Sim1^{fl/fl}$), who were also weaned onto a HF diet and weighed weekly (Figure IV.17 A–B). Again, we saw no difference in weight of cHet-Oxt or cKO-Oxt in either sex. The experiment was terminated early because of these results and the qPCR data.

Expression of Sim1 and Oxt mRNAs in oxytocin neuron conditional Sim1 deletion

Concurrent to the cKO-Oxt experiment, we collected hypothalami from cHet-Oxt mice that had completed that study and performed qPCR. Our results indicated no reduction of expression of *Sim1* (Figure IV.18 A) or *Oxt* (Figure IV.18 B) in heterozygotes compared to control littermates.

DISCUSSION

Evidence for both developmental (Michaud et al., 1998; Michaud et al., 2001) and post-developmental roles (Kublaoui et al., 2006b; Yang et al., 2006) for *Sim1* exist; to answer which is important for the regulation of feeding, we took advantage of CamKII-Cre expression in post-mitotic neurons to generate conditional postnatal *Sim1* deficient mice. The results of our studies strongly support a postnatal role for *Sim1* in hyperphagic obesity.

As some Cre transgenes have been reported to cause weight phenotypes (Schmidt-Supprian and Rajewsky, 2007), it was important for us to confirm that neither of the Cre lines would confound our results. To control for possible Cre effects, we

collected weight curves of the Cre93 and 159 transgenes compared to their wild type littermates out to 18 weeks, which is older the ages of the mice used in the conditional *Sim1* knockout experiments. Additionally, we included Cre positive, loxP negative controls in our conditional experiments. None of our Cre transgenes had a significant effect on any parameters that we observed.

The sex differences in some of our results are consistent with commonly observed differences between male and female responses; many studies have shown variance in response to high-fat diets, regulation of the neuropeptide Y signaling system in the hypothalamus, and leptin levels (Kennedy et al., 1997; Zammaretti et al., 2007; Huang et al., 2008; Hwang et al., 2009). While there is not a clear-cut explanation for these differences, sex hormone levels may be involved.

Given the incomplete efficiency of conditional gene inactivation in most Cre-loxP systems, including Cre159 (Minichiello et al., 1999), and the fact that these experiments were conducted on animals of mixed background, the conditional deletion of *Sim1* with Cre93 and 159 exhibited a robust phenotype. The development of early onset obesity even on a low fat diet suggests that the hyperphagic obesity of *Sim1* deficient mice is largely, if not entirely, due to a physiological effect of *Sim1* haploinsufficiency rather than a fixed developmental defect. Additionally, we were successful in creating viable conditional *Sim1* homozygous mice lacking 90% of *Sim1* expression. The severity of hyperphagic obesity correlated with the reduction of *Sim1* expression in conditional heterozygotes vs. homozygotes and in Cre93 vs. Cre159 progeny, corroborating our previous inference from studies of germline heterozygotes and *Sim1* overexpressing

transgenics that *Sim1* has dose dependent effects (Holder et al., 2004; Kublaoui et al., 2006b).

Whether or not the PVN of *Sim1* heterozygous mice is hypocellular is contested. Conventional *Sim1* homozygous mice lack the PVN and SON and die shortly after birth (Michaud et al., 1998). While the absence of these nuclei in these mice was originally attributed to cell death or fate switching (Michaud et al., 1998), it has since been shown that the $Sim1^{-/-}$ neurons survive until birth, but do not properly migrate (Xu and Fan, 2007). As germline *Sim1* homozygous mice do not survive postnatally, they were unable to determine the survival of *Sim1* neurons beyond birth. Initial reports on the conventional *Sim1* heterozygous mice showed a 24% decrease in cellularity (Michaud et al., 2001), but our data did not show a decrease in the number of *Sim1* neurons (Kublaoui et al., 2006a). While the differing findings could represent genetic background effects, neither our previous data nor those of Michaud et al. were corrected for double-counting, e.g., by the method of Abercrombie (Abercrombie and Johnson, 1946) or by using a stereological technique (Coggeshall and Lekan, 1996). Our cKO93 mice allowed us to examine whether ongoing *Sim1* expression is needed for the survival of PVN neurons into adulthood as well as to further address the relationship between PVN cellularity and hyperphagic obesity in *Sim1*-deficient animals. If there were a reduction in PVN cellularity in conventional *Sim1* heterozygotes, then this would be expected to be more magnified in cKO93 mice. Using unbiased stereological analysis, we show that neither conventional *Sim1* heterozygotes nor conditional *Sim1* homozygotes have significant hypocellularity. The normal cellularity of the PVN even in adult cKO93 mice strongly argues that hypocellularity is not the mechanism of hyperphagia in *Sim1* deficiency and

definitely dissociates the hyperphagic obesity of these mice from the formation of the PVN. We cannot rule out a small, selective deficit of a subpopulation of PVN neurons, but as all PVN neurons are affected in *Sim1*$^{-/-}$ mice, we consider this unlikely.

Another possible developmental defect that could cause the hyperphagia of these mice is the abnormal development of PVN neuronal projections. Neurogenesis of the mouse and rat PVN is completed by 13-15 days post-coitum, 8-10 days before birth (Angevine, 1970; Shimada and Nakamura, 1973; Karim and Sloper, 1980) and therefore prior to the expression of our Cre93 and 159 lines. However, PVN neuronal projections – in particular, oxytocinergic neurons projecting to the NTS – continue to develop postnatally. Data from mice are not available, but in rats, the development of PVN to hindbrain projections (reviewed in (Rinaman, 2006)) is completed by postnatal day 20. We examined the projections from the PVN to the hindbrain as well as the median eminence (ME) in conventional *Sim1* heterozygotes and wild type littermates and saw no qualitative difference. Together with the results from the conditional heterozygotes and homozygotes, these results argue strongly that the hyperphagic obesity of these mice is not due to a fixed developmental defect (Michaud et al., 2001) and support the hypothesis that *Sim1* plays a physiologic role in feeding regulation (Kublaoui et al., 2006a; Kublaoui et al., 2006b; Yang et al., 2006).

Sim1 is closely associated evolutionarily with oxytocin neurons (Eaton and Glasgow, 2006). The previous observation of reduced oxytocin (*Oxt*) expression in *Sim1* heterozygotes (Kublaoui et al., 2008) was reproduced in mice with conditional postnatal *Sim1* deficiency. The present findings show that the amount of *Sim1* reduction correlates with the amount of *Oxt* reduction, which in turn correlates with the severity of

hyperphagic obesity. These results support previous findings indicating the importance of Oxt deficiency in mediating the phenotype of *Sim1* deficient mice (Kublaoui et al., 2008). Although the most likely cause of the differing severity of obesity between the cKO93 and cKO159 mice is the difference in the levels of *Sim1* and *Oxt* reduction, we cannot rule out the possibility that later expression of the Cre159 line could also be a factor.

We previously showed that PVN neurons of *Sim1*$^{+/-}$ mice are hyporesponsive to activation by MTII, an MC3R/MC4R agonist (Kublaoui et al., 2006a), with no reduction of *Mc4r* expression in whole hypothalamus of these mice (Holder et al., 2004). However, in the present study using LCM to isolate the PVN, we found that *Mc4r* expression was decreased by > 30% in *Sim1*$^{+/-}$ mice and > 70% in cKO93 compared to their respective control littermates. To our knowledge, this is the first time that another gene has been shown to affect *Mc4r* expression.

It is notable that decreased *Mc4r* expression is consistent with our previous data showing resistance of *Sim1* heterozygous mice to the effect of MTII on food intake as well as c-Fos activation in the PVN (Kublaoui et al., 2006a). While the decrease in PVN *Mc4r* expression is intriguing, we do not yet know if this deficiency is partially or fully responsible for the obesity phenotype of *Sim1* deficient mice. Inactivation of *Mecp2* in *Sim1* neurons is sufficient to cause hyperphagic obesity without a decrease in *Mc4r* (Fyffe et al., 2008), but it has also been demonstrated that *Mc4r* expression in *Sim1* neurons controls food intake (Balthasar et al., 2005). It is not clear if there is direct regulation of *Mc4r* or *Oxt* by *Sim1*, or *Oxt* by *Mc4r*, but PVN *Oxt* neurons and Oxt itself are known to interact with leptin and CCK in the NTS to control food intake (Blevins et al., 2003; Blevins et al., 2004). In addition we showed that ICV replacement of Oxt

rescued the hyperphagia of *Sim1* heterozygous mice (Kublaoui et al., 2008). It is unclear if Mc4r activation and *Oxt* expression and activity are in a linear pathway, or if they function in parallel. If they are in parallel pathways, it is unclear which is the predominant cause of the hyperphagic obesity of *Sim1* deficient mice.

Whether these decreases in *Oxt* and *Mc4r* represent defects in specific signaling pathways, or are part of a global dysfunction of these neurons has yet to be determined. Neither gene has been shown to be a direct transcriptional target of Sim1 (Liu et al., 2003a). The previously observed abnormal response of PVN neurons in *Sim1*$^{+/-}$ mice to MTII but not to hypertonic saline (Kublaoui et al., 2006a) suggests a selective defect. On the other hand, it is possible that *Sim1* is required to maintain the differentiated gene expression program of PVN neurons, and as with neuroanatomic lesions (Heinbecker et al., 1944; Leibowitz et al., 1981), the predominant phenotypic effect of global PVN dysfunction is a change in feeding regulation. Further neuroendocrine studies of conditional *Sim1* homozygotes should allow us to resolve this issue.

Our results with the Oxt-Cre mice were inconclusive. No weight phenotype was observed, even on a high fat diet at 20 weeks of age. While initial data suggested that this Cre transgene would cause widespread recombination in the Oxt neurons, we observed no decrease in the amount of *Sim1* expression. Although it is likely that the Oxt-Cre transgene did not cause a decrease in *Sim1* due to lack of recombination of the floxed allele, it is also possible that we could not detect the small difference since the qPCR was of the hypothalamus and not solely the PVN and SON. The lab that created these mice have concluded that the transgene is ineffective and have been working on creating another line. It is, however, a possibility that our results were correct and that *Sim1*

deficiency in oxytocin neurons is not sufficient to cause hyperphagic obesity, particularly if the reported *Sim1* interneurons are the critical neurons for the obesity phenotype (Cowley et al., 1999).

Regardless of the specific mechanism(s) by which *Sim1* deficiency causes hyperphagia, our results corroborate previous findings that *Sim1* acts postnatally in a dosage-sensitive manner to regulate feeding (Yang et al., 2006). *Sim1* and it's yet to be identified transcriptional target genes are thus potential targets for pharmacologic agents for the treatment obesity. Importantly, *Sim1* neurons in the PVN (and/or possibly amygdala) that express *Mc4r* regulate food intake but not energy expenditure, and the predominant phenotype of *Sim1* deficiency appears to be hyperphagia. Therefore, targeting *Sim1* neurons for appetite suppression may have fewer side effects than other therapeutic strategies.

METHODS

Animals and genotyping

Studies were performed in animals of mixed genetic background; therefore littermates were used as controls for all experiments. Animals were group housed and maintained in a temperature-controlled room under a standard 12 h:12 h light-dark cycle with *ad libitum* access to water and low fat (LF), low phytoestrogen diet (Teklad Global Diet 2016) unless specifically indicated otherwise. All experimental protocols were approved by the UT Southwestern Institutional Animal Care and Use Committee and are in accord with accepted standards of humane animal care. Male and female C57Bl/6 mice were obtained from the National Cancer Institute at 4-5 weeks of age for breeding. Floxed

Sim1 mice (The Jackson Laboratory (JAX) stock number 007570, *Sim1*$^{fl/fl}$), whose first exon of *Sim1* is flanked by 2 loxP sites, were obtained as previously described (Holder et al., 2004). EIIa-Cre mice were obtained from JAX (stock number 003314) and exhibit early widespread Cre recombinase expression (Lakso et al., 1996). α-calcium/calmodulin-dependent protein kinase II-Cre (CamKII-Cre) 93 and 159 lines were obtained from Rudolf Jaenisch, Whitehead Institute, Cambridge, MA and have been previously described (Minichiello et al., 1999; Rios et al., 2001). Oxt-Cre transgenic mice were generated by Dr. David Olson in the laboratory of Dr. Bradford Lowell at Beth Israel Deaconess Medical Center, Boston, MA. He subcloned a fragment of genomic DNA containing all Oxt exons plus 10 kb of upstream flanking sequences as well as the vasopressin gene and flanking sequences. He then inserted an open reading frame encoding Cre recombinase and a polyadenylation signal after the initiator methionine codon of the Oxt gene. To prevent vasopressin overexpression, he deleted its initiator methionine and 5' flanking sequences. The resulting construct was injected into pronuclei of fertilized mouse oocytes, and a transgenic line expressing Cre recombinase in the hypothalamus was obtained. Rosa-eYFP (Srinivas et al., 2001) mice were obtained from the Jackson Laboratory (JAX stock number 006148).

Genomic DNA was isolated from tail biopsies using HotSHOT as previously described (Truett et al., 2000) and postmortem liver biopsies using Wizard Genomic DNA Purification Kit (Promega, Madison, WI), and was genotyped using polymerase chain reaction (PCR). The floxed *Sim1* allele was detected using primers L2R 5'-GAC TTT TCT TTC ATC GTG TCT CGG-3' and Z1F 5'-CAT TCG TGT CTT CCC GGA GCA AAC TTC-3'. The Rosa-eYFP transgene was detected using the primers described

on The Jackson Laboratory's website (http://jaxmice.jax.org/); 2163 Rosa 5'-GCG AAG AGT TTG TCC TCA ACC-3', 2164 Rosa 5'-GGA GCG GGA GAA ATG GAT ATG-3', 2165 Rosa 5'-AAA GTC GCT CTG AGT TGT TAT-3'. To detect Cre transgenes primers Cre800 5'-GCT GCC ACG ACC AAG TGA CAG CAA TG-3' and Cre1200 5'-GTA GTT ATT CGG ATC ATC AGC TAC AC-3' (Holtwick et al., 2002) were used with OL260 5'-CAT ACT GCA TGT GTC TTG GTG GGC TGA GCC-3' and OL261 5'-GAA TCC TGT GCA ATA CTC ACC ACT CCA GGC-3' as internal controls.

Growth and Feeding Studies

Mice were genotyped and weaned onto their respective diets at three weeks of age and fed *ad libitum* with either a low fat (LF), low phytoestrogen diet (Global Diet 2016; Teklad, Madison, WI; 3.2 kcal/g, with 56.0% available carbohydrate, 4.2% crude fat, and 16.7% crude protein) or a high fat (HF) diet (D12492; Research Diets, New Brunswick, NJ; 5.24 kcal/g, with 26.3% available carbohydrate, 34.9% available fat, and 26.2% available protein) unless stated otherwise. Animals of both sexes were group housed, except cohorts used to measure food intake which were individually housed. Food consumption and body weight were measured weekly, and data were analyzed and plotted as mean ± standard error.

Tissue collection for immunostaining and stereology

For immunostaining and stereology, mice were deeply anesthetized with pentobarbital (7.5mg/0.15ml, IP) and transcardially perfused with 10 ml of heparinized saline (10U/ml, 2 ml/min) followed by 10 ml of phosphate-buffered 4% paraformaldehyde (PFA). Brains

were removed, post-fixed for 24 hours in 4% PFA, and then equilibrated in 30% sucrose in PBS for 72 hours. Brains were coronally sectioned (35 μm for immunostaining, 50 μm for stereology) on a sliding microtome (Leica SM 2000R; Wetzlar, Germany).

Immunohistochemistry

Immunohistochemistry was performed as described previously (Beuckmann et al., 2004; Kublaoui et al., 2006a; Kublaoui et al., 2008). For fluorescent YFP labeling, 35 μm coronal brain sections that had been stored in PBS at 4º were permeabilized and blocked in 3% normal goat serum/0.3% Triton X-100 for 1 hour, incubated at 4º overnight in GFP antibody (FITC) (1:5,000, ab6662, Abcam Inc., Cambridge, MA). Sections were placed in 4',6-diamidino-2-phenylindole (DAPI) (0.2 μg /ml, 236276; Roche, Indianapolis, IN) for 10 minutes and then mounted on plus coated slides and coverslipped using Vectashield (H-1000; Vector Laboratories, Burlingame, CA). For fluorescent GFP and Oxt double labeling, sections were incubated for 48 hours in rabbit anti-GFP antiserum (A6455, 1:5000; Molecular Probes, Eugene, OR) and mouse anti-Oxt antiserum. Sections were then incubated with fluorescein isothiocyanate goat antirabbit IgG secondary antiserum and Cy-2 affiniPure goat antimouse IgG secondary antiserum (115-225-166, 1:400; Jackson ImmunoResearch) for 2 hours at room temperature. Sections were treated with DAPI and mounted as described above. Images of sections containing PVN and SON were captured on an Olympus BX61 microscope using Cytovision software (Applied Imaging Corp., San Jose, CA).

For diaminobenzidine tetrahydrochloride (DAB) staining of YFP positive cells, brain sections were pretreated with 0.3% hydrogen peroxide in PBS for 30 minutes at

room temperature and then blocked with 3% normal goat serum/0.3% Triton X-100/PBS for 2 hours at room temperature. Sections were incubated overnight at 4º with GFP rabbit primary antiserum (1:80,000, A6455, Molecular Probes, Eugene, OR) in 0.3% Triton X-100/PBS. After washing in PBS, sections were incubated in biotinylated goat anti-rabbit secondary antibody diluted in 0.3% Triton X-100/PBS (1:600, BA-1000, Vector Laboratories, Burlingame, CA) for 30 minutes and then washed in PBS, followed by Horseradish peroxidase strepaviden diluted in 0.5% Triton X-100/PBS for 30 minutes (1:500, SA-5004, Vector Laboratories, Burlingame, CA), both at room temperature. After washing in PBS, the sections were incubated in a solution of hydrogen peroxide charged DAB (DAB Chromogen, Dako North America, Inc., Carpinteria, CA) in 0.05% Tris pH 7.6 with nickel enhancement. Sections were mounted on plus coated slides, air-dried, dehydrated in graded ethanols, cleared in xylenes, and coverslipped with Permount (Fisher Scientific, Pittsburgh, PA). Images of sections containing PVN and SON were captured on a Leica DM2000 with Microfire camera and PictureFrame 2.0 software (Optronics, Goleta, CA).

Stereological analyses

Nissl staining was performed as previously described (Gerfen, 2003). Briefly, coronal sections (50 μm) were mounted on plus coated slides and allowed to dry, then incubated for one minute in thionin solution, washed in water, dehydrated in graded ethanols, cleared in xylenes and coverslipped with Permount (Fisher Scientific, Pittsburgh, PA).

For stereological analyses the PVN of Nissl stained serial sections were outlined at low magnification (4×, 0.16 numerical aperture, UPlanApo, Japan) on the live

computer image as described previously (Chakraborty et al., 2008) and with the help of The Mouse Brain in Stereotaxic Coordinates (Paxinos and Franklin, 2001). The optical fractionator (West et al., 1991) was used to estimate the total number of cells in the regions of interest. A 100× immersion oil, 1.3 numerical aperture objective (UPlanFI, Olympus, Japan) was used to achieve optimal optical sectioning during stereologic analysis. All counts were done by the same investigator, who was blinded to the genotype of the animals. The Stereo Investigator v8 software (Micro-BrightField Inc., Wiliston, VT) placed disector frames using a systematic-random design within each contour outlining a 70×77 μm grid to give ~10 counting frames per section, and the Nissl stained cells were counted within 20×20 μm optical disectors in the x–y axis. The final postprocessing thickness of the sections, as measured by the microcator, was on average 12 μm, so the counting frame height was kept at 10 μm for all sections studied to keep a 1 μm guard zone. Bilateral PVN cell counts were estimated using the optical fractionator to count sections with periodicity n=2, and 5-6 serial sections from each brain were counted. The cell number estimates did not depend on a direct measurement of the volume of reference of the region considered because of the use of the optical fractionator, and therefore the shrinkage of the tissue during histologic processing does not influence the precision of these estimates (Chakraborty et al., 2003). On an average 300−500 cells were sampled in the PVN in each animal. The Coefficient of Error (Gundersen, m=1) was 0.05 or less for all samples.

Quantitative analyses were performed using a computer assisted morphometry system consisting of an Olympus BX61 microscope equipped with an LEP XY computer/joystick controlled motorized stage (LUDL Electronic Products Ltd,

Hawthorne, NY), a Microfire digital camera (Optronics, Goleta, CA), a Dell computer, and StereoInvestigator8 software. Images of sections containing PVN were captured on a Leica DM2000 with Microfire camera and PictureFrame 2.0 software (Optronics, Goleta, CA).

Retrograde labeling of PVN neurons

In order to label PVN neurons that send monosynaptic projections to the dorsal vagal complex (DVC) (Saper et al., 1976), mice were stereotactically injected with the retrograde tracer cholera toxin b subunit (CTb 1% in 0.9% saline; List Biological Laboratories, Campbell, California; product#104; lot#10427B1). Briefly, mice were anesthetized with Ketamine HCl/Xylazine HCl (80/12 mg/kg, i.p.) and restrained in a Kopf stereotaxic apparatus. A glass micropipette connected to an air pressure injector system was positioned via the stereotaxic manipulator. CTb was unilaterally injected into the DVC (+0.16 from the obex, ±0.23 mm lateral, -0.36mm from the surface of the brainstem). After injection, the micropipette was removed and the incision was closed with surgical staples. Injection site was confirmed by immunostaining hindbrain sections.

In order to simultaneously label PVN neurons that send projections to the median eminence (Horvath, 1998), the same mice received a single intraperitoneal injection of Fluoro-Gold (FG) (100µg/mouse in 0.9% saline; Fluorochrome, Inc., Englewood, CO).

Perfusion and histology for retrograde tract tracing

Seven days post-surgery, mice were deeply anesthetized with chloral hydrate (500 mg/kg, i.p.), and then were perfused transcardially with 0.9% saline followed by 10% formalin

(Sigma Aldrich, St. Louis, MO). The brain was removed, postfixed 2 hours, and submerged in 20% sucrose overnight at 4°C. Coronal sections were cut at 25μm using a freezing microtome (1:5 series). Sections were collected in 0.1 M phosphate buffered saline (PBS) (pH 7.4), transferred in a cryoprotectant solution and stored at -20°C. After washing in PBS, brain sections were pretreated with 0.3% hydrogen peroxide in PBS for 15 minutes at room temperature. Sections were incubated overnight in a goat polyclonal antibody raised against CTb (1:50,000; List Biological Laboratories; product# 703; lot# 7032A3) in 3% normal donkey serum (Jackson ImmunoResearch Laboratories Inc., West Grove, PA) with 0.25% Triton X-100 in PBS (PBT). This antibody has been validated to detect CTb-labeled neurons in the rat central nervous system (Fuzesi et al., 2008). Another series of sections were incubated in a rabbit polyclonal antibody raised against FG (1:20,000; Chemicon, cat#AB153, lot#LV1446350) in 3% normal donkey serum PBT. This antibody has been validated to detect FG-labeled neurons in the rat central nervous system (Kaufling et al., 2009).

After washing in PBS, sections were incubated in biotinylated donkey anti-rabbit IgG (Jackson ImmunoResearch Laboratories Inc., West Grove, PA; cat#711065152, lot#77648; 1:1,000) or biotinylated donkey anti-goat IgG (Jackson ImmunoResearch Laboratories Inc., West Grove, PA; cat# 705065147, lot# 72100; 1:1,000) for 1 hour at room temperature, followed by a solution of ABC (Vectastain Elite ABC Kit; Vector Laboratories, Burlingame, CA; 1:1,000) dissolved in PBS for 1 hour. After washing in PBS, the sections were incubated in a solution of 0.04% diaminobenzidine tetrahydrochloride and 0.01% hydrogen peroxide (Sigma Aldrich, St. Louis, MO). It resulted in the accumulation of punctate brown precipitate in the cytoplasm of

retrogradely-labeled neurons. DAB-labeled sections were mounted on gelatin-coated slides, air-dried, dehydrated in graded ethanols, cleared in xylenes, and coverslipped with Permaslip (Alban Scientific, St Louis, MO). DAB staining was viewed using an Axioskop2 microscope (Zeiss, Oberkochen, Germany) using brightfield optics. Digital images were captured using an Axiocam digital camera and Axiovision 3.1 software (Zeiss, Oberkochen, Germany).

Quantitative Real Time PCR

Hypothalamic tissue for qPCR was collected as previously described (Kublaoui et al., 2006b). Hypothalami were dissected from fresh brains with a mouse brain block (Model PA 002; David Kopf Instruments, Tujunga, CA), using the following landmarks: posteriorly, posterior aspect of median eminence; anteriorly, 5mm anterior to the median eminence; dorsally, the thalamus; laterally, medial to the dentate gyrus. Total RNA was extracted using Tripure reagent (Roche Applied Science, Indianapolis, IN). cDNA was generated using an iScript cDNA Synthesis kit (Bio-Rad Laboratories, Hercules, CA).

Alternatively, tissue was isolated from the PVN using laser capture microdissection (LCM). Briefly, mice were sacrificed and brains dissected manually and frozen immediately. The frozen brains were mounted in Tissue-Tek OCT 4583 compound (Sakura, Tokyo, Japan) and then were sectioned on a cryostat (Leica, Nussloch, Germany) to a thickness of 30 μm. Sections were adhered to Silane (2%) treated glass membrane slides (Molecular Devices, Sunnyvale, CA). Sections were prepared for 1 minute in 70% EtOH and then dipped in water. Sections were stained with a filtered thionin solution for 2 minutes. Next, sections were rinsed and dehydrated with

EtOH, and finally cleared with xylene for 5 minutes. All solutions were made with autoclaved 0.1% DEPC water. The PVN region was microdissected out of a series of 20 evenly spaced thionin-stained sections using a Veritas LCM system (Molecular Devices, Arcturus Bioscience, Sunnyvale, CA). The collected tissue, adherent to the underside of the LCM cap, was then dissolved in digestion buffer (Stratagene, La Jolla, CA) and frozen at -80°C. Later, RNA was extracted from these samples using the Picopure RNA isolation kit (Arcturus Bioscience, Sunnyvale, CA). Approximately 20 evenly spaced sections were pooled to eliminate any potential rostrocaudal gene expression bias. Typical pools contained around 600 ng of RNA. Microdissected RNA was reverse transcribed using iScript (Bio-Rad, Hercules, CA) and then pre-amplified with Taqman PreAmp master mix kit (Applied Biosystems, Foster City, CA).

Quantitative real-time PCR was performed using TaqMan Universal PCR Master Mix with an ABI 3700 instrument (Applied Biosystems, Foster City, CA). Taqman assays were used to measure *Sim1*, *Oxt*, and *Mc4r* mRNA levels (Mm00441390_m1, Mm00726655_s1 and Mm00457483_s1; Applied Biosystems, Foster City, CA). For Mc4r, which does not contain an intron, a parallel experiment using mock reverse transcribed samples from LCM tissue was used as a control for genomic DNA contamination, and showed negligible PCR product. Mouse *Gapdh* (4352339E, Applied Biosystems, Foster City, CA) was the endogenous control used for normalization. Standard curves were generated using reference cDNA prepared from control mouse hypothalamus or PVN. All measurements were made in the exponential phase of the real-time PCR. Reactions were performed in triplicate and the results averaged. Results were

analyzed using SDS 2.3 software (Applied Biosystems, Foster City, CA) and Microsoft Excel.

Statistical Analysis

Data were analyzed using Microsoft Excel and Prism5 software (GraphPad Software, San Diego, CA) and are presented as mean ± SEM. Single comparisons were made using unpaired, two-tailed Student's t-test. Multiple comparisons were performed using one-way ANOVA with Tukey's post hoc test. Differences were considered statistically significant if $p<0.05$.

Acknowledgements:

This research was conducted in collaboration with Terry Gemelli, Laurent Gautron, Joel Elmquist, Dave Olson, Bradford Lowell, Bassil Kublaoui and Andrew Zinn. This work was supported by grants from the American Heart Association 0865266F and 0665077Y (B.M.K.) and National Institutes of Health DK79986 (A.R.Z.), as well as DK071320, DK53301, DK081185 (J. K. E.) and the American Diabetes Association 1-07-RA-41 (L.G. and J.K.E.). Grants 5UL1DE019584 (Jay Horton) and 5RL1DK081185 (J.K.E) support the Task Force for Obesity Research at Southwestern.

We thank Ying-Hue Lee, Rudolph Jaenisch, Lane Jaeckle Santos, Viren Amin, Amelia Eisch, John Shelton and James Richardson for their assistance.

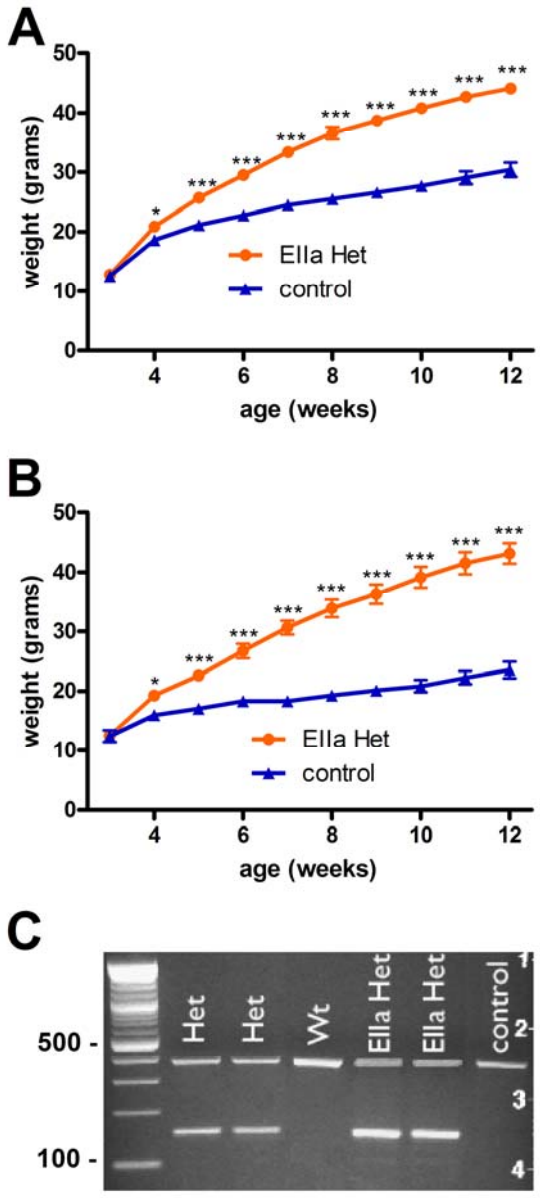

Figure IV.1 Recombination of floxed *Sim1* allele with EIIa-Cre. ***A-B,*** *Sim1* heterozygous mice generated with EIIa-Cre on a high fat diet. ***A,*** Males (EIIa Het, n = 13; control, n = 14) ***B,*** Females (EIIa Het, n = 14; control, n = 7). ***C,*** The genotypes of germline and EIIa heterozygotes and wild types shown by PCR. The 371bp band shows the wild type allele and the 160bp band shows the recombined allele. Groups were compared by unpaired two-tailed t-test. * $p<0.05$ and *** $p<0.005$. Error bars indicate SEM. WT, Wild type.

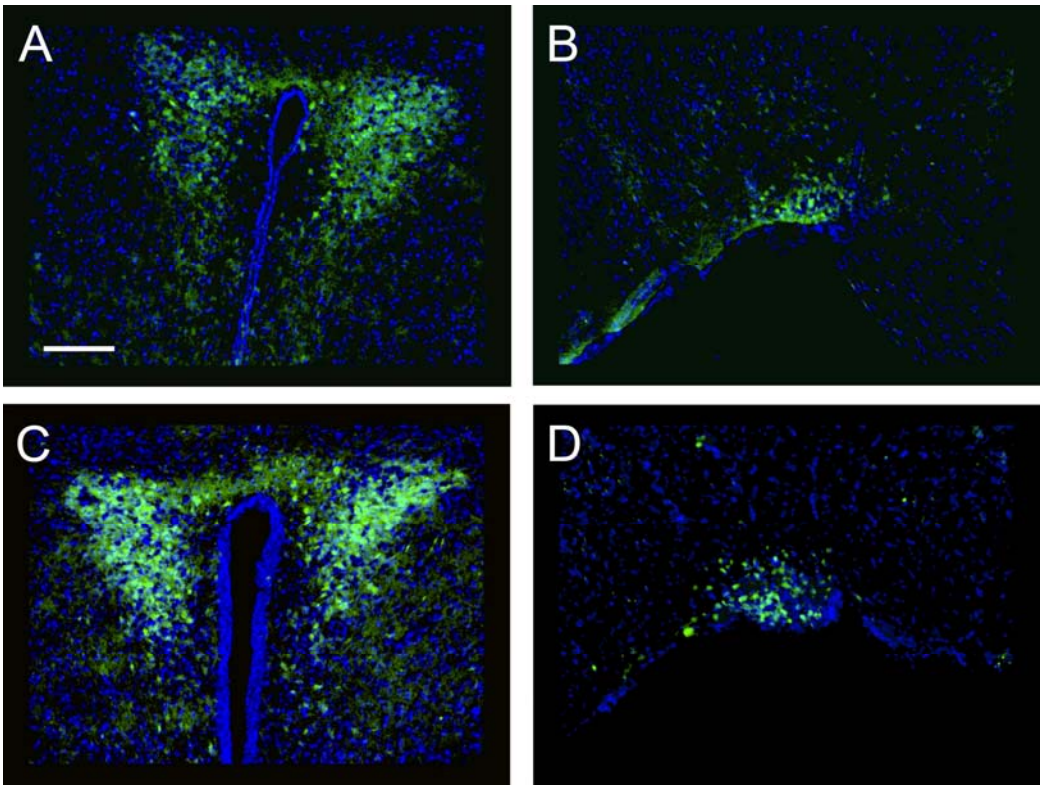

Figure IV.2 CamKII-Cre93 is expressed in the PVN and the SON. Mice expressing eYFP under the control of the Rosa26 promoter were bred with CamKII-Cre93 mice. A-B, The PVN (***A***) and SON (***B***) of an adult female mouse. eYFP is represented by green and DAPI is shown in blue. ***C-D,*** The PVN (***C***) and SON (***D***) of an adult male mouse. Scale bar: 200μm.

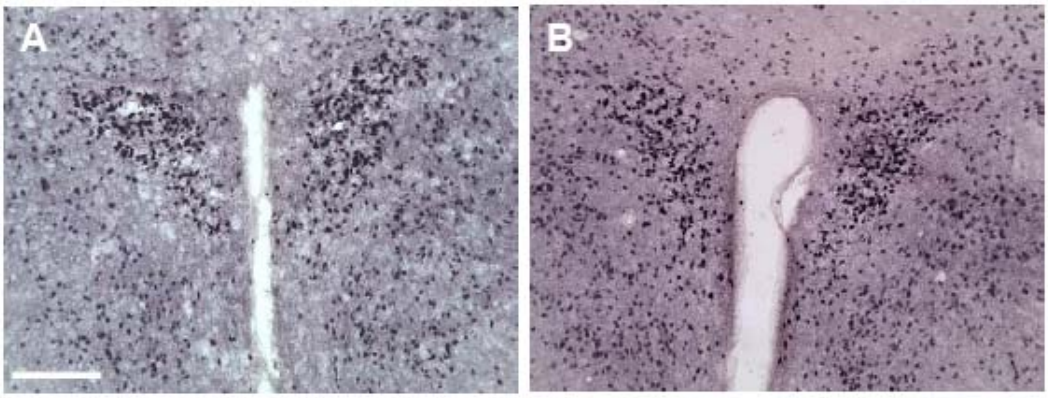

Figure IV.3 Hypothalamic CamKII-Cre159 expression includes the PVN. Mice expressing eYFP under the control of the Rosa26 promoter were bred with CamKII-Cre159 mice. ***A,*** The PVN of an adult female mouse. ***B,*** The PVN of an adult male mouse. Scale bar: 200μm.

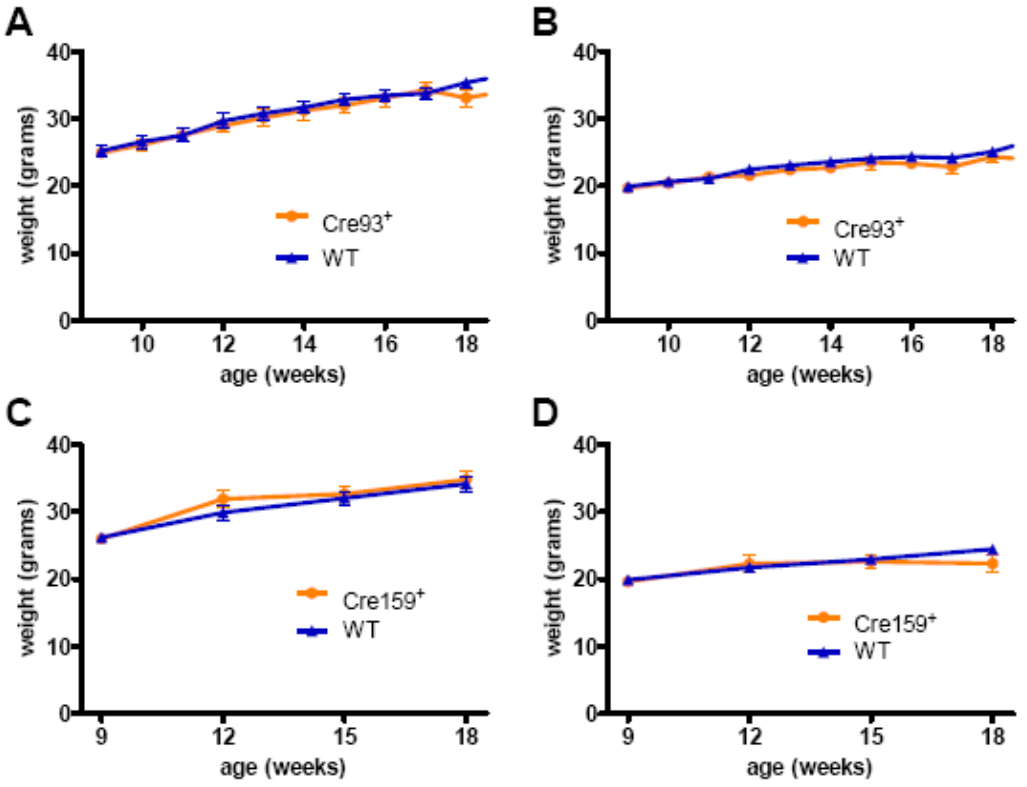

Figure IV.4 Cre93 and 159 transgenes on a low fat diet. ***A-B,*** Growth curves of mice carrying the Cre93 transgene (***A,*** Males: Cre93, n = 5; WT, n = 5; ***B,*** Females: Cre93, n = 4; WT, n = 4). ***C-D*** Growth curves of mice carrying the Cre159 transgene (***C,*** Males: Cre159, n = 11; WT, n = 11; ***D,*** Females: Cre159, n = 7; WT, n = 11). Mice were weaned at 3-4 weeks of age and weights monitored between 9 to 18 weeks of age. Error bars indicate SEM.

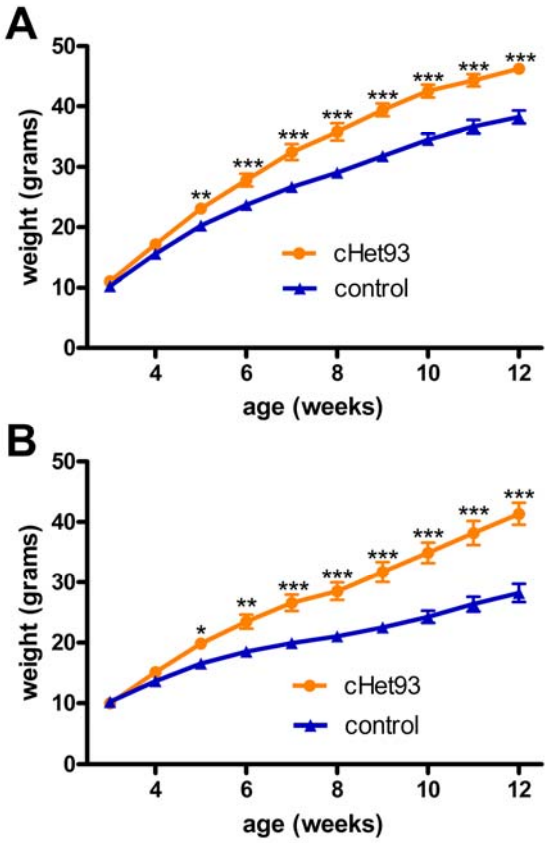

Figure IV.5 Conditional postnatal *Sim1* heterozygotes on a high fat diet. Growth curves of male male (***A***) and female (***B***) conditional heterozygotes (cHet93: Cre93, $Sim1^{+/fl}$) after being weaned onto high fat at 3 weeks of age. Mice were group housed with the same sex and weighed weekly. Males (cHet93, n = 12; control, n = 15), Females (cHet93, n = 7; control, n = 7). Groups were compared by unpaired two-tailed t-test. * $p<0.05$, ** $p<0.01$ and *** $p<0.005$. Error bars indicate SEM.

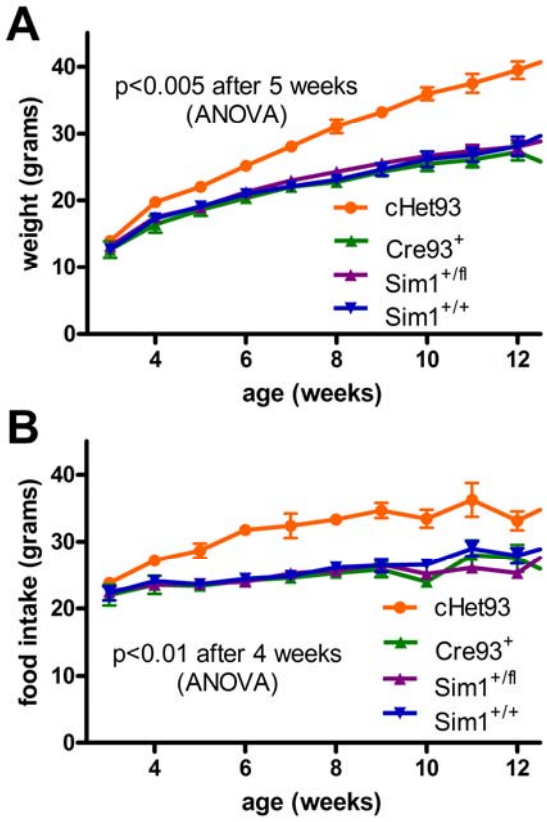

Figure IV.6 Conditional postnatal heterozygotes on a low fat diet. ***A,*** Growth curves of male conditional heterozygotes on a low fat diet. ***B,*** Weekly food intake of male cHet93 mice on a low fat diet. (cHet93, n = 7; $Cre93^{+}$, n = 6; $Sim1^{+/fl}$, n = 15; WT, n = 6). Mice were individually housed to monitor food intake and weight weekly. Multiple comparisons were performed using one-way ANOVA with Tukey's post hoc test. Error bars indicate SEM. WT, Wild type.

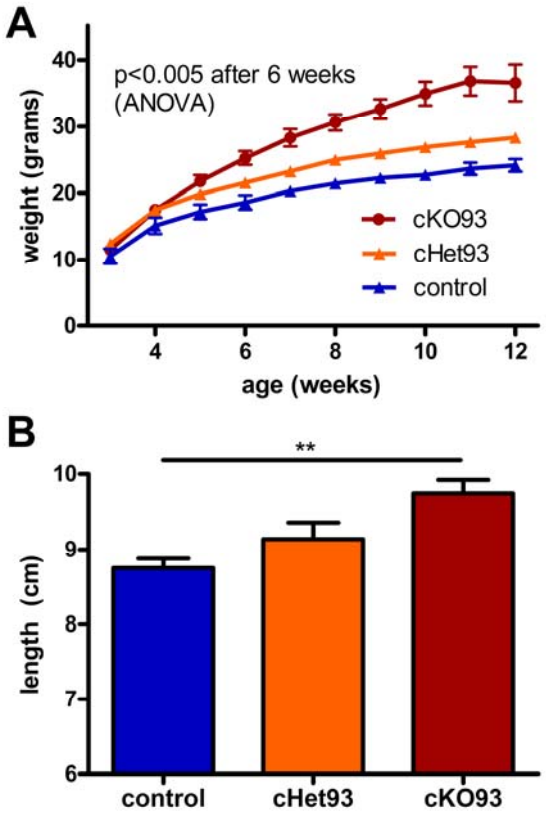

Figure IV.7 Postnatal conditional *Sim1* homozygotes on a low fat diet. ***A,*** Weekly growth curves showing male conditional *Sim1* homozygotes (cKO93: Cre93, $Sim1^{fl/fl}$), heterozygotes (cHet93) and their littermate controls on a low fat diet. Mice were group housed with the same sex and weighed weekly. (cKO93; n = 5, cHet93; n = 7, control n = 6). ***B,*** Nose to anus length of male cKO93 mice at 13 weeks of age. (cKO93, n = 5; cHet93, n = 7; control n = 6). Multiple comparisons were performed using one-way ANOVA with Tukey's post hoc test. ***p*<0.01. Error bars indicate SEM.

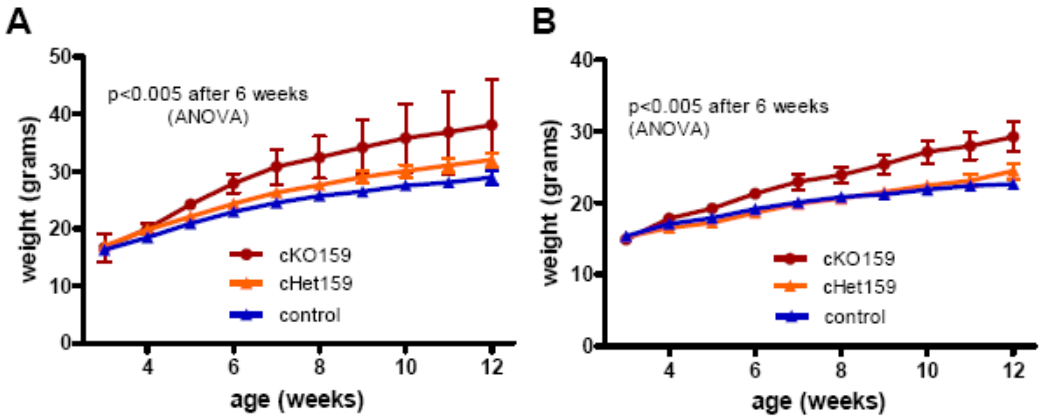

Figure IV.8 Cre159 conditional postnatal heterozygotes and homozygotes on a low fat diet. *A-B,* Weekly growth curves showing conditional *Sim1* homozygotes (cKO159: Cre159, *Sim1*$^{fl/fl}$), heterozygotes (cHet159: Cre159, *Sim1*$^{+/fl}$) and their littermate controls on a low fat diet. Mice were group housed with the same sex and weighed weekly. (***A,*** Males: cKO159, n = 2; cHet159, n = 7; control n = 8; ***B,*** Females: cKO159, n = 8; cHet159, n = 9; control n = 17). Multiple comparisons were performed using one-way ANOVA with Tukey's post hoc test. Error bars indicate SEM.

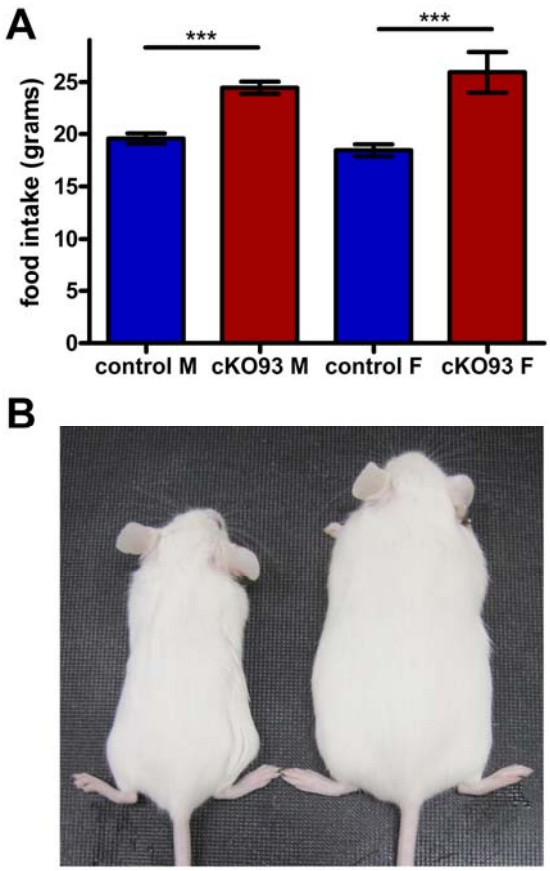

Figure IV.9 Food intake and gross appearance of postnatal conditional *Sim1* homozygotes on a low fat diet. ***A,*** Weekly food intake of cKO93 male and female mice at 6 weeks of age on a low fat diet compared to control littermates. (Males: cKO93, n = 13; control n = 13; Females: cKO93, n = 7; control n = 16). ***B,*** Gross appearance of control littermates and cKO93 female mice on a low fat diet at 12 weeks of age (left = control, right = cKO93). Mice were individually housed to monitor food intake and weight weekly. ***$p<0.001$. Error bars indicate SEM.

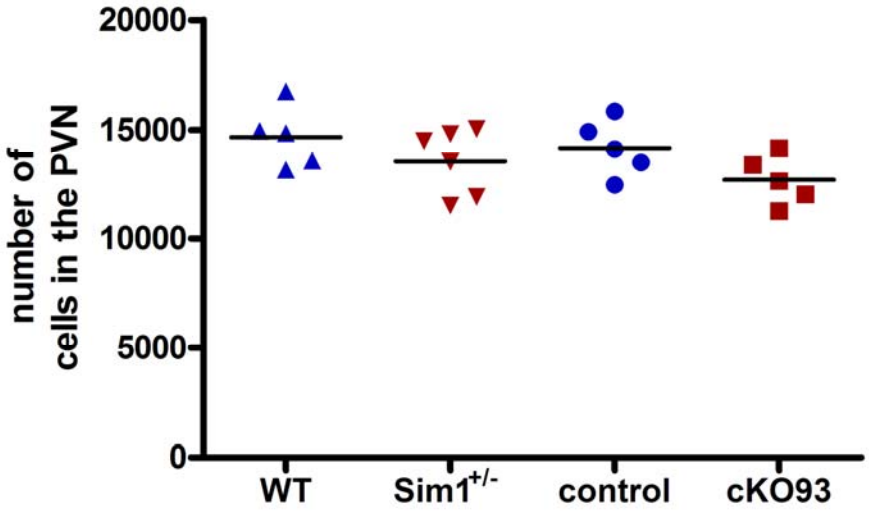

Figure IV.10 Unbiased stereologic analyses of the PVN of germline *Sim1* heterozygotes and conditional postnatal *Sim1* homozygotes. Unbiased stereologic cell counting of the PVN of female WT *vs.* *Sim1*$^{+/-}$ and control *vs.* cKO93 mice (WT, n = 5; *Sim1*$^{+/-}$, n = 6; control, n = 5; cKO93, n = 5). WT *vs.* *Sim1*$^{+/-}$, $p = 0.2433$; control *vs.* cKO93, $p = 0.0952$. All counting was done by the same investigator, who was blinded to the genotypes of the mice. Groups were compared by unpaired two-tailed t-test. WT, Wild type.

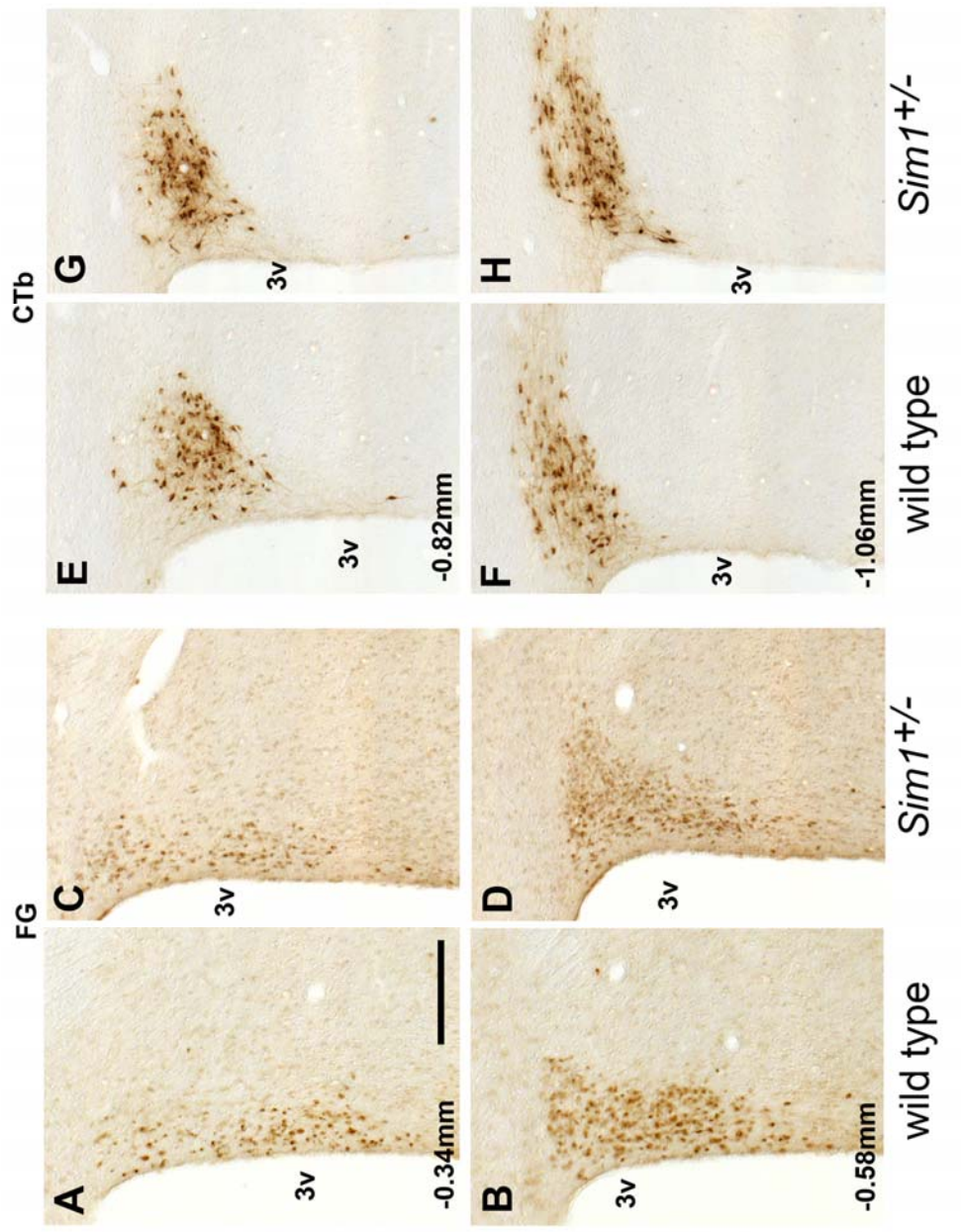

Figure IV.11 Projections from the PVN to the median eminence (ME) and the dorsal vagal complex (DVC) in germline *Sim1* heterozygotes. ***A-D,*** projections to the ME were traced using Fluoro-Gold (FG) in wild type and *Sim1*$^{+/-}$ mice. ***E-H*** show retrograde tract tracing from the DVC using the cholera toxin b subunit (CTb) in wild type and *Sim1*$^{+/-}$ mice. The estimated distance from Bregma of each rostrocaudal level of the PVN is indicated. 3v, third ventricle. Scale bar: 200μm.

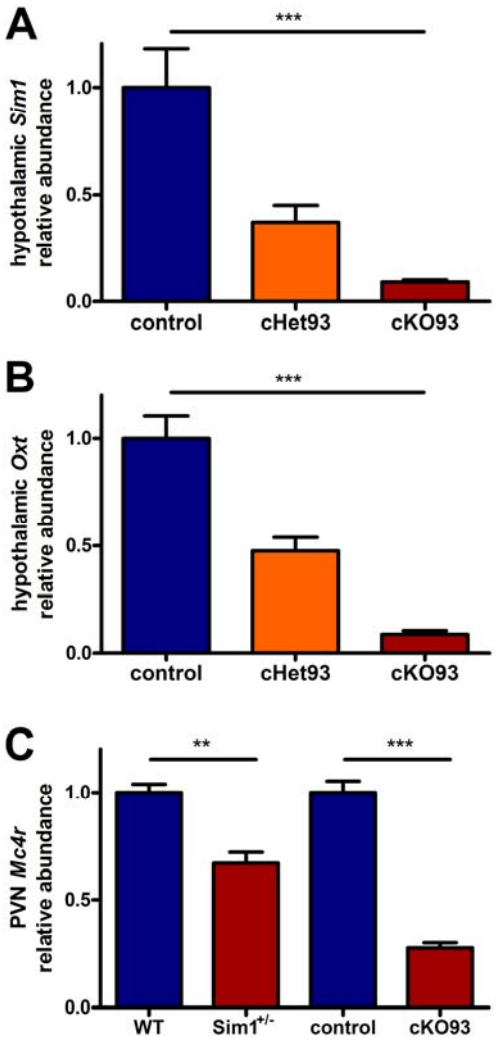

Figure IV.12 Quantitative real time PCR analysis of hypothalamic expression of *Sim1* and *Oxt,* and *Mc4r* expression in the PVN. *A,* *Sim1* expression in the whole hypothalamus of male cHet93 and cKO93 compared to their control littermates. ***B,*** *Oxt* expression in the whole hypothalamus of male cHet93 and cKO93 compared to their control littermates. (cHet93, n = 6; cKO93, n = 6; control, n = 4). ***C,*** *Mc4r* expression in the PVN of $Sim1^{+/-}$ mice and cKO93 compared to their respective control littermates (WT, n = 6; $Sim1^{+/-}$, n = 5; control, n = 5; cKO93, n = 6). Groups of two were compared by unpaired two-tailed t-test, and multiple comparisons were performed using one-way ANOVA with Tukey's post hoc test. $^{**}p<0.01$, $^{***}p<0.001$. Error bars indicate SEM.

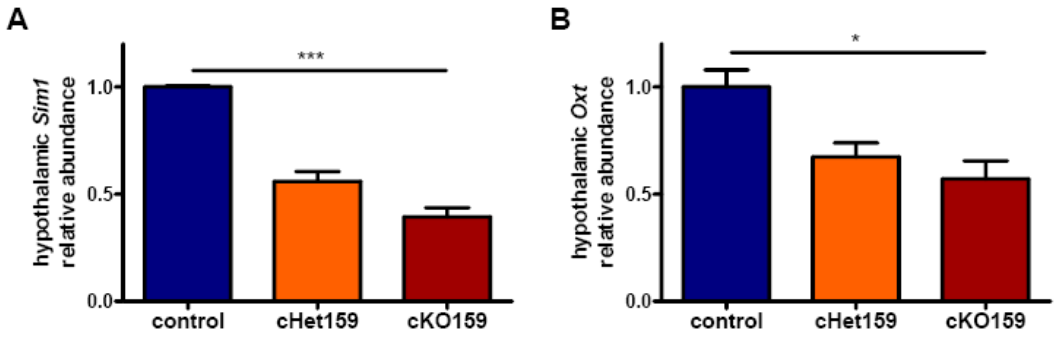

Figure IV.13 Quantitative real time PCR analysis of hypothalamic expression of *Sim1* and *Oxt*. *A,* *Sim1* expression in the whole hypothalamus of female cHet159 and cKO159 compared to their control littermates. ***B,*** *Oxt* expression in the whole hypothalamus of male cHet159 and cKO159 compared to their control littermates. (cHet159, n = 3, cKO159, n = 3, control, n = 2). Multiple comparisons were performed using one-way ANOVA with Tukey's post hoc test. *$p<0.05$, ***$p<0.001$. Error bars indicate SEM.

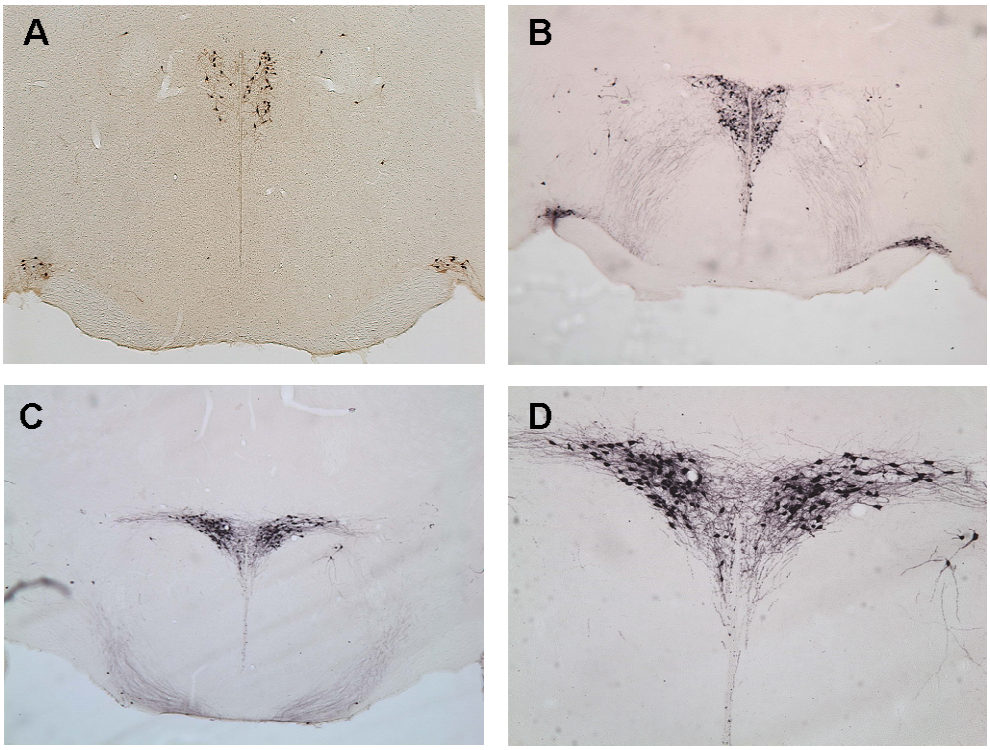

Figure IV.14 Oxt-Cre expression in the PVN and SON. Mice expressing eYFP under the control of the Rosa26 promoter were bred with Oxt-Cre. ***A,*** Cre expression data from David Olson showing recombination in about 35% of Oxt neurons in the PVN and SON. ***B-D,*** Cre expression data from our lab showing recombination in the PVN and SON.

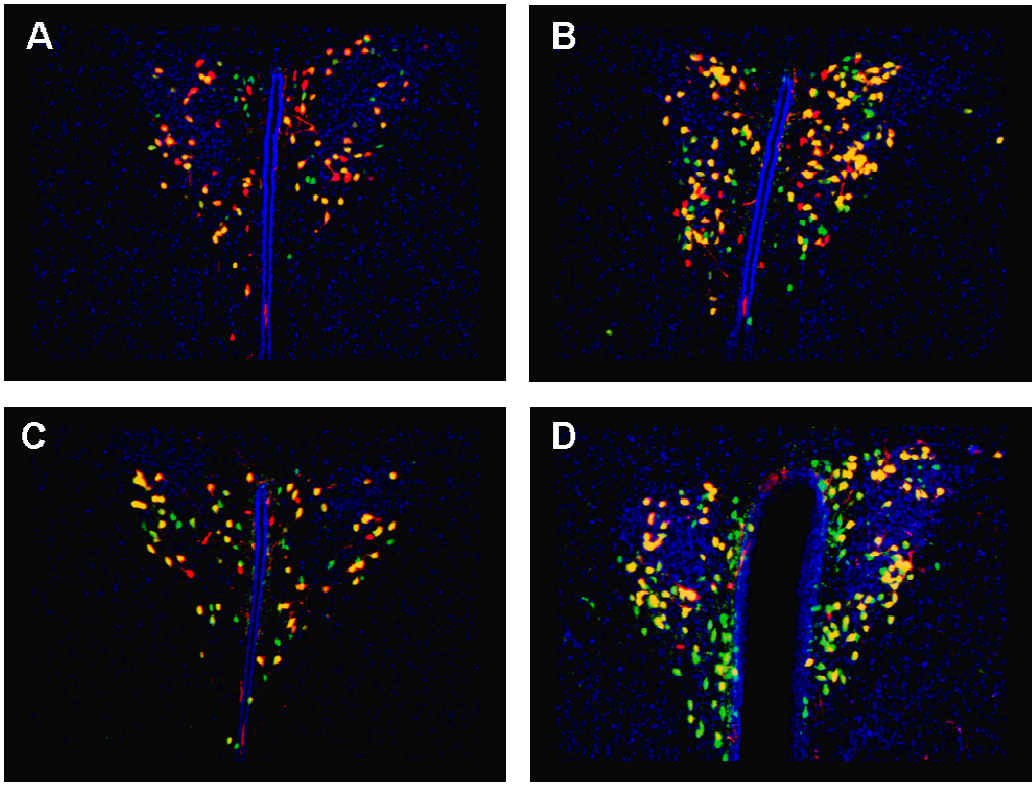

Figure IV.15 Oxt-Cre recombination colocalizes with Oxt immunostaining. Mice expressing eYFP under the control of the Rosa26 promoter were bred with Oxt-Cre. ***A-D,*** Double immunohistochemistry data showing eYFP and Oxt positive neurons in the PVN. eYFP is represented by green, Oxt by red, and DAPI is shown in blue. Yellow indicates colocalization of eYFP and Oxt.

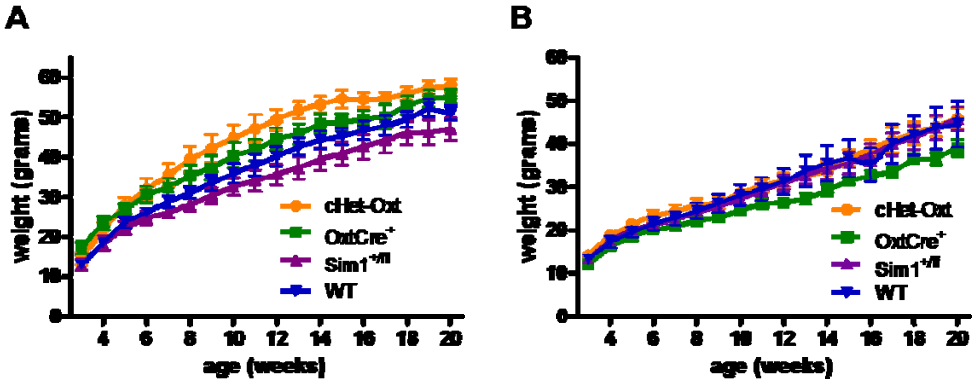

Figure IV.16 Oxt-Cre conditional heterozygotes on a high fat diet. ***A,*** Growth curves of male conditional heterozygotes (cHet-Oxt: Oxt-Cre, *Sim1*$^{+/fl}$) on a high fat diet up to 20 weeks of age. (cHet-Oxt, n = 5, OxtCre^{+}, n = 5, *Sim1*$^{+/fl}$, n = 6, WT, n = 5). ***B,*** Growth curves of female conditional heterozygotes on a high fat diet up to 20 weeks of age. (cHet-Oxt, n = 6, OxtCre^{+}, n = 7, *Sim1*$^{+/fl}$, n = 7, WT, n = 6). Multiple comparisons were performed using one-way ANOVA with Tukey's post hoc test. Error bars indicate SEM.

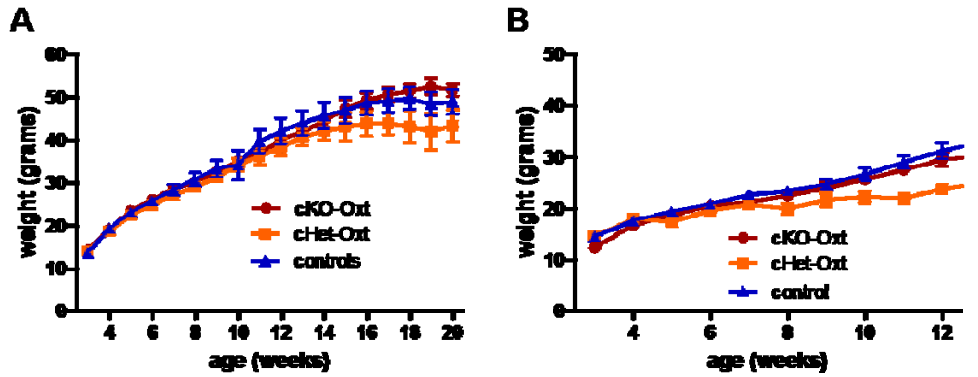

Figure IV.17 Oxt-Cre conditional homozygotes on a high fat diet. ***A****,* Growth curves of male conditional homozygotes (cKO-Oxt: Oxt-Cre, *Sim1*$^{fl/fl}$) and heterozygotes on a high fat diet up to 20 weeks of age. (cKO-Oxt, n = 5, cHet-Oxt, n = 8, control, n = 9). ***B****,* Growth curves of female conditional homozygotes and heterozygotes on a high fat diet. (cKO-Oxt, n = 5, cHet-Oxt, n = 2, control, n = 10). Multiple comparisons were performed using one-way ANOVA with Tukey's post hoc test. Error bars indicate SEM.

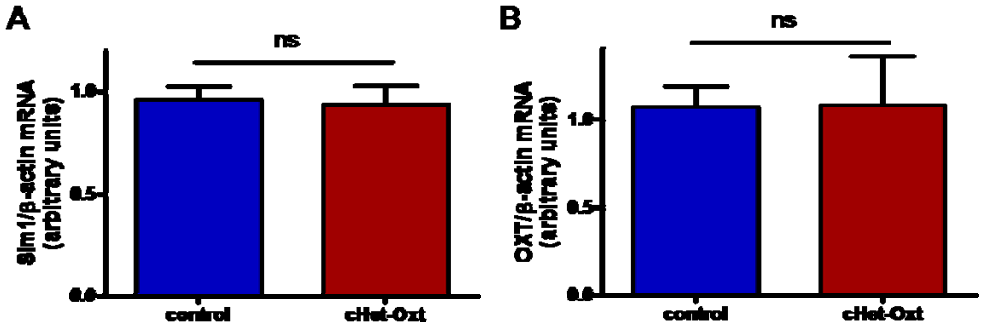

Figure IV.18 Quantitative real time PCR analysis of hypothalamic expression of *Sim1* and *Oxt* mRNAs. ***A****, Sim1* expression in male cHet-Oxt compared to their control littermates. ***B****, Oxt* expression in male cHet-Oxt compared to their control littermates. (control, n = 3, cHet-Oxt, n = 3). Groups were compared by unpaired two-tailed t-test. Error bars indicate SEM.

Chapter V

Conclusions and Recommendations

The results of these studies strongly support a postdevelopmental, physiological role for *Sim1*, and certainly highlights the importance of *Sim1* in the development of hyperphagic obesity. Much work remains to be done in order to fully understand the function of *Sim1*.

Further characterization of the cKO93 mice could yield interesting and important results. Our new finding of reduction of PVN *Mc4r* expression in these mice is intriguing, but we do not yet know if this deficiency is partially or fully responsible for the obesity phenotype of *Sim1* deficient mice. It is not clear if there is direct regulation of *Mc4r* or *Oxt* by *Sim1*, or *Oxt* by *Mc4r*. It is also uncertain if Mc4r activation and *Oxt* expression and activity are in a linear pathway, or if they function in parallel. If they are in parallel pathways, which is the predominant cause of the hyperphagic obesity of *Sim1* deficient mice will need to be determined. Recently, *Nesfatin-1* was shown to regulate PVN oxytocin signaling that causes a reduction in food intake (Maejima et al., 2009); the relationship between *Sim1* and *Nesfatin-1* is not yet known and could prove to be one of our pathway's missing links.

Additionally, whether these decreases in *Oxt* and *Mc4r* represent defects in specific signaling pathways, or are part of a global dysfunction of these neurons has yet to be determined. The previously observed abnormal response of PVN neurons in *Sim1*$^{+/-}$ mice to MTII but not to hypertonic saline (Kublaoui et al., 2006a) suggests a selective defect. On the other hand, it is possible that *Sim1* is required to maintain the differentiated gene expression program of PVN neurons, and as with neuroanatomic lesions (Heinbecker et al., 1944; Leibowitz et al., 1981), the predominant phenotypic effect of global PVN dysfunction is a change in feeding regulation.

Another area of interest is the status of the other PVN/SON neuropeptides in these mice. We saw a modest reduction in the *Sim1*$^{+/-}$ mice that may or may not be exacerbated in the cKO93. We have also not done immunostaining for any of these neuropeptides, so while we know that *Oxt* mRNA is decreased, we have not confirmed protein levels. As their hypothalamic Oxt is severely decreased, are these mice able to successfully breed and/or keep their pups alive? We have also never investigated the circulating levels of these neuropeptides or the hormones they control.

Recently we have started investigating possible behavioral differences in *Sim1*$^{+/-}$ mice, and while there have been some suggestive trends, nothing has been significantly different. The cKO93 mice could again prove useful in this area, as it is likely that any mild phenotype in *Sim1*$^{+/-}$ mice would be exacerbated in cKO93 mice. Metabolic cages may be able to help us establish whether the hyperphagia manifests in the form of larger meals or more frequent meals.

Previously we were able to rescue the hyperphagia of *Sim1*$^{+/-}$ mice with Oxt injections; would this also apply to our cKO93 mice? As shown in the data presented here, we saw no difference in projections from the PVN to the DVC and ME in *Sim1*$^{+/-}$ mice, but we have yet to show that in the cKO93 mice.

An unexpected tangent of the research above was the creation of mice that appear to lack a defined PVN and SON. These mice were created when male Cre93, Sim1$^{fl/wt}$ were bred with female Sim1$^{fl/fl}$ mice; aberrant recombination occurs in the testes of the males, causing germline deletion of the floxed allele. Progeny that should have been Cre93, Sim1$^{fl/fl}$ (cKO93) were in fact Cre93, Sim1$^{-/fl}$. These mice are viable and were

indistinguishable from other cKO93 by weight. They came to our attention because 1) their Cre negative littermates who should have been $Sim1^{fl/fl}$ in fact already contained an aberrant germline recombined allele ($Sim1^{-/fl}$), and 2) when the brains from these mice were Nissl stained, the lack of dense nuclei where the PVN and SON should have been was apparent. Neither we nor Carol Elias were able to observe any other affected areas of the brain; specifically the amygdala, which also expresses *Sim1*, seems to be intact in these mice. This lack of PVN and SON created many questions that we would like to answer. Are the nuclei not there because the neurons have not migrated properly, or have they died? If they are alive, where are they located, and are they functional? It is believed that the neuropeptides produced by the PVN are necessary for life, so if the neurons are dead or non-functional how are these mice alive? We do not currently possess an assay to track these neurons, but we can test the mRNA expression of the neuropeptides in the hypothalamus. If they are not present in the hypothalamus, circulating levels should also be evaluated. As it is believed that the death of germline *Sim1* homozygotes is due to neuroendocrine insufficiency, these mice may be useful in confirming or disproving this.

While our studies show a postnatal role for *Sim1*, we cannot claim a postdevelopmental role yet, as the projections and connections of the neurons may still be forming when Cre93 and 159 begin expressing. Therefore, we plan to use a tamoxifen inducible CaMK-$CreER^{T2}$ mouse line (Erdmann et al., 2007). Using this transgene, we should be able to induce *Sim1* recombination well after the brain is fully formed. We are also working on importing other various Cre lines (Crh, Trh, and the new Oxt) to answer the question of neuronal subtype importance. As mentioned previously, both Cre93 and 159 lines show expression in both the PVN and the amygdala, and we have not been able

to differentiate between the roles of *Sim1* in the PVN *vs.* the amygdala. If Cre lines could be obtained that expressed specifically in one or the other, this could finally give us answers to this area of questions. Alternatively, viral-mediated Cre expression could be used to inactivate *Sim1* with spatial specificity.

Another unanswered question is whether it is the neuropeptides or the neurons that happen to express them that are important in mediating the hyperphagic obesity of *Sim1* deficient mice. Our Oxt rescue injection data would imply that at least Oxt is important, but it is possibile that these neuropeptides are merely markers for neurons that use GABA and glutamate for signaling (van den Pol, 2003; Cone, 2005). We plan to use diphtheria toxin expressed in specific neuronal subtypes to ablate these neurons in adulthood. This technique was previously used to determine the function of NPY/Agrp, and showed that while neonatal ablation effected feeding minimally, ablation in adults resulted in rapid starvation (Luquet et al., 2005).

Research on the transcriptional targets and native localization of *Sim1* have been confounded by the lack of a specific antibody. While the creation of a specific antibody would be ideal, this has proven to be an expensive and thus far fruitless endeavor. One of the best studied bHLH-PAS proteins, the aryl hydrocarbon (dioxin) receptor (AHR), heterodimerizes with its partner ARNT and translocates to the nucleus in a ligand-dependent fashion (Hankinson, 1995). By contrast, no ligand has yet been identified for SIM1, which is thought to constitutively heterodimerize with its partner ARNT2.

Multiple bHLH-PAS family members have been shown to undergo regulated translocation to the nucleus (Hankinson, 1995; Kallio et al., 1998; Ward et al., 1998; Dekanty et al., 2005; Kwon et al., 2006; Teh et al., 2006), but the natural localization of

Sim1 has remained enigmatic. Sim1 has an atypical nuclear localization signal that is potentially a substrate for phosphorylation (Yamaki et al., 2004). The potential phosphorylation of Sim1, particularly as a mechanism by which signal transduction and transcriptional regulation is controlled, has not been studied. Protein phosphorylation of transcription factors can modulate nuclear translocation, DNA binding activity, protein stability, and protein-protein interactions including interactions with transcriptional co-activators. A number of bHLH-PAS proteins are known to undergo serine/threonine phosphorylation, which has been shown to modulate their activity and in some cases their nuclear localization (Conrad et al., 1999; Long et al., 1999; Lee et al., 2001; Toh et al., 2001; Kondratov et al., 2003; Kewley and Whitelaw, 2005; To et al., 2006)

Lacking a specific antibody, we hope to use microarrays with the cKO93 to elucidate some of the genes *Sim1* deficiency is affecting, though this will still not tell us which DNA sequences *Sim1* specifically binds to and therefore which are being directly regulated. A possible different approach is to make a mouse line that has a tagged-*Sim1* allele knocked in. This could allow us to perform experiments such as ChIP-chip and ChIP-Seq to look at Sim1 transcriptional targets. It would also allow us to look at *in vivo* localization of Sim1 under various circumstances; for example, in different feeding-related states. SIM1 is generally thought to be constitutively localized to the nucleus, based on developmental studies of the homologous *Drosophila Singleminded* (*Sim*) gene and cell culture studies of epitope-tagged mammalian Sim1 or *Sim1*-GFP fusion proteins. However, in our preliminary immunohistochemical and immunocytochemical studies of hypothalamic tissue and cultured cells, we observed that a substantial proportion of native Sim1 is actually cytoplasmic or perinuclear *in vivo*. Conclusive data would be

useful in understanding the regulation of Sim1, whether by subcellular localization, phosphorylation state, ligand alone or in combination.

Here we have shown that *Sim1* haploinsufficiency causes human and mouse phenotypes similar to that of mutations in the melanocortin-4 receptor (hyperphagic obesity, increased linear growth, sensitivity to dietary fat) and also that overexpression of *SIM1* in mice protects against diet induced obesity. We have now shown that conditional postnatal *Sim1* haploinsufficiency, after the formation of the PVN, is sufficient to cause hyperphagic obesity. Furthermore, we show that the PVN of *Sim1* heterozygotes is normocellular, and PVN neurons project normally to the median eminence and hindbrain. Additionally, we show that a conditional *Sim1* homozygous knockout is viable, demonstrating that *Sim1* is not required for postnatal survival of PVN neurons. Using the conditional knockout, we find that *Mc4r* and *Oxytocin* expression are dependent upon *Sim1* dosage, corroborating our earlier work implicating *Sim1* in the leptin-melanocortin-oxytocin signaling pathway regulating food intake. Our results provide new mechanistic insights into the hyperphagic obesity phenotype of *Sim1* deficiency in humans and mice and suggest that *Sim1* and the genes it regulates may provide new targets for drugs to treat obesity.

BIBLIOGRAPHY

Abbott CR, Rossi M, Kim M, AlAhmed SH, Taylor GM, Ghatei MA, Smith DM, Bloom SR (2000) Investigation of the melanocyte stimulating hormones on food intake. Lack Of evidence to support a role for the melanocortin-3-receptor. Brain Res 869:203-210.

Abercrombie M, Johnson ML (1946) Quantitative histology of Wallerian degeneration: I. Nuclear population in rabbit sciatic nerve. J Anat 80:37-50.

Acampora D, Postiglione MP, Avantaggiato V, Di Bonito M, Vaccarino FM, Michaud J, Simeone A (1999) Progressive impairment of developing neuroendocrine cell lineages in the hypothalamus of mice lacking the Orthopedia gene. Genes Dev 13:2787-2800.

Ahituv N, Kavaslar N, Schackwitz W, Ustaszewska A, Martin J, Hebert S, Doelle H, Ersoy B, Kryukov G, Schmidt S, Yosef N, Ruppin E, Sharan R, Vaisse C, Sunyaev S, Dent R, Cohen J, McPherson R, Pennacchio LA (2007) Medical sequencing at the extremes of human body mass. Am J Hum Genet 80:779-791.

Allison DB, Faith MS, Nathan JS (1996) Risch's lambda values for human obesity. Int J Obes Relat Metab Disord 20:990-999.

Angevine JB, Jr. (1970) Time of neuron origin in the diencephalon of the mouse. An autoradiographic study. J Comp Neurol 139:129-187.

Arletti R, Benelli A, Bertolini A (1989) Influence of oxytocin on feeding behavior in the rat. Peptides 10:89-93.

Arletti R, Benelli A, Bertolini A (1990) Oxytocin inhibits food and fluid intake in rats. Physiol Behav 48:825-830.

Balthasar N (2006) Genetic dissection of neuronal pathways controlling energy homeostasis. Obesity (Silver Spring) 14 Suppl 5:222S-227S.

Balthasar N, Dalgaard LT, Lee CE, Yu J, Funahashi H, Williams T, Ferreira M, Tang V, McGovern RA, Kenny CD, Christiansen LM, Edelstein E, Choi B, Boss O, Aschkenasi C, Zhang CY, Mountjoy K, Kishi T, Elmquist JK, Lowell BB (2005) Divergence of melanocortin pathways in the control of food intake and energy expenditure. Cell 123:493-505.

Barlow SE, Dietz WH (1998) Obesity evaluation and treatment: Expert Committee recommendations. The Maternal and Child Health Bureau, Health Resources and Services Administration and the Department of Health and Human Services. Pediatrics 102:E29.

Barsh GS, Farooqi IS, O'Rahilly S (2000) Genetics of body-weight regulation. Nature 404:644-651.

Baskin DG, Blevins JE, Schwartz MW (2001) How the brain regulates food intake and body weight: the role of leptin. J Pediatr Endocrinol Metab 14 Suppl 6:1417-1429.
Bernardis LL (1984) Paraventricular nucleus lesions in weanling female rats result in normophagia, normal body weight and composition, linear growth and normal levels of several plasma substrates. Physiol Behav 32:507-510.
Beuckmann CT, Sinton CM, Williams SC, Richardson JA, Hammer RE, Sakurai T, Yanagisawa M (2004) Expression of a poly-glutamine-ataxin-3 transgene in orexin neurons induces narcolepsy-cataplexy in the rat. J Neurosci 24:4469-4477.
Blevins JE, Schwartz MW, Baskin DG (2004) Evidence that paraventricular nucleus oxytocin neurons link hypothalamic leptin action to caudal brain stem nuclei controlling meal size. Am J Physiol Regul Integr Comp Physiol 287:R87-96.
Blevins JE, Eakin TJ, Murphy JA, Schwartz MW, Baskin DG (2003) Oxytocin innervation of caudal brainstem nuclei activated by cholecystokinin. Brain Res 993:30-41.
Bray GA, Tartaglia LA (2000) Medicinal strategies in the treatment of obesity. Nature 404:672-677.
Burbach JP (2002) Regulation of gene promoters of hypothalamic peptides. Front Neuroendocrinol 23:342-369.
Butler AA, Kesterson RA, Khong K, Cullen MJ, Pelleymounter MA, Dekoning J, Baetscher M, Cone RD (2000) A unique metabolic syndrome causes obesity in the melanocortin-3 receptor-deficient mouse. Endocrinology 141:3518-3521.
Caqueret A, Coumailleau P, Michaud JL (2005) Regionalization of the anterior hypothalamus in the chick embryo. Dev Dyn 233:652-658.
Castel M, Morris JF (1988) The neurophysin-containing innervation of the forebrain of the mouse. Neuroscience 24:937-966.
Chakraborty S, Sachdev A, Salton SR, Chakraborty TR (2008) Stereological analysis of estrogen receptor expression in the hypothalamic arcuate nucleus of ob/ob and agouti mice. Brain Res 1217:86-95.
Chakraborty TR, Hof PR, Ng L, Gore AC (2003) Stereologic analysis of estrogen receptor alpha (ER alpha) expression in rat hypothalamus and its regulation by aging and estrogen. J Comp Neurol 466:409-421.
Chen AS et al. (2000) Inactivation of the mouse melanocortin-3 receptor results in increased fat mass and reduced lean body mass. Nat Genet 26:97-102.
Cheung CC, Clifton DK, Steiner RA (1997) Proopiomelanocortin neurons are direct targets for leptin in the hypothalamus. Endocrinology 138:4489-4492.

Choi YH, Hartzell D, Azain MJ, Baile CA (2002) TRH decreases food intake and increases water intake and body temperature in rats. Physiol Behav 77:1-4.
Chrast R, Scott HS, Chen H, Kudoh J, Rossier C, Minoshima S, Wang Y, Shimizu N, Antonarakis SE (1997) Cloning of two human homologs of the Drosophila single-minded gene SIM1 on chromosome 6q and SIM2 on 21q within the Down syndrome chromosomal region. Genome Res 7:615-624.
Coggeshall RE, Lekan HA (1996) Methods for determining numbers of cells and synapses: a case for more uniform standards of review. J Comp Neurol 364:6-15.
Cone RD (2005) Anatomy and regulation of the central melanocortin system. Nat Neurosci 8:571-578.
Conrad PW, Freeman TL, Beitner-Johnson D, Millhorn DE (1999) EPAS1 trans-activation during hypoxia requires p42/p44 MAPK. The Journal of biological chemistry 274:33709-33713.
Cowley MA, Pronchuk N, Fan W, Dinulescu DM, Colmers WF, Cone RD (1999) Integration of NPY, AGRP, and melanocortin signals in the hypothalamic paraventricular nucleus: evidence of a cellular basis for the adipostat. Neuron 24:155-163.
Cowley MA, Smart JL, Rubinstein M, Cerdan MG, Diano S, Horvath TL, Cone RD, Low MJ (2001) Leptin activates anorexigenic POMC neurons through a neural network in the arcuate nucleus. Nature 411:480-484.
Cummings DE, Schwartz MW (2003) Genetics and pathophysiology of human obesity. Annu Rev Med 54:453-471.
Dekanty A, Lavista-Llanos S, Irisarri M, Oldham S, Wappner P (2005) The insulin-PI3K/TOR pathway induces a HIF-dependent transcriptional response in Drosophila by promoting nuclear localization of HIF-alpha/Sima. J Cell Sci 118:5431-5441.
Dhillon H, Zigman JM, Ye C, Lee CE, McGovern RA, Tang V, Kenny CD, Christiansen LM, White RD, Edelstein EA, Coppari R, Balthasar N, Cowley MA, Chua S, Jr., Elmquist JK, Lowell BB (2006) Leptin directly activates SF1 neurons in the VMH, and this action by leptin is required for normal body-weight homeostasis. Neuron 49:191-203.
Douglas AJ, Johnstone LE, Leng G (2007) Neuroendocrine mechanisms of change in food intake during pregnancy: a potential role for brain oxytocin. Physiol Behav 91:352-365.
Eaton JL, Glasgow E (2006) The zebrafish bHLH PAS transcriptional regulator, single-minded 1 (sim1), is required for isotocin cell development. Dev Dyn 235:2071-2082.
Elmquist JK, Elias CF, Saper CB (1999) From lesions to leptin: hypothalamic control of food intake and body weight. Neuron 22:221-232.

Ema M, Morita M, Ikawa S, Tanaka M, Matsuda Y, Gotoh O, Saijoh Y, Fujii H, Hamada H, Kikuchi Y, Fujii-Kuriyama Y (1996) Two new members of the murine Sim gene family are transcriptional repressors and show different expression patterns during mouse embryogenesis. Mol Cell Biol 16:5865-5875.

Emmons RB, Duncan D, Estes PA, Kiefel P, Mosher JT, Sonnenfeld M, Ward MP, Duncan I, Crews ST (1999) The spineless-aristapedia and tango bHLH-PAS proteins interact to control antennal and tarsal development in Drosophila. Development 126:3937-3945.

Emond M, Schwartz GJ, Ladenheim EE, Moran TH (1999) Central leptin modulates behavioral and neural responsivity to CCK. Am J Physiol 276:R1545-1549.

Emond M, Ladenheim EE, Schwartz GJ, Moran TH (2001) Leptin amplifies the feeding inhibition and neural activation arising from a gastric nutrient preload. Physiol Behav 72:123-128.

Erdmann G, Schutz G, Berger S (2007) Inducible gene inactivation in neurons of the adult mouse forebrain. BMC Neurosci 8:63.

Faivre L, Cormier-Daire V, Lapierre JM, Colleaux L, Jacquemont S, Genevieve D, Saunier P, Munnich A, Turleau C, Romana S, Prieur M, De Blois MC, Vekemans M (2002) Deletion of the SIM1 gene (6q16.2) in a patient with a Prader-Willi-like phenotype. J Med Genet 39:594-596.

Fan CM, Kuwana E, Bulfone A, Fletcher CF, Copeland NG, Jenkins NA, Crews S, Martinez S, Puelles L, Rubenstein JL, Tessier-Lavigne M (1996) Expression patterns of two murine homologs of Drosophila single-minded suggest possible roles in embryonic patterning and in the pathogenesis of Down syndrome. Mol Cell Neurosci 7:1-16.

Farooqi IS, O'Rahilly S (2005) Monogenic obesity in humans. Annu Rev Med 56:443-458.

Farooqi IS, Keogh JM, Yeo GS, Lank EJ, Cheetham T, O'Rahilly S (2003) Clinical spectrum of obesity and mutations in the melanocortin 4 receptor gene. N Engl J Med 348:1085-1095.

Farooqi IS, Bullmore E, Keogh J, Gillard J, O'Rahilly S, Fletcher PC (2007) Leptin regulates striatal regions and human eating behavior. Science 317:1355.

Flegal KM, Carroll MD, Kuczmarski RJ, Johnson CL (1998) Overweight and obesity in the United States: prevalence and trends, 1960-1994. Int J Obes Relat Metab Disord 22:39-47.

Flynn MC, Scott TR, Pritchard TC, Plata-Salaman CR (1998) Mode of action of OB protein (leptin) on feeding. Am J Physiol 275:R174-179.

Froguel P, Boutin P (2001) Genetics of pathways regulating body weight in the development of obesity in humans. Exp Biol Med (Maywood) 226:991-996.
Fuzesi T, Sanchez E, Wittmann G, Singru PS, Fekete C, Lechan RM (2008) Regulation of cocaine- and amphetamine-regulated transcript-synthesising neurons of the hypothalamic paraventricular nucleus by endotoxin; implications for lipopolysaccharide-induced regulation of energy homeostasis. J Neuroendocrinol 20:1058-1066.
Fyffe SL, Neul JL, Samaco RC, Chao HT, Ben-Shachar S, Moretti P, McGill BE, Goulding EH, Sullivan E, Tecott LH, Zoghbi HY (2008) Deletion of Mecp2 in Sim1-expressing neurons reveals a critical role for MeCP2 in feeding behavior, aggression, and the response to stress. Neuron 59:947-958.
Gerfen CR (2003) Basic Neuroanatomical Methods. Current Protocols in Neuroscience:1.1.7-1.1.8.
Gilhuis HJ, van Ravenswaaij CM, Hamel BJ, Gabreels FJ (2000) Interstitial 6q deletion with a Prader-Willi-like phenotype: a new case and review of the literature. Eur J Paediatr Neurol 4:39-43.
Gimpl G, Fahrenholz F (2001) The oxytocin receptor system: structure, function, and regulation. Physiol Rev 81:629-683.
Gong S, Zheng C, Doughty ML, Losos K, Didkovsky N, Schambra UB, Nowak NJ, Joyner A, Leblanc G, Hatten ME, Heintz N (2003) A gene expression atlas of the central nervous system based on bacterial artificial chromosomes. Nature 425:917-925.
Gould BR, Zingg HH (2003) Mapping oxytocin receptor gene expression in the mouse brain and mammary gland using an oxytocin receptor-LacZ reporter mouse. Neuroscience 122:155-167.
Griffond B, Deray A, Bahjaoui-Bouhaddi M, Colard C, Bugnon C, Fellmann D (1994) Induction of Fos-like immunoreactivity in rat oxytocin neurons following insulin injections. Neurosci Lett 178:119-123.
Grill HJ, Kaplan JM (2002) The neuroanatomical axis for control of energy balance. Front Neuroendocrinol 23:2-40.
Gu YZ, Hogenesch JB, Bradfield CA (2000) The PAS superfamily: sensors of environmental and developmental signals. Annual review of pharmacology and toxicology 40:519-561.
Hankinson O (1995) The aryl hydrocarbon receptor complex. Annu Rev Pharmacol Toxicol 35:307-340.
Heinbecker P, White HL, Rolf D (1944) Experimental obesity in the dog. Am J Physiol 141:549-565.

Holder JL, Jr., Butte NF, Zinn AR (2000) Profound obesity associated with a balanced translocation that disrupts the SIM1 gene. Hum Mol Genet 9:101-108.
Holder JL, Jr., Zhang L, Kublaoui BM, DiLeone RJ, Oz OK, Bair CH, Lee YH, Zinn AR (2004) Sim1 gene dosage modulates the homeostatic feeding response to increased dietary fat in mice. Am J Physiol Endocrinol Metab 287:E105-113.
Holtwick R, Gotthardt M, Skryabin B, Steinmetz M, Potthast R, Zetsche B, Hammer RE, Herz J, Kuhn M (2002) Smooth muscle-selective deletion of guanylyl cyclase-A prevents the acute but not chronic effects of ANP on blood pressure. Proc Natl Acad Sci U S A 99:7142-7147.
Hosoya T, Oda Y, Takahashi S, Morita M, Kawauchi S, Ema M, Yamamoto M, Fujii-Kuriyama Y (2001) Defective development of secretory neurones in the hypothalamus of Arnt2-knockout mice. Genes Cells 6:361-374.
Hoybye C (2004) Endocrine and metabolic aspects of adult Prader-Willi syndrome with special emphasis on the effect of growth hormone treatment. Growth Horm IGF Res 14:1-15.
Huang X, Charbeneau RA, Fu Y, Kaur K, Gerin I, MacDougald OA, Neubig RR (2008) Resistance to diet-induced obesity and improved insulin sensitivity in mice with a regulator of G protein signaling-insensitive G184S Gnai2 allele. Diabetes 57:77-85.
Hung CC, Luan J, Sims M, Keogh JM, Hall C, Wareham NJ, O'Rahilly S, Farooqi IS (2007) Studies of the SIM1 gene in relation to human obesity and obesity-related traits. Int J Obes (Lond) 31:429-434.
Huszar D, Lynch CA, Fairchild-Huntress V, Dunmore JH, Fang Q, Berkemeier LR, Gu W, Kesterson RA, Boston BA, Cone RD, Smith FJ, Campfield LA, Burn P, Lee F (1997) Targeted disruption of the melanocortin-4 receptor results in obesity in mice. Cell 88:131-141.
Hwang LL, Wang CH, Li TL, Chang SD, Lin LC, Chen CP, Chen CT, Liang KC, Ho IK, Yang WS, Chiou LC (2009) Sex Differences in High-fat Diet-induced Obesity, Metabolic Alterations and Learning, and Synaptic Plasticity Deficits in Mice. Obesity (Silver Spring).
Johnson AK, Epstein AN (1975) The cerebral ventricles as the avenue for the dipsogenic action of intracranial angiotensin. Brain Res 86:399-418.
Kallio PJ, Okamoto K, O'Brien S, Carrero P, Makino Y, Tanaka H, Poellinger L (1998) Signal transduction in hypoxic cells: inducible nuclear translocation and recruitment of the CBP/p300 coactivator by the hypoxia-inducible factor-1alpha. Embo J 17:6573-6586.
Karim MA, Sloper JC (1980) Histogenesis of the supraoptic and paraventricular neurosecretory cells of the mouse hypothalamus. J Anat 130:341-347.

Kaufling J, Veinante P, Pawlowski SA, Freund-Mercier MJ, Barrot M (2009) Afferents to the GABAergic tail of the ventral tegmental area in the rat. J Comp Neurol 513:597-621.
Keith SW, Redden DT, Katzmarzyk PT, Boggiano MM, Hanlon EC, Benca RM, Ruden D, Pietrobelli A, Barger JL, Fontaine KR, Wang C, Aronne LJ, Wright SM, Baskin M, Dhurandhar NV, Lijoi MC, Grilo CM, DeLuca M, Westfall AO, Allison DB (2006) Putative contributors to the secular increase in obesity: exploring the roads less traveled. Int J Obes (Lond) 30:1585-1594.
Kennedy A, Gettys TW, Watson P, Wallace P, Ganaway E, Pan Q, Garvey WT (1997) The metabolic significance of leptin in humans: gender-based differences in relationship to adiposity, insulin sensitivity, and energy expenditure. J Clin Endocrinol Metab 82:1293-1300.
Kent WJ, Sugnet CW, Furey TS, Roskin KM, Pringle TH, Zahler AM, Haussler D (2002) The human genome browser at UCSC. Genome Res 12:996-1006.
Kewley RJ, Whitelaw ML (2005) Phosphorylation inhibits DNA-binding of alternatively spliced aryl hydrocarbon receptor nuclear translocator. Biochemical and biophysical research communications 338:660-667.
Kirchgessner AL, Sclafani A, Nilaver G (1988) Histochemical identification of a PVN-hindbrain feeding pathway. Physiol Behav 42:529-543.
Kondratov RV, Chernov MV, Kondratova AA, Gorbacheva VY, Gudkov AV, Antoch MP (2003) BMAL1-dependent circadian oscillation of nuclear CLOCK: posttranslational events induced by dimerization of transcriptional activators of the mammalian clock system. Genes & development 17:1921-1932.
Kortelainen ML (1997) Adiposity, cardiac size and precursors of coronary atherosclerosis in 5 to 15-year-old children: a retrospective study of 210 violent deaths. Int J Obes Relat Metab Disord 21:691-697.
Krahn DD, Gosnell BA, Majchrzak MJ (1990) The anorectic effects of CRH and restraint stress decrease with repeated exposures. Biol Psychiatry 27:1094-1102.
Krahn DD, Gosnell BA, Grace M, Levine AS (1986) CRF antagonist partially reverses CRF- and stress-induced effects on feeding. Brain Res Bull 17:285-289.
Kublaoui BM, Holder JL, Jr., Gemelli T, Zinn AR (2006a) Sim1 haploinsufficiency impairs melanocortin-mediated anorexia and activation of paraventricular nucleus neurons. Mol Endocrinol 20:2483-2492.
Kublaoui BM, Holder JL, Jr., Tolson KP, Gemelli T, Zinn AR (2006b) SIM1 overexpression partially rescues agouti yellow and diet-induced obesity by normalizing food intake. Endocrinology 147:4542-4549.

Kublaoui BM, Gemelli T, Tolson KP, Wang Y, Zinn AR (2008) Oxytocin deficiency mediates hyperphagic obesity of Sim1 haploinsufficient mice. Mol Endocrinol 22:1723-1734.
Kwon I, Lee J, Chang SH, Jung NC, Lee BJ, Son GH, Kim K, Lee KH (2006) BMAL1 shuttling controls transactivation and degradation of the CLOCK/BMAL1 heterodimer. Mol Cell Biol 26:7318-7330.
Lakso M, Pichel JG, Gorman JR, Sauer B, Okamoto Y, Lee E, Alt FW, Westphal H (1996) Efficient in vivo manipulation of mouse genomic sequences at the zygote stage. Proc Natl Acad Sci U S A 93:5860-5865.
Lee C, Etchegaray JP, Cagampang FR, Loudon AS, Reppert SM (2001) Posttranslational mechanisms regulate the mammalian circadian clock. Cell 107:855-867.
Leibowitz SF, Alexander JT (1991) Analysis of neuropeptide Y-induced feeding: dissociation of Y1 and Y2 receptor effects on natural meal patterns. Peptides 12:1251-1260.
Leibowitz SF, Hammer NJ, Chang K (1981) Hypothalamic paraventricular nucleus lesions produce overeating and obesity in the rat. Physiol Behav 27:1031-1040.
Liu C, Goshu E, Wells A, Fan CM (2003a) Identification of the downstream targets of SIM1 and ARNT2, a pair of transcription factors essential for neuroendocrine cell differentiation. J Biol Chem 278:44857-44867.
Liu H, Kishi T, Roseberry AG, Cai X, Lee CE, Montez JM, Friedman JM, Elmquist JK (2003b) Transgenic mice expressing green fluorescent protein under the control of the melanocortin-4 receptor promoter. J Neurosci 23:7143-7154.
Long WP, Chen X, Perdew GH (1999) Protein kinase C modulates aryl hydrocarbon receptor nuclear translocator protein-mediated transactivation potential in a dimer context. The Journal of biological chemistry 274:12391-12400.
Loots GG, Ovcharenko I, Pachter L, Dubchak I, Rubin EM (2002) rVista for comparative sequence-based discovery of functional transcription factor binding sites. Genome Res 12:832-839.
Lu D, Willard D, Patel IR, Kadwell S, Overton L, Kost T, Luther M, Chen W, Woychik RP, Wilkison WO, et al. (1994) Agouti protein is an antagonist of the melanocyte-stimulating-hormone receptor. Nature 371:799-802.
Luquet S, Perez FA, Hnasko TS, Palmiter RD (2005) NPY/AgRP neurons are essential for feeding in adult mice but can be ablated in neonates. Science 310:683-685.
Maejima Y et al. (2009) Nesfatin-1-regulated oxytocinergic signaling in the paraventricular nucleus causes anorexia through a leptin-independent melanocortin pathway. Cell Metab 10:355-365.

Maes HH, Neale MC, Eaves LJ (1997) Genetic and environmental factors in relative body weight and human adiposity. Behav Genet 27:325-351.
Mantella RC, Rinaman L, Vollmer RR, Amico JA (2003) Cholecystokinin and D-fenfluramine inhibit food intake in oxytocin-deficient mice. Am J Physiol Regul Integr Comp Physiol 285:R1037-1045.
Martin NM, Houston PA, Patterson M, Sajedi A, Carmignac DF, Ghatei MA, Bloom SR, Small CJ (2006) Abnormalities of the somatotrophic axis in the obese agouti mouse. Int J Obes (Lond) 30:430-438.
Matson CA, Ritter RC (1999) Long-term CCK-leptin synergy suggests a role for CCK in the regulation of body weight. Am J Physiol 276:R1038-1045.
Matson CA, Reid DF, Ritter RC (2002) Daily CCK injection enhances reduction of body weight by chronic intracerebroventricular leptin infusion. Am J Physiol Regul Integr Comp Physiol 282:R1368-1373.
Matson CA, Wiater MF, Kuijper JL, Weigle DS (1997) Synergy between leptin and cholecystokinin (CCK) to control daily caloric intake. Peptides 18:1275-1278.
Matson CA, Reid DF, Cannon TA, Ritter RC (2000) Cholecystokinin and leptin act synergistically to reduce body weight. Am J Physiol Regul Integr Comp Physiol 278:R882-890.
Michaud JL, Rosenquist T, May NR, Fan CM (1998) Development of neuroendocrine lineages requires the bHLH-PAS transcription factor SIM1. Genes Dev 12:3264-3275.
Michaud JL, DeRossi C, May NR, Holdener BC, Fan CM (2000) ARNT2 acts as the dimerization partner of SIM1 for the development of the hypothalamus. Mech Dev 90:253-261.
Michaud JL, Boucher F, Melnyk A, Gauthier F, Goshu E, Levy E, Mitchell GA, Himms-Hagen J, Fan CM (2001) Sim1 haploinsufficiency causes hyperphagia, obesity and reduction of the paraventricular nucleus of the hypothalamus. Hum Mol Genet 10:1465-1473.
Miller MW, Duhl DM, Vrieling H, Cordes SP, Ollmann MM, Winkes BM, Barsh GS (1993) Cloning of the mouse agouti gene predicts a secreted protein ubiquitously expressed in mice carrying the lethal yellow mutation. Genes Dev 7:454-467.
Minichiello L, Korte M, Wolfer D, Kuhn R, Unsicker K, Cestari V, Rossi-Arnaud C, Lipp HP, Bonhoeffer T, Klein R (1999) Essential role for TrkB receptors in hippocampus-mediated learning. Neuron 24:401-414.
Mizuno TM, Kleopoulos SP, Bergen HT, Roberts JL, Priest CA, Mobbs CV (1998) Hypothalamic pro-opiomelanocortin mRNA is reduced by fasting and [corrected] in ob/ob and db/db mice, but is stimulated by leptin. Diabetes 47:294-297.

Moran TH (2000) Cholecystokinin and satiety: current perspectives. Nutrition 16:858-865.
Moran TH, Schwartz GJ (1994) Neurobiology of cholecystokinin. Crit Rev Neurobiol 9:1-28.
Morton GJ, Cummings DE, Baskin DG, Barsh GS, Schwartz MW (2006) Central nervous system control of food intake and body weight. Nature 443:289-295.
Morton GJ, Blevins JE, Williams DL, Niswender KD, Gelling RW, Rhodes CJ, Baskin DG, Schwartz MW (2005) Leptin action in the forebrain regulates the hindbrain response to satiety signals. J Clin Invest 115:703-710.
Ogden CL, Carroll MD, Curtin LR, McDowell MA, Tabak CJ, Flegal KM (2006) Prevalence of overweight and obesity in the United States, 1999-2004. JAMA 295:1549-1555.
Olson BR, Drutarosky MD, Stricker EM, Verbalis JG (1991a) Brain oxytocin receptors mediate corticotropin-releasing hormone-induced anorexia. Am J Physiol 260:R448-452.
Olson BR, Drutarosky MD, Chow MS, Hruby VJ, Stricker EM, Verbalis JG (1991b) Oxytocin and an oxytocin agonist administered centrally decrease food intake in rats. Peptides 12:113-118.
Paxinos G, Franklin KBJ (2001) The Mouse Brain in Stereotaxic Coordinates, Second Edition. San Diego: Academic Press.
Rinaman L (1998) Oxytocinergic inputs to the nucleus of the solitary tract and dorsal motor nucleus of the vagus in neonatal rats. J Comp Neurol 399:101-109.
Rinaman L (2006) Ontogeny of hypothalamic-hindbrain feeding control circuits. Dev Psychobiol 48:389-396.
Rinaman L, Vollmer RR, Karam J, Phillips D, Li X, Amico JA (2005) Dehydration anorexia is attenuated in oxytocin-deficient mice. Am J Physiol Regul Integr Comp Physiol 288:R1791-1799.
Rios M, Fan G, Fekete C, Kelly J, Bates B, Kuehn R, Lechan RM, Jaenisch R (2001) Conditional deletion of brain-derived neurotrophic factor in the postnatal brain leads to obesity and hyperactivity. Mol Endocrinol 15:1748-1757.
Saper CB, Loewy AD, Swanson LW, Cowan WM (1976) Direct hypothalamo-autonomic connections. Brain Res 117:305-312.
Satoh N, Ogawa Y, Katsuura G, Numata Y, Masuzaki H, Yoshimasa Y, Nakao K (1998) Satiety effect and sympathetic activation of leptin are mediated by hypothalamic melanocortin system. Neurosci Lett 249:107-110.
Schioth HB, Muceniece R, Mutulis F, Bouifrouri AA, Mutule I, Wikberg JE (1999) Further pharmacological characterization of the selective

melanocortin 4 receptor antagonist HS014: comparison with SHU9119. Neuropeptides 33:191-196.
Schmidt-Supprian M, Rajewsky K (2007) Vagaries of conditional gene targeting. Nat Immunol 8:665-668.
Schwartz MW, Woods SC, Porte D, Jr., Seeley RJ, Baskin DG (2000) Central nervous system control of food intake. Nature 404:661-671.
Schwartz MW, Seeley RJ, Woods SC, Weigle DS, Campfield LA, Burn P, Baskin DG (1997) Leptin increases hypothalamic pro-opiomelanocortin mRNA expression in the rostral arcuate nucleus. Diabetes 46:2119-2123.
Sclafani A, Rinaman L, Vollmer RR, Amico JA (2007) Oxytocin knockout mice demonstrate enhanced intake of sweet and nonsweet carbohydrate solutions. Am J Physiol Regul Integr Comp Physiol 292:R1828-1833.
Shimada M, Nakamura T (1973) Time of neuron origin in mouse hypothalamic nuclei. Exp Neurol 41:163-173.
Srinivas S, Watanabe T, Lin CS, William CM, Tanabe Y, Jessell TM, Costantini F (2001) Cre reporter strains produced by targeted insertion of EYFP and ECFP into the ROSA26 locus. BMC Dev Biol 1:4.
Steward CA, Horan TL, Schuhler S, Bennett GW, Ebling FJ (2003) Central administration of thyrotropin releasing hormone (TRH) and related peptides inhibits feeding behavior in the Siberian hamster. Neuroreport 14:687-691.
Stock S, Granstrom L, Backman L, Matthiesen AS, Uvnas-Moberg K (1989) Elevated plasma levels of oxytocin in obese subjects before and after gastric banding. Int J Obes 13:213-222.
Stunkard AJ, Harris JR, Pedersen NL, McClearn GE (1990) The body-mass index of twins who have been reared apart. N Engl J Med 322:1483-1487.
Stunkard AJ, Sorensen TI, Hanis C, Teasdale TW, Chakraborty R, Schull WJ, Schulsinger F (1986) An adoption study of human obesity. N Engl J Med 314:193-198.
Swaab DF, Purba JS, Hofman MA (1995) Alterations in the hypothalamic paraventricular nucleus and its oxytocin neurons (putative satiety cells) in Prader-Willi syndrome: a study of five cases. J Clin Endocrinol Metab 80:573-579.
Swanson LW, Kuypers HG (1980) The paraventricular nucleus of the hypothalamus: cytoarchitectonic subdivisions and organization of projections to the pituitary, dorsal vagal complex, and spinal cord as demonstrated by retrograde fluorescence double-labeling methods. J Comp Neurol 194:555-570.
Teh CH, Lam KK, Loh CC, Loo JM, Yan T, Lim TM (2006) Neuronal PAS domain protein 1 is a transcriptional repressor and requires

arylhydrocarbon nuclear translocator for its nuclear localization. J Biol Chem 281:34617-34629.
To KK, Sedelnikova OA, Samons M, Bonner WM, Huang LE (2006) The phosphorylation status of PAS-B distinguishes HIF-1alpha from HIF-2alpha in NBS1 repression. The EMBO journal 25:4784-4794.
Toh KL, Jones CR, He Y, Eide EJ, Hinz WA, Virshup DM, Ptacek LJ, Fu YH (2001) An hPer2 phosphorylation site mutation in familial advanced sleep phase syndrome. Science 291:1040-1043.
Traurig M, Mack J, Hanson RL, Ghoussaini M, Meyre D, Knowler WC, Kobes S, Froguel P, Bogardus C, Baier LJ (2009) Common variation in SIM1 is reproducibly associated with BMI in Pima Indians. Diabetes 58:1682-1689.
Travers JB, Travers SP, Norgren R (1987) Gustatory neural processing in the hindbrain. Annu Rev Neurosci 10:595-632.
Truett GE, Heeger P, Mynatt RL, Truett AA, Walker JA, Warman ML (2000) Preparation of PCR-quality mouse genomic DNA with hot sodium hydroxide and tris (HotSHOT). Biotechniques 29:52, 54.
Turleau C, Demay G, Cabanis MO, Lenoir G, de Grouchy J (1988) 6q1 monosomy: a distinctive syndrome. Clin Genet 34:38-42.
Vaisse C, Clement K, Guy-Grand B, Froguel P (1998) A frameshift mutation in human MC4R is associated with a dominant form of obesity. Nat Genet 20:113-114.
Valassi E, Scacchi M, Cavagnini F (2008) Neuroendocrine control of food intake. Nutr Metab Cardiovasc Dis 18:158-168.
van den Pol AN (2003) Weighing the role of hypothalamic feeding neurotransmitters. Neuron 40:1059-1061.
Varela MC, Simoes-Sato AY, Kim CA, Bertola DR, De Castro CI, Koiffmann CP (2006) A new case of interstitial 6q16.2 deletion in a patient with Prader-Willi-like phenotype and investigation of SIM1 gene deletion in 87 patients with syndromic obesity. Eur J Med Genet 49:298-305.
Verbalis JG, Blackburn RE, Olson BR, Stricker EM (1993) Central oxytocin inhibition of food and salt ingestion: a mechanism for intake regulation of solute homeostasis. Regul Pept 45:149-154.
Vettor R, Fabris R, Pagano C, Federspil G (2002) Neuroendocrine regulation of eating behavior. J Endocrinol Invest 25:836-854.
Villa A, Urioste M, Bofarull JM, Martinez-Frias ML (1995) De novo interstitial deletion q16.2q21 on chromosome 6. Am J Med Genet 55:379-383.
Wang W, Lufkin T (2000) The murine Otp homeobox gene plays an essential role in the specification of neuronal cell lineages in the developing hypothalamus. Dev Biol 227:432-449.

Ward MP, Mosher JT, Crews ST (1998) Regulation of bHLH-PAS protein subcellular localization during Drosophila embryogenesis. Development 125:1599-1608.
Wardle J, Carnell S, Haworth CM, Plomin R (2008) Evidence for a strong genetic influence on childhood adiposity despite the force of the obesogenic environment. Am J Clin Nutr 87:398-404.
West MJ, Slomianka L, Gundersen HJ (1991) Unbiased stereological estimation of the total number of neurons in thesubdivisions of the rat hippocampus using the optical fractionator. Anat Rec 231:482-497.
Wisse BE, Schwartz MW (2003) The skinny on neurotrophins. Nat Neurosci 6:655-656.
Wolff GL (1963) Growth of Inbred Yellow (Aya) and Non-Yellow (Aa) Mice in Parabiosis. Genetics 48:1041-1058.
Woods SL, Whitelaw ML (2002) Differential activities of murine single minded 1 (SIM1) and SIM2 on a hypoxic response element. Cross-talk between basic helix-loop-helix/per-Arnt-Sim homology transcription factors. The Journal of biological chemistry 277:10236-10243.
Xu B, Goulding EH, Zang K, Cepoi D, Cone RD, Jones KR, Tecott LH, Reichardt LF (2003) Brain-derived neurotrophic factor regulates energy balance downstream of melanocortin-4 receptor. Nat Neurosci 6:736-742.
Xu C, Fan CM (2007) Allocation of paraventricular and supraoptic neurons requires Sim1 function: a role for a Sim1 downstream gene PlexinC1. Mol Endocrinol 21:1234-1245.
Yamaki A, Kudoh J, Shimizu N, Shimizu Y (2004) A novel nuclear localization signal in the human single-minded proteins SIM1 and SIM2. Biochem Biophys Res Commun 313:482-488.
Yang C, Gagnon D, Vachon P, Tremblay A, Levy E, Massie B, Michaud JL (2006) Adenoviral-mediated modulation of Sim1 expression in the paraventricular nucleus affects food intake. J Neurosci 26:7116-7120.
Yanovski SZ, Yanovski JA (2002) Obesity. N Engl J Med 346:591-602.
Yen TT, McKee MM, Stamm NB (1984) Thermogenesis and weight control. Int J Obes 8 Suppl 1:65-78.
Yen TT, McKee MM, Stamm NB, Bemis KG (1983) Stimulation of cyclic AMP and lipolysis in adipose tissue of normal and obese Avy/a mice by LY79771, a phenethanolamine, and stereoisomers. Life Sci 32:1515-1522.
Yen TT, Gill AM, Frigeri LG, Barsh GS, Wolff GL (1994) Obesity, diabetes, and neoplasia in yellow A(vy)/- mice: ectopic expression of the agouti gene. FASEB J 8:479-488.
Yeo GS, Farooqi IS, Aminian S, Halsall DJ, Stanhope RG, O'Rahilly S (1998) A frameshift mutation in MC4R associated with dominantly inherited human obesity. Nat Genet 20:111-112.

Zammaretti F, Panzica G, Eva C (2007) Sex-dependent regulation of hypothalamic neuropeptide Y-Y1 receptor gene expression in moderate/high fat, high-energy diet-fed mice. J Physiol 583:445-454.
Ziotopoulou M, Mantzoros CS, Hileman SM, Flier JS (2000) Differential expression of hypothalamic neuropeptides in the early phase of diet-induced obesity in mice. . Am J Physiol Endocrinol Metab 279:E838-E845.